SYNTHESIS OF NANOSTRUCTURE ACTIVE PHARMACEUTICAL INGREDIENTS FOR ISONIAZID AND GRISEOFULVIN BY CRYOGENIC TECHNOLOGY

LAYTH ABDULATEEF HASHIM

A DISSERTATION SUBMITTED FULFILLMENT OF THE REQUIREMENTS FOR THE DEGREE OF MASTERS OF ENGINEERING SCIENCE

FACULTY OF ENGINEERING
UNIVERSITY OF MALAYA
KUALA LUMPUR

SEPTEMBER 2011

ABSTRACT

One of the major challenges in the pharmaceutical industries is to improve the physicochemical properties of newly discovered Active Pharmaceutical Ingredients (API). It is reported that 40% of the newly developed APIs are bioavailability limited, which means the API are not released at a desirable dissolution rate.

The limitations are mainly due to low physicochemical properties such as solubility, dissolution rate and permeability. Improving physicochemical properties of APIs can be achieved through control of particle size distributions during production with the introduction of water-soluble polymers and/or surfactants, which act as additives to prevent particle agglomeration and crystal growth.

Venturing into the nano-particle world by producing APIs at nano-scale through nano-particle formation processes are expected to enhance physicochemical properties of APIs. On the other hand, cryogenic and nucleation technologies are promising process that creates highly porous nano-structured particles compared to conventional process such as wet milling and high pressure homogenization which normally lead to degradation in API activities.

This study consists of three main steps. Firstly, cryogenic surface was designed and fabricated using liquid nitrogen as a refrigeration media. The surface temperature range from -110°C to -90°C and the thermal conductivity of the surface made of stainless steel is 16 W/m.K. The procedure consists of dropping of solution from a nozzle with internal diameter of 0.8 mm into cryogenic surface and forming freezing disk of solution, with drop of volume measuring 7.7 mm diameter $\times$ 0.139mm height. This technique is called Ultra Rapid Freezing (URF). These frozen drops are then collected for drying in a freeze dryer. By utilizing cryogenic surface instead of atomization into liquid nitrogen, spreads of drop due to the complexity of cryogen evaporation (Leidenfrost effect) are eliminated.

Secondly, by employing the URF techniques developed, investigation of the effect of polymer (Polyvinylpyrrolidone) inclusion on the efficiency of this process was conducted. Isoniazid (Iso-Nicotinic Acid Hydrazide) was used as API and distilled water as the solvent. A comparison was also made with a nano-particle produced through URF and lyophilization by using a freeze dryer. Nano particle formation through freeze dryer is depending on freeze-drying cycle which is divided into three steps: freezing (solidification), primary drying (ice sublimation) and secondary drying (desorption of unfrozen water). Through this comparison, the effect of freezing rate on nano formation was observed. Furthermore, Differential Scanning Calorimetry (DSC) was utilized to prevent phase separation with the changing of freezing rate through introduction of heat. The hypothesis of this study is that the rate of freezing is critical in preventing phase separation during freezing, through this way API molecular grow can be inhabited and dispersed with the polymer.

Thirdly, to apply the URF technique developed to overcome the low bioavailability limitation, in which enhancement of dissolution rate is targeted. Griseofulvin (GF) was used in the dissolution study. GF is classified as Class II poorly soluble but highly permeable API, according to biopharmaceutical classification system (BCS). In addition to the inclusion of polymer, surfactant (Sodium dodecyl sulphate) was added. DSC is utilized to determine the amorphousity or crystallinity of the product, by observing the melting point.

The results demonstrated that URF technique developed offers a highly effective approach to produce nanoparticles, amorphous API and enhancing dissolution rates. Due to increasing freezing rate, phase separation prevention led to control size of crystal formation in nano range. Crystalline API (Isoniazid) yield was higher than 98% particles with size ≤200 nm were successfully recovered.

It can be concluded convincingly, that developed technique is an effective particle formation process for pharmaceutical development (particularly Isoniazid & Griseofulvin) and manufacturing to improve dissolution rates of poorly water soluble APIs.

ABSTRAK

Salah satu cabaran utama dalam industri farmaseutikal adalah untuk memperbaiki sifat-sifat bahan active farmasi (API) fizikokimia. laporan menunjukkan 40% API yang baru dihasilkan adalah bioavailabiliti terhad dalam ini bermaksud API tidak dilepaskan pada kadar pembubaran yang diingini.

Ini adalah disebabkan oleh kekurangan sifat-sifat fizikokimia seperti kelarutan, kadar pembubaran dan kebolehtelapan. sifat-sifat fizikokimia API boleh ditingkatkan melalui kawalan pengagihan saiz zarah semasa pengeluaran dengan pengenalan polimer larut air dan / atau surfaktan, yang bertindak sebagai bahan tambahan untuk mencegah aglomerasi zarah dan pertumbuhan kristal.

Nano-zarah dunia, pengeluaran API pada skala nano melalui proses pembentukan zarah nano dijangka dapat meningkatkan sifat-sifat fizikokimia API. Sebaliknya, teknologi kriogenik dan penukleusan menjanjikan proses yang mencipta zarah berstruktur nano yang sangat poros berbanding dengan proses konvensional seperti pengilangan yang basah dan penyeragaman tekanan tinggi yang biasanya membawa kepada degradasi dalam aktiviti-aktiviti API.

Kajian ini terdiri daripada tiga langkah utama. Pertama, permukaan kriogenik direkakan dan menggunakan cecair nitrogen sebagai media penyejukan. Julat permukaan suhu dari -110 ° C hingga -90 ° C dan kekonduksian haba permukaan yang dibuat daripada keluli tahan karat adalah 16 W / mK. Prosedur terdiri daripada jatuh penyelesaian dari muncung dengan diameter dalaman sebanyak 0.8 mm ke permukaan kriogenik dan membentuk cakera pembekuan penyelesaian, dengan penurunan sebanyak isipadu berukuran 7.7 mm diameter × ketinggian 0.139mm. Teknik ini

dipanggil Pembekuan Ultra Rapid (URF). Titis beku ini kemudiannya dikumpulkan untuk mengeringkan di dalam pengering pembekuan. Dengan menggunakan permukaan kriogenik bukan pengabusan ke dalam nitrogen cecair, merebak kejatuhan yang disebabkan oleh kerumitan penyejatan cryogen (Leidenfrost kesan) dihapuskan.

Kedua, dengan menggunakan teknik URF yang maju, penyiasatan kesan kemasukan polimer (Polyvinylpyrrolidone) pada kecekapan proses ini dijalankan. Isoniazid (Asid Hydrazide Iso-nikotinik) digunakan sebagai API dan air suling sebagai pelarut. Perbandingan juga dibuat dengan zarah nano yang dihasilkan melalui URF dan lyophilization dengan menggunakan rambut beku. Nano pembentukan zarah melalui rambut pembekuan adalah bergantung kepada kitaran beku-kering yang dibahagikan kepada tiga langkah: pembekuan (pemejalan), pengeringan utama (ais pemejalwapan) dan pengeringan menengah (desorption air unfrozen). Melalui perbandingan ini, kesan kadar pembekuan ke atas pembentukan nano akan diperhatikan . Tambahan pula, Calorimetry Mengimbas Pembezaan (DSC) digunakan untuk mencegah pemisahan fasa dengan mengubah kadar pembekuan melalui pengenalan haba. Hipotesis kajian ini adalah bahawa kadar pembekuan adalah kritikal dalam mencegah pemisahan fasa semasa pembekuan, melalui cara ini API molekul berkembang boleh didiami dan bersurai dengan menggunakan polimer.

Ketiga, menggunakan memohon teknik urf yang untuk mengatasi had bioavailabiliti yang rendah, di mana peningkatan kadar pembubaran adalah disasarkan. Griseofulvin (GF) telah digunakan dalam kajian pembubaran. GF dikelaskan sebagai Kelas II API yang kurang larut tetapi sangat telap, mengikut sistem klasifikasi biofarmaseutikal (Beluran). Di samping itu kemasukan polimer, surfactant (dodecyl Natrium sulfat) telah ditambah. DSC adalah digunakan untuk menentukan amorphousity atau crystallinity for produk, melalue memerhatikan takat lebur.

Keputusan menunjukkan bahawa kemajuaa teknik urf menawarkan pendekatan yang amat berkesan untuk menghasilkan nanopartikel, API amorfus dan meningkatkan kadar pembubaran. Disebabkan oleh peningkatan kadar pembekuan, mencegah pemisahan fasa mengakibatkan pengawalan saiz pembentukan kristal dalam julat nano. hasilan API kristal (Isoniazid) adalah lebih tinggi daripada zarah 98% dengan saiz ≤200 nm telah dengan berjaya pulih.

Ia boleh disimpulkan secara yakin, bahawa teknik yang dibangunkan adalah proses pembentukan zarah berkesan untuk pembangunan farmaseutikal (terutamanya Isoniazid & Griseofulvin) dan pembuatan untuk meningkatkan kadar pembubaran buruk API larut air.

DEDICATION

To my wonderful, supportive, loving wife, Zeena, for always standing by me. Throughout our years together, you're always there to help me remember who I really am.

ACKNOWLEDGEMENT

In the name of Allah, the Most Gracious and the Most Merciful.

Alhamdulillah, all praises to Allah for the strengths and His blessing in completing this thesis.

Special appreciation goes to my supervisor, ***Dr. Ezzat Chan Abdullah***, for his supervision and constant support. His valuable help of constructive comments and suggestions throughout the experimental and thesis works have contributed to the success of this research. Not forgotten, my appreciation to my co-supervisor, ***Dr. Abdul Aziz Abdul Raman*** for his support and knowledge regarding this topic. My acknowledgement also goes to all the technicians and office staffs of department of Chemical Engineering for their co-operations.

I am deeply and forever indebted to my parents for their love, support and encouragement throughout my entire life. I am also very grateful to my brothers and to my only sister.

Last but not least I would like to thank my wife for her continuous support, love and patience as well as my little girl Lara for her understanding and presence during darkest moments of doubt.

TABLE OF CONTENTS

CHAPTER5: CONCLUSION AND RECOMMENDATION

LIST OF FIGURES

LIST OF TABLES

LIST OF NOMENCLATURE

		Units in SI System
A	Specific Surface Area of Drug Particles	m^{-1}
A*	Entire Gastrointestinal Surface Area	m^{-2}
C	The Concentration of The Drug in Dissolution Media At Time T.	mg
C_s	Local equilibrium concentration of the drug in the diffusion layer surrounding the particle	mg
C_w	Drug concentration at the membrane (intestinal) surface.	kg/kg
D	Diffusion coefficient of drug molecules in dissolution media	m^2/s
h	Diffusion layer thickness	m
J_w	Drug flux (mass· (area×time)-1) through the intestinal wall	kg/m^2s
k_B	Boltzmann constant Ratio of the universal gas constant to Avogadro's number It has a value of 1.380662 × 10-23	J/K
M*	Total mass of drug absorbed at time t.	kg
P_c	Critical pressure	MN/m^2
P_w	Permeability of the membrane.	mg
R	Ideal gas constant 8314	J/kmol K
r	Particle radius	m
r*	Critical nuclear size	m
S	Solubility at temperature T.	mg/L
S*	Saturation Ratio	J
S_o	solubility on a flat, solid sheet	mg/L
T_c	Critical Temperature	°C
Tg	glass-transition temperature	°C
β_a	Surface conversion factors (βa = surface area/r2)	-
β_v	Volume conversion factors (βv = volume/r3)	-
γ	interfacial tension	N/m

		Units in SI System
$\gamma`$	Surface free energy per unit area	J/m^2
ΔG	Gibbs free energy	J
μ_1 and μ_2	Chemical potentials of phase 1 and phase 2	J
ν	Molecular volume of the precipitated embryo	$m^3/kmol$
ρ	Density	kg/m^3

LIST OF ABBREVIATIONS

API	Active Pharmaceutical Ingredient
ASES	Aerosol Solvent Extraction System
BCS	Biopharmaceutics Classification System
CAN-BD	Carbon Dioxide Assisted Nebulization-Bubble Drying
CD	Cyclodextrin
DELOS	Depressurization of an Expanded Liquid Organic Solution
GAS	Gas AntiSolvent
GF	Griseofulvin
GI	Gastrointestinal
HPMC	Hypromellose
HTS	Hydrothermal synthesis
HTS-SCW	Hydrothermal synthesis in supercritical water
INH	Isoniazid (isonicotinic acid hydrazide)
PCA	Precipitation by Compressed Antisolvent
PMMA	Polymethylmethacrylate
PVP	Polyvinylpyrrolidone
RESS	Rapid Expansion of Supercritical Solutions
SAA	Supercritical Assisted Atomization
SAS	Supercritical Antisolvent
SAS-EM	Supercritical AntiSolvent with Enhanced Mass transfer
SCF	Supercritical Fluid
ScMM	Solution Supercritical Melting Micronization
SCW	Supercritical water
SDS	Sodium Dodecyl Sulphate
SEDDS	Self-emulsifying or self micro-emulsifying drug delivery systems

SF	Spray Freezing
SFL	Spray Freezing into Liquid
SFN	Supercritical Fluid Nucleation
SFV/L	Spray Freezing into Vapor over Liquid
TB	Tuberculosis
THC	Δ^9-tetrahydrocannabinol
URF	Ultra Rapid Freezing
VLE	Vapor-Liquid Equilibria
PXRD	Powder X-ray Diffraction

UNIVERSITI MALAYA

PERAKUAN KEASLIAN PENULISAN

Nama: Layth Abulateef Hashim

No. Pendaftaran/Matrik: KGA 080015

Nama Ijazah: Master of Engineering Science

Tajuk Kertas Projek/Laporan Penyelidikan/Disertasi/Tesis ("Hasil Kerja ini"):

SYNTHESIS OF NANOSTRUCTURE ACTIVE PHARMACEUTICAL INGREDIENTS FOR ISONIAZID AND GRISEOFULVIN BY CRYOGENIC TECHNOLOGY

Bidang Penyelidikan: Nanoparticle Technology

Saya dengan sesungguhnya dan sebenarnya mengaku bahawa:

(1) Saya adalah satu-satunya pengarang/penulis Hasil Kerja ini;
(2) Hasil Kerja ini adalah asli;
(3) Apa-apa penggunaan mana-mana hasil kerja yang mengandungi hakcipta telah dilakukan secara urusan yang wajar dan bagi maksud yang dibenarkan dan apa-apa petikan, ekstrak, rujukan atau pengeluaran semula daripada atau kepada mana-mana hasil kerja yang mengandungi hakcipta telah dinyatakan dengan sejelasnya dan secukupnya dan satu pengiktirafan tajuk hasil kerja tersebut dan pengarang/penulisnya telah dilakukan di dalam Hasil Kerja ini;
(4) Saya tidak mempunyai apa-apa pengetahuan sebenar atau patut semunasabahnya tahu bahawa penghasilan Hasil Kerja ini melanggar suatu hakcipta hasil kerja yang lain;
(5) Saya dengan ini menyerahkan kesemua dan tiap-tiap hak yang terkandung di dalam hakcipta Hasil Kerja ini kepada Universiti Malaya ("UM") yang seterusnya mula dari sekarang adalah tuan punya kepada hakcipta di dalam Hasil Kerja ini dan apa-apa pengeluaran semula atau penggunaan dalam apa jua bentuk atau dengan apa juga cara sekalipun adalah dilarang tanpa terlebih dahulu mendapat kebenaran bertulis dari UM;
(6) Saya sedar sepenuhnya sekiranya dalam masa penghasilan Hasil Kerja ini saya telah melanggar suatu hakcipta hasil kerja yang lain sama ada dengan niat atau sebaliknya, saya boleh dikenakan tindakan undang-undang atau apa-apa tindakan lain sebagaimana yang diputuskan oleh UM.

Tandatangan Calon Tarikh

Diperbuat dan sesungguhnya diakui di hadapan,

Tandatangan Saksi Tarikh

Nama:
Jawatan:

UNIVERSITI MALAYA

ORIGINAL LITERARY WORK DECLARATION

Name of Candidate: Layth Abulateef Hashim

Registration/Matric No: KGA 080015

Name of Degree: Master of Engineering Science

Title of Project Paper/Research Report/Dissertation/Thesis ("this Work"):

SYNTHESIS OF NANOSTRUCTURE ACTIVE PHARMACEUTICAL INGREDIENTS FOR ISONIAZID AND GRISEOFULVIN BY CRYOGENIC TECHNOLOGY

Field of Study: Nanoparticle Technology

I do solemnly and sincerely declare that:

(1) I am the sole author/writer of this Work;
(2) This Work is original;
(3) Any use of any work in which copyright exists was done by way of fair dealing and for permitted purposes and any excerpt or extract from, or reference to or reproduction of any copyright work has been disclosed expressly and sufficiently and the title of the Work and its authorship have been acknowledged in this Work;
(4) I do not have any actual knowledge nor do I ought reasonably to know that the making of this work constitutes an infringement of any copyright work;
(5) I hereby assign all and every rights in the copyright to this Work to the University of Malaya ("UM"), who henceforth shall be owner of the copyright in this Work and that any reproduction or use in any form or by any means whatsoever is prohibited without the written consent of UM having been first had and obtained;
(6) I am fully aware that if in the course of making this Work I have infringed any copyright whether intentionally or otherwise, I may be subject to legal action or any other action as may be determined by UM.

Candidate's Signature Date

Subscribed and solemnly declared before,

Witness's Signature Date

Name:
Designation:

1.0 INTRODUCTION

Recent advances in synthesis and development of drug delivery in the areas of pharmaceutical industries have brought about a number of new active pharmaceutical ingredients (APIs) which hold promise in treating many of today's diseases and disorders (Muller et al., 2001). However, these APIs exhibit poor water solubility and low permeability in vivo resulting in poor absorption and limited and/or erratic bioavailability. Therefore, improving bioavailability of APIs is prerequisite to proper disease treatment. The main strategies to eliminate decreasing bioavailability of APIs are enhancing its solubility and changing the route of administration (Pandey et al., 2003).

Numerous researchers introduce the administration of APIs drugs in the form of vesicular systems and inhalations (Pandey et al., 2003) or injectable (Quenelle et al., 1999) preparations either through needle or free-needle techniques, as microparticulate systems through dermatology (Barrow et al., 1998). The main targets are to reduce APIs doses, doses frequency and toxicity, improvement in patient compliance and, most importantly, targeting drug delivery for Tuberculosis (TB) treatment. TB is an infectious disease infecting through inhalation of air polluted with the bacterium (Mycobacterium tuberculosis) (Riley et al., 1959) and uptake of the bacterium by alveolar macrophages. Treatment of TB is a complicated process involving long-term oral administration of multiple drugs for curing as well as preventing and/or combating multi-drug resistance (Fox et al., 1999). However due to long-term oral administration, the high blood levels of antitubercular drugs, is not effective for killing mycobacteria in the whole body especially those residing in lung [alveolar macrophages] the part that disease start from and containing a large number of bacilli (Russell, 2001). O'Hara and Hickey suggested the administration of

biodegradable microspheres through the bronchio-pulmonary route for better therapy of TB (O'Hara and Hickey, 2000). This strategy involves the direct steady delivery of antibiotic such Isoniazid (INH) to infected cellular tissue. Delivery of drugs to the lungs in sustained release formulations requires the encapsulation of drugs in microparticle or nanoparticle structures (Heyder et al., 1986).

Other advantage for using microparticle or nanoparticle structures is enhancing the dissolution rate as in Griseofulvin (GF) an antifungal API. This drug has appeared so frequently in the literature of pharmaceutical sciences owing to its incomplete and erratic absorption after oral administration of conventional or micronized forms. The slow dissolution rate is the dominating factor in producing irregular and incomplete absorption of this drug. Griseofulvin is an important example for enhancing the bioavailability, it is one of the antifungal drugs with systemic effect; it has been used since 1958 (Kucers and Bennet, 1988).

Nanoparticle formulations offer two main benefits: first the size of a particle decreases, where a greater number of its molecules will be found at its surface rather than inside the particle (Pison et al., 2006); second by giving nanoparticles a large surface area to volume ratio (Sung et al., 2007). This increase in the total surface area leads to an increase in dissolution rate and saturation solubility, as described by the Noyes-Whitney equation and the Kelvin and Ostwald-Freundlich equation (Muller et al., 2001).

Interestingly, the size-dependence becomes apparent only after the particle size falls below approximately 1 mm, making it entirely unique to nanoparticles. These phenomena make nanoparticle formulations a highly effective means to enhance mass transfer from the particle into the surrounding medium. For this reason, nanoparticle

formulations have been used to enhance the bioavailability of insoluble hydrophobic drugs (Pison et al., 2006). By suspending the drugs as nanoparticles, one can achieve a dose that is higher than that of a solution, which is thermodynamically limited by the aqueous solubility of the drug. In addition to the enhancement of mass transfer properties offered by nanoparticles, several studies have demonstrated that nanoparticles bind to and can be internalized by a variety of cell types (Foster et al., 2001; Chambers and Mitragotri, 2004; Foster et al., 2002; Koch et al., 2005; Suh et al.,2003). Davda and Labhasetwar showed that vascular endothelial cells rapidly internalize nanoparticles into the cytoplasm (Davda and Labhasetwar, 2002). Another study demonstrated that pulmonary epithelial cells internalize particles 0.5 mm or smaller 10 times more than 1 mm particles and 100 times more than 2 or 3 mm particles (Foster et al., 2001). These studies, and many others, suggest that nanoparticle formulations may be an effective way to enhance drug internalization by cells.

To date, researchers have made great strides in the development of precise pulmonary drug delivery technologies, both in terms of inhaler design and advances in particle engineering. Some of the most promising advances have manifested from applying nanotechnology to particle engineering (Becker et al., 2007). Nanotechnology refers to the methods used for the construction of nanomaterials and nanodevices and methods of handling of nano objects. Nanotechnologies produce nanometre-size particles. These technologies are based on methods allowing the construction of objects with sizes that are thousand or even million times smaller than those visible to the human eye. The systematic and purposeful development of the fundamentals of nanotechnologies started several decades ago. Many chemical processing technologies have been used to produce nanostructured materials; one of those is Cryogenic processing techniques.

Cryogenic processing techniques have shown to promising in the areas of oral delivery, pulmonary delivery, and nanoparticle encapsulation (Vaughn et al., 2005). These techniques been developed to produce nanostructured amorphous particles with high degrees of porosity (Yu et al., 2002). Cryogenic processes allow for a reduction in the primary particle size of drug particles without the intense frictional or mechanical forces involved in ball-milling or other processes relying on frictional comminution or trituration with a mortar and pestle, which can cause degradation of the drug through thermal stress (Leach et al.,2005; Overhoff et al.,2006).

Spray-freezing into liquid (SFL) is classified as cryogenic process because it involves atomizing of solution API and surfactant into a cryogenic liquid, such as nitrogen. High and sustained lung tissue concentrations were achieved via inhalation of an amorphous nanoparticulate which produced by SFL (Rogers et al., 2002; Vaughn et al., 2006). The disadvantage on this process is forming of droplet/cryogenic liquid interface, therefore vapor pocket existed due to the increased temperature difference between the feedstock and the cryogen liquid which affect the rate of freezing [Leidenfrost effect] (Hall et al.,1969).

The development of Ultra Rapid Freezing (URF) as Cryogenic technologies, the rapid freezing of the API/polymer composition is critical in preventing phase separation during freezing, allowing for the API to be molecularly dispersed with the polymer. Recrystallization of the APIs is avoided by the inclusion of high glass-transition temperature (Tg) polymers such as polyvinylpyrrolidone (PVP) or hypromellose (HPMC) (Purvis et al., 2006). URF process would overcome the limitation of transferring heat through a gas film by eliminating the gas interface element and using direct contact with the cryogenic substrate [Leidenfrost effect]. Low energy

consumption, intimate contact between the solution and cold solid surface without the complexity of cryogen evaporation [Leidenfrost effect] and without any contaminations effect.

Polyvinylpyrrolidone (PVP) is a commonly used water-soluble polymer in a variety of pharmaceutical formulations due to its low toxicity and chemical stability. Improved stability and dissolution properties of hydrophobic drugs prepared with PVP have been demonstrated for several kinds of drugs (Gohel and Patel, 2003).

Sodium dodecyl sulphate (SDS) has been used as an emulsifying agent in pharmaceutical formulations. Because of intrinsic toxicity problems, SDS is often used in combination with other excipients to obtain enhanced solubility and dispersion stability of drug particles (Craig, 2002).

The objectives of this study are:

- To design and fabricate a laboratory sized of cryogenic surface URF atomization system.
- To determine the degree of conversion of Isoniazid (INH) nanoparticles formation in the URF process.
- To investigate the effect of Sodium Dodecyl Sulfate (SDS) and Polyvinylpyrrolidone (PVP) emulsifusion effect on the dissolution rate of Griseofulvin (GF).

2.0 INTRODUCTION

Nanoparticle formation can be categorized by two general strategies, i.e. particle reduction is also popularly known as top-down technique and particle nucleation and stabilization also known as bottom-up technique.

For the particle reduction strategy, large API particles are fractured into smaller particles using a variety of processes and equipment. These nanoparticles are generally stabilized using various polymers and surfactants which can modify the surface charge of the particle preventing aggregation caused by electrostatic forces. On the other hand, for the bottom-up technique nanoparticles may be formed by particle nucleation from solution in which the API is dissolved, with or without stabilizing agents.

Particle growth is arrested using stabilizing polymers or surfactants, and controlled by manipulating process parameters in order to obtain particles within a desired size range. This chapter will review recently reported strategies of nano-particle formation and also discusses the background knowledge of bioavailability and crystallization.

2.1. BIOAVAILABILITY AND DISSOLUTION RATE

Throughout the past decade, formulation and delivery of APIs have played a crucial role in the development and commercialization of new pharmaceutical products. The major objective of formulation chemistry is to improve bioavailability, stability and convenience to the patient. Among the several routes of administration i.e.: oral, transdermal, parenteral, intranasal, intravenous, intramuscular, intraocular and subcutaneous; oral administration is still the most popular because it offers improved convenience (painless and simple) and patient compliance.

The bioavailability of an orally administered drug depends on its dissolution rate in aqueous media over the pH range of 1 – 8 and its permeability across membranes of the epithelial cells in the gastrointestinal tract (FDA, 2002).

Enhancing dissolution rate is a prerequisite to drug absorption and clinical response for almost all drugs given orally. The drug flux [mass· (area×time)$^{-1}$] through the intestinal wall at any position and time can be expressed by Fick's First Law as (Cussler, 1986):

$$J_w(x,y,z,t)=P_w(x,y,z,t).C_w(x,y,z,t) \quad (2.1)$$

Where $P_w(x,y,z,t)$ is the permeability of this membrane and $C_w(x,y,z,t)$ is the drug concentration at the membrane (intestinal) surface. It is assumed that sink condition (drug concentration equals zero) exist for the drug inside this membrane and P_w is an effective permeability.

The plasma may be assumed to be the physiological sink since concentration in the plasma is generally more than several orders of magnitude below that in the intestinal lumen in human (Lennernäs *et al.*, 1992). The drug absorption rate assuming no luminal reactions, at any time is:

$$Absorption\ rate = dm/dt = \iint_A P_w\, C_w dA` \quad (2.2)$$

Where A is over the entire gastrointestinal surface. The total mass, M`, of drug absorbed at time t is:

$$M(t) = \int_0^t \int \int_A P_w\, C_w dA` dt \quad (2.3)$$

The maximal absorption rate occurs when the drug concentration is at its solubility, C_s,

$$J^{max} = P_w C_{w,s} \quad (2.4)$$

and

$$M^{max}(t) = \int_0^t \int \int_A P_w C_w dA` dt \quad (2.5)$$

Where C_w=C_s, $C \leq C_s$ for permeability limited absorption; C_w=C_s, $C \leq C_s$, for solubility limited absorption.

For high solubility drugs that are dosed in solution or in dosage forms that dissolve very rapidly, a good correlation between drug absorption and intestinal membrane permeability is often obtained (Lennernas *et al*., 1992; Lennernas *et al*., 1994). A drug with permeability greater than 2 to 4 × 10^{-4} cm/s or about 1 cm/hr would be well absorbed with the expected fraction absorbed being greater than 95% (Amidon *et al*., 1995).

Amidon *et al*. divided drugs into four classes on the basis of their aqueous solubility and their ability to permeate the mucosa in the gut from the apical to the basolateral side (Amidon *et al*., 1995). Class I drugs are defined as those with high permeability which are able to dissolve readily in aqueous media over the pH range 1 to 8. The drug is well absorbed (though its systemic availability may be low due to first pass extraction/metabolism) and the rate limiting step to drug absorption is drug dissolution or gastric emptying if dissolution is very rapid.

Class II drugs are defined as those with high permeability but whose solubility in aqueous media is insufficient for the whole dose to be dissolved in the gastrointestinal contents under usual conditions. For these substances, dissolution is the rate limiting step to absorption.

Class III drug are defined as those with high solubility but low permeability which is the rate limiting step in drug absorption.

Class IV drugs are defined as those with low solubility and low permeability. Class II-IV drugs present significant problems for effective oral delivery. In this dissertation, Ultra rapid Freezing (URF) process, were applied to increase the dissolution rates of Class II drugs which have low solubility in water but high permeability into intestinal membranes.

Table 2.1
Biopharmaceutical Classification System
adopted from Amidon *et al* (1995).

Class	Dissolution in aqueous environment	Permeation over (intestinal) membrane
I	Fast	Fast
II	Slow	Fast
III	Fast	Slow
IV	Slow	Slow

The dissolution rate of a drug into an aqueous solution is described by Noyes-Whitney equation,

$$\frac{dm}{dt} = \frac{DA(C_S - C)}{h} \qquad (2.6)$$

The dissolution rate depends upon the diffusion coefficient of drug molecules in dissolution media, D; the specific surface area of drug particles, A; the local equilibrium concentration of the drug in the diffusion layer surrounding the particle, C_s; the diffusion layer thickness, h; and the concentration of the drug in dissolution media at time t, C (Noyes and Whitney, 1897).

In sink conditions, the dissolution rate may be increased by increasing surface area S and drug solubility in dissolution media C_s. The surface area S may be increased by reducing the particle size to sub-micro range, (Liversidge and Cundy, 1995) by increasing the porosity and by enhancing wetting of the particles by the dissolution media.

Reducing the particle size can also increase the solubility of the API according to the Ostwald-Freundlich equation, which assumes spherical particles:

$$\ln \frac{S}{S_{\circ}} = \frac{2\nu\gamma}{rRT} = \frac{2M\gamma}{\rho rRT} \qquad (2.7)$$

Where r is the particle radius, υ is the molar volume, ρ is the density, γ is the interfacial tension, and S is the solubility at temperature T. S_o is the solubility on a flat, solid sheet, M is the molecular weight of the solid, and R is the ideal gas constant. However, increases in solubility due to particle size reduction are negligible until particle size is decreased to well below 200 nm (Kipp, 2004).

As the particle size is decreased below 200 nm, the solubility relative to the equilibrium solubility (i.e. the solubility ratio, S/So) increases exponentially (Kipp, 2004). Therefore, increasing the intrinsic solubility allows for more API to dissolve leading to increase dissolution rates. This can have a profound effect on increasing absorption of APIs in which the rate limiting step is dissolution.

Wetting may be enhanced with hydrophilic excipients that are surface active at the API-aqueous interface (Reddy *et al.*, 1976). The solubility of drugs, C_s, may be enhanced by

trapping the API in metastable crystalline or amorphous states with higher free energies than the lowest energy equilibrium crystalline state.

2.2. METHODS TO INCREASE SOLUBILITY AND DISSOLUTION RATE OF APIs

Several strategies can be used to increase the amount of dissolved drug at the absorption site. The most straightforward method is to use a dosage form in which drug molecules are already dissolved in an aqueous solution. However, this may require large volumes of the liquid to dissolve the complete drug dose, which is highly unwanted. To increase the solubility buffers, surfactants or complex forming excipients (e.g. cyclodextrins) can be applied.

Cyclodextrins are cyclic dextrins that have the most polar side of the glucose units oriented outwards, resulting in a more a polar cavity in which the hydrophobic drug can be entrapped (Bayomi *et al*., 2002). They can increase the aqueous solubility of lipophilic molecules significantly. Moreover, cyclodextrin-drug complexes are solid at room temperature and can be used in solid dosage forms as well. Surfactants can form micelles entrapping hydrophobic molecules.

Capsules can be used to deliver the drug in dissolved state to the gastrointestinal tract, and surfactants keep the drug solubilized when it is exposed to the aqueous intestinal fluids. For example, this strategy has been successfully applied for danazol. The bioavailability of a capsule in which danazol was dissolved in Tween80® was increased 15.8 times compared to a powder filled capsule (Erlich *et al*., 1999). For a number of drugs, reproducible and extensive absorption after oral administration can be established by using surfactants (Torchilin, 2001). However, their use is limited, for example when

used for pulmonary administration, surfactants or most cyclodextrin-derivatives can cause irritation in the lung and are therefore highly undesirable (de Boer *et al.*, 2001). Furthermore, due to the liquid state, molecular mobility is high and therefore in these formulations chemically unstable drugs are susceptible to degradation.

A third option is to dissolve the drug in an oily liquid. An example of such an application is the soft gelatine capsule that contains sesame oil in which a hydrophobic drug, i.e. Δ^9-tetrahydrocannabinol (THC), is dissolved. It is marketed in the USA as Marinol®. However, the oil forms droplets inside the aqueous environment of the gastrointestinal tract. The hydrophobic drug has to be transferred from the oil phase to the aqueous environment of the gastro-intestinal lumen before membrane passage can occur, a process that will significantly decelerate the absorption.

In-vivo studies indeed revealed that the onset of action of Marinol® capsules is very slow and that only a small amount of the drug reaches the systemic blood circulation (Grotenhermen, 2003). To solve this problem micro-emulsions and self-emulsifying systems have been developed. Micro-emulsions are thermodynamically stable dispersions of two immiscible liquids, such as oil and water, stabilised by surfactant molecules (Constantinides, 1995). Self-emulsifying or self micro-emulsifying drug delivery systems (SEDDS) form under conditions of mild agitation very fine dispersions (<100nm in diameter). SEDDS usually contain triglyceride oils and at least 25%w/w hydrophilic surfactants and 0-50%w/w hydrophilic co-solvents (Pouton, 1997). The large surface of the oil-intestinal fluid interface provided by the small droplets guarantees a rapid and complete transfer of the lipophilic drug into the intestinal fluids. Sandimmune Neoral® is an example of a marketed product based on self emulsification. It contains Cyclosporine A and the inter- and intra-individual variability

of the pharmacokinetics has been claimed to be reduced compared to Sandimmune®, the latter forming a coarse emulsion in the gut.

The fourth strategy to deal with drugs that suffer from dissolution-limited absorption is to increase their dissolution rate. Often the absorption of lipophilic drugs is decelerated by the slow rate of dissolution from the solid drug particles. Dispersion of the drug as very fine particles will increase the surface area available for dissolution. According to the classical Noyes-Whitney equation this will increase the dissolution rate. Particle size reduction may go to the nano-scale. However, even this size reduction will not lead to concentrations above the maximum solubility of the drug in the intestinal fluids.

Alternatively, solid dispersions can be used to increase the dissolution rate of poorly soluble drugs (Gohel and Patel, 2003), and they have proven to increase the amount of dissolved drug at the absorption site sometimes to supersaturated concentrations and consequently improve the bioavailability. Solid dispersions are investigated in many studies because they are highly versatile in their application. They can form the basis of products applied for various routes of administration and for various dosage forms, including the most popular dosage form; i.e. the tablet.

2.2.1. Solid dispersions

The term solid dispersion refers to a group of solid products consisting of at least two different components, generally a hydrophilic matrix and a hydrophobic drug. The matrix can be either crystalline or amorphous. The drug can be dispersed molecularly, in amorphous particles (clusters) or in crystalline particles (Chiou and Riegelman, 1971). Therefore, based on their molecular arrangement, six different types of solid dispersions can be distinguished. They are described in Table 2.2 Moreover, certain combinations

can be encountered, i.e. in the same sample; some molecules are present in clusters while some are molecularly dispersed. Confusingly, in various studies the designation of solid dispersions is based on the method of preparation.

However, since different preparation methods can result in the same subtypes or similar preparation methods can result in different subtypes, it can be argued that solid dispersions should preferably be designated according to their molecular arrangement. Moreover, not the preparation method but the molecular arrangement governs the properties of solid dispersions. Therefore, it is essential to use terms that indicate the molecular arrangement in the solid dispersion. Knowledge about the molecular arrangement will enlarge comprehension of the properties and behavior of solid dispersions. Furthermore, it will facilitate optimization of their properties required for a specific application. For example, the mechanism underpinning the dissolution of solid dispersions is poorly understood (Craig, 2002).

Many case studies showed accelerated dissolution of hydrophobic compounds using solid dispersions but mechanisms are rarely discussed. The most important reason for that is the lacking knowledge about the mode of incorporation of the hydrophobic drug in the matrix, despite numerous efforts to clarify this. A question like, “is the drug present as a crystalline phase or as amorphous nano-particles or molecularly dispersed throughout the matrix” is rarely discussed (Kaushal *et al.*, 2004). All three situations result in different drug concentrations at the dissolving interface. Still it has not been fully elucidated how this affects dissolution behavior of solid dispersions.

Secondly, the physical and chemical stability of the matrix or the incorporated drug depends on the mode of incorporation. If drug molecules, for example, are present in amorphous nano-particles, crystallization requires only rotational rearrangement.

On the other hand, for a molecularly dispersed drug, translational diffusion is necessary before crystallization can occur by rotational rearrangements. The physical state of the matrix is also important for the chemical stability of the drug: the crystallinity of the matrix influences the translational and rotational rearrangements of the drug necessary for degradation reactions.

Finally, the influence of drug load and method of preparation on dissolution behavior and stability of solid dispersions can only be understood and predicted when the relation between these characteristics and the mode of incorporation is known.

Table 2.2
Classification of solid dispersions in six subtypes
(Torchilin, 2001).

	Solid Dispersion Type	Matrix*	Drug**	Remarks	No. Phases
I	Eutectics	C	C	The first type of solid dispersions prepared	2
II	amorphous precipitations in crystalline matrix	C	A	Rarely encountered	2
III	Solid Solutions				
	Continuous Solid solutions	C	M	Miscible at all compositions, never prepared	1
	Discontinuous solid solutions	C	M	Partially miscible, 2 phases even though drug is molecularly dispersed	2
	Substitutional solid solutions	C	M	Molecular diameter of drug (solute) differs less than 15% from matrix (solvent) diameter. In that case the drug and matrix are substitutional. Can be continuous or discontinuous. When discontinous: 2 phases even though drug is molecularly dispersed	1 or 2
	interstitial solid solutions	C	M	Drug (solute) molecular diameter less than 59% of matrix (solvent) diameter. Usually limited miscibility, discontinous. Example: Drug in helical interstitial spaces of PEG.	2
IV	glass suspension	A	C	Particle size of dispersed phase dependent on cooling/evaporation rate. Obtained after crystallization of drug in amorphous matrix	2
V	glass suspension	A	A	Particle size of dispersed phase dependent on cooling/evaporation rate many solid dispersions are of this type	2
VI	glass solution	A	M	Requires miscibility/solid solubility, complex formation or upon fast cooling/evaporation during preparation, many (recent) examples especially with PVP	1

*: A: matrix in the amorphous state
C: matrix in the crystalline state
**: A: drug dispersed as amorphous clusters in the matrix
C: drug dispersed as crystalline particles in the matrix
M: drug molecularly dispersed throughout the matrix

2.3. CRYSTALLIZATION

2.3.1. Thermodynamic background

A crystal is defined as a solid composed of atoms or molecules arranged in an orderly, repetitive array. Crystallization is an important process in pharmaceutical industry because a large number of pharmaceutical products are marketed in crystalline form. Crystallization may be carried out from vapor, melt or solution. Most industrial applications of the operation are solution-based crystallization.

There are two steps involved in crystallization process from solution: (1) nucleation, i.e. formation of new solid phase and (2) growth, i.e. increase in the size of the nucleus. The rate of nucleation plays an important role in controlling the final particle size distribution; this step is the most complex and still the most poorly understood. Nucleation process is composed of primary homogenous, primary heterogeneous and secondary nucleation (Dirksen and Ring, 1991).

Primary nucleation is prevailing in supersaturated solutions free from solute particles. Homogenous primary nucleation occurs in the absence while the heterogeneous one occurs in the presence of a solid interface of a foreign seed. In practice, primary heterogeneous nucleation is more important, because nucleation on a foreign surface takes place at lower critical supersaturation. However, once the heteronuclei are used up, heterogeneous nucleation stops, thus the maximum possible heterogeneous nucleation rate is limited (Perry and Green, 1984; Mullin, 2001).

Secondary nucleation refers to several mechanisms of nuclei production which have all in common mechanical aspects induced by the stirring of the medium and the

interaction between the crystals already present and their environment: fluid, stirrer, reactor wall and other crystals. Secondary nucleation is predominant in continuous industrial crystallizers operated at low supersaturation levels. On the contrary, at high level of supersaturation, primary nucleation is the main source of nuclei (Kashchiev, 2000).

Both nucleation and crystal growth have supersaturation as common driving force. The level of supersaturation is characterized by the saturation ratio (S`) which means the ratio of the actual concentration to the equilibrium concentration of the solute.

$$S = \frac{C}{C_S} \tag{2.8}$$

The phase change associated with crystallization and precipitation processes can be explained by thermodynamic principles. When a substance is transformed from one phase to another, the change in the molar Gibbs free energy (ΔG) of the transformation, at constant pressure and temperature, is given by

$$\Delta G = (\mu_1 - \mu_{12}) \tag{2.9}$$

Where μ_1 and μ_2 are the chemical potentials of phase 1 and phase 2, respectively. In crystallization process, Gibbs free energy can also be expressed in terms of supersaturation.

$$\Delta G = -RT \ln S` \tag{2.10}$$

When $C>C_S$, $\Delta G<0$ crystals are growing in the supersaturated solution. Alternatively, when $C<C_S$, $\Delta G>0$ crystals are dissolving. In equilibrium $C = C_S$, $\Delta G = 0$ and the solution is saturated.

Classical theories of primary homogenous nucleation assume that solute molecules in a supersaturated solution combine to produce embryos. In a supersaturated solution embryos larger than the critical size become stable nuclei which grow to form macroscopic particles. The critical nuclear size is defined as follows:

$$r^* = \frac{3\beta_a \gamma \nu}{3\beta_\nu \kappa_B T \ln S} \qquad (2.11)$$

where β_a and β_v are the surface and volume conversion factors, respectively (βa = surface area/r^2 and β_v = volume/r^3); k_B is the Boltzmann constant, ν is the molecular volume of the precipitated embryo and γ` is the surface free energy per unit area. For a given value of S all particles with r > r* will grow and all particles with r < r* will dissolve. Crystal growth is a layer-by-layer process that occurs only at the face of the crystal, so that material must be transported to that face from the bulk of the solution (Strickland, 1968).

Crystal growth consists of the two steps: diffusion of molecules to the growing crystal face and integration of molecules into the crystal lattice. In fact, different faces have different rates of growth. The ratio of these growth rates as well as the geometry of the unit cell determines the final crystal habit.

The shape of a crystal can be either thermodynamically or kinetically controlled. The thermodynamically controlled one is only important for crystals grown at very low saturation ratios. In most cases, kinetic factors are governing crystal growth i.e. fast-growing faces disappear and slow faces dominate the final shape (overlapping principle).

There are several methods that aim to modify the shape: combination of two or more forms, crystal twinning, crystallization under controlled conditions (i.e.: temperature) or in presence of additives and trace impurities.

In solution based crystallization, drug is dissolved in solution, and supersaturation is induced by mechanical means which finally leads to precipitation. There are several ways to induce supersaturation in a solution including heating, cooling, evaporation and addition of a third component (non-solvent, precipitant or reactant) (**Table 2.3**).

The possible paths of cooling and antisolvent crystallization processes are shown in **Figure 2.1** and **Figure 2.2.** Both diagrams are divided into three domains. In the stable region concentration of solute is below the solubility ($C<C_S$, $\Delta G>0$); neither nucleation nor crystal growth occurs in this zone. In the metastable region, the system is not in equilibrium; still the driving force is too low to induce nucleation ($C>C_S$, $\Delta G<0$, $r<r^*$). However, if seed crystals are added to the solution they provide surface area for crystal growth and nucleation (**Figure 2.1**).

Seeding is widely used for preparing relatively large but easy-to-handle crystals because it allows controlling the size and number of crystals produced, as well as the polymorphic form. In the labile zone ($C>C_S$, $\Delta G<0$, $r>r^*$), spontaneous homogeneous nucleation and crystal growth occur simultaneously (**Figure 2.1**). High nucleation rates lead to very fine particles which are often difficult to separate from mother liquor and show high tendency to aggregate.

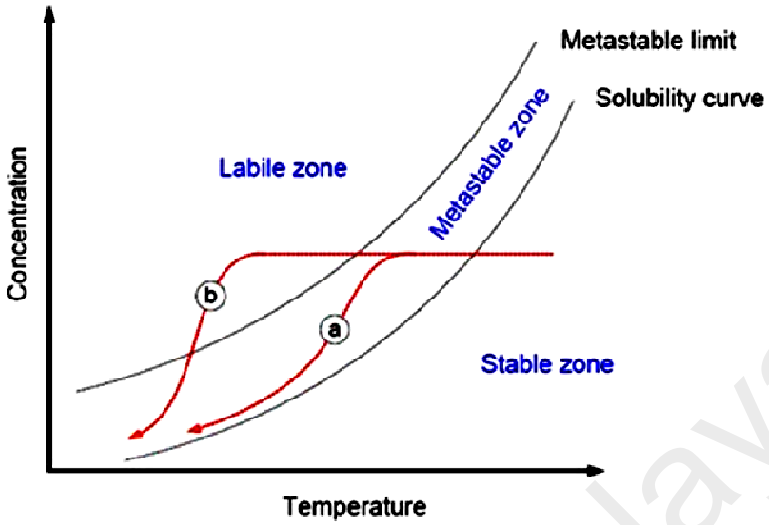

Figure 2.1
The paths of (a) seeded and (b) unseeded cooling crystallization (Perry and Green, 1984; Kashchiev, 2000).

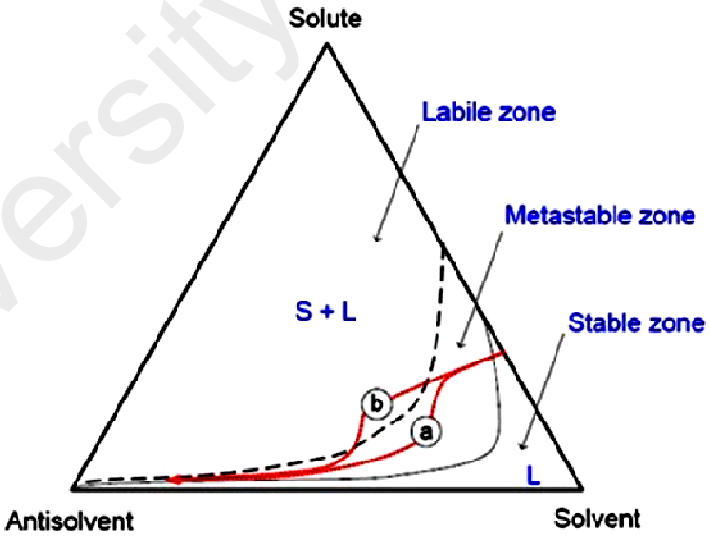

Figure 2.2
The paths of (a) seeded and (b) unseeded antisolvent crystallization (Perry and Green, 1984; Kashchiev, 2000).

Table 2.3
Operating principles of different crystallizers
(Perry and Green, 1984).

Operating Principles	Mechanisms
Cooling	↓Temperature ⇒↓ Solubility [a]
Heating	↑Temperature ⇒ Solvent evaporation ⇒↑Concentration ⇒↓Solubility [b]
Vacuum	↓Pressure ⇒ Solvent evaporation⇒↑Concentration ⇒↓Temperature ⇓⇒↓Solubility
Antisolvent	+ Antisolvent ⇒↓Solubility
Precipitant	+ Precipitant ⇒↓Solubility
Chemical reaction	+ Reactant ⇒Chemical reaction ⇒ Insoluble product

[a] the solubility is proportional to the temperature; [b] the solubility is inversely proportional to the temperature.

2.3.2. Polymorphism

Some materials may exist in more than one crystal structure, this is called polymorphism. Nowadays, more than 50 % of the APIs are known to exist in several crystal forms as polymorphs or pseudopolymorphs (hydrates or solvates) or both. Although, polymorphs are identical in the liquid and vapour states, owing to the same chemical composition, they may exhibit different physical and chemical properties such as melting point, density, solubility, crystal morphology and habit, physical and chemical stability, dissolution kinetics and spectroscopic behavior. Two polymorphs can form an enantiotropic or a monotropic system and phase transitions can be observed, as described below.

In **enantiotropic** systems each form has a temperature range over which it is stable with respect to the other form. A schematic Gibbs free energy diagram of an enantiotropic system is shown in **Figure 2.3** The free energy curves of the two enantiotropic forms (A, B) intersect below the melting points (T_{mA} and T_{mB}) when plotted against temperature. The x-coordinate of the point of intersection is (T_{AB}) is called transition

point. The form showing the smaller free energy at a given temperature is the most stable form. For a temperature below TAB, form A is stable and form B is metastable while the contrary is true above TAB. The solubility versus temperature curves also intersect in the transition point **Figure 2.4** the stable form exhibits lower solubility.

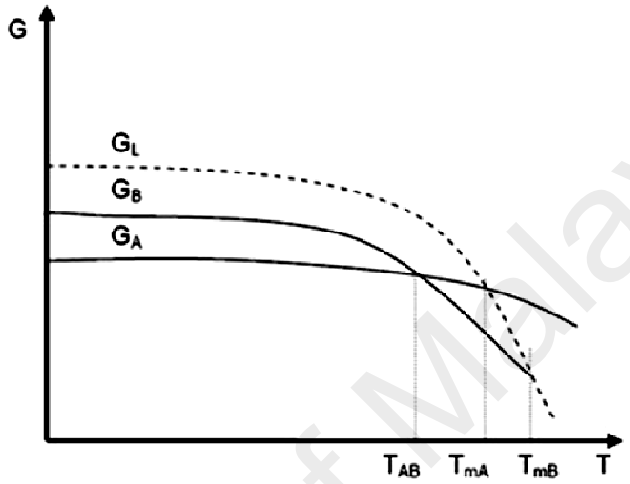

Figure 2.3
Free energy versus temperature diagram for an enantiotropic system.
(Perry and Green, 1984; Mullin, 1988)

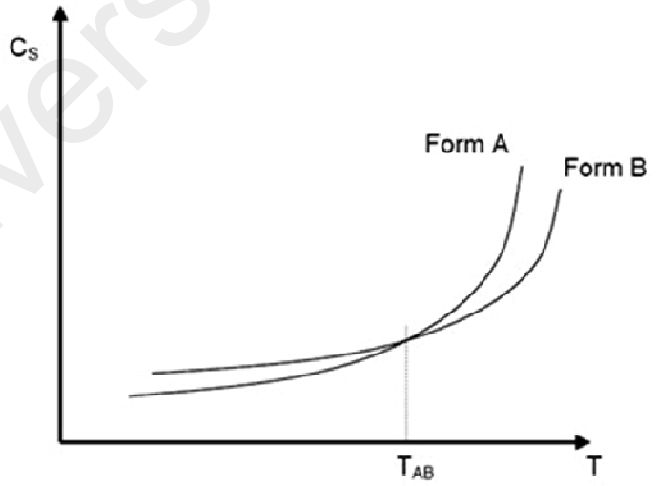

Figure 2.4
Solubility versus temperature curves for an enantiotropic system
(Perry and Green, 1984*;* Mullin, 1988).

In a **monotropic** system one form is metastable with respect to the other form at all temperatures. There is no observable transition point, although thermodynamics imply a theoretical transition point above the melting point. The free energy curves of such systems do not intersect below the melting points (**Figure 2.5**), neither do their solubility curves (**Figure 2.6**).

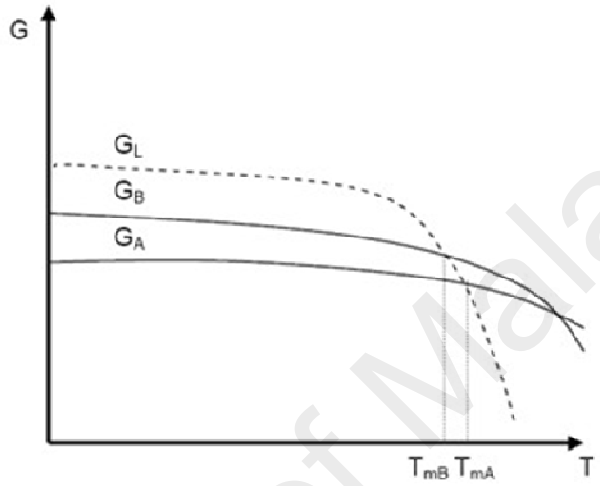

Figure 2.5
Free energy versus temperature diagram for a monotropic system
(Perry and Green, 1984).

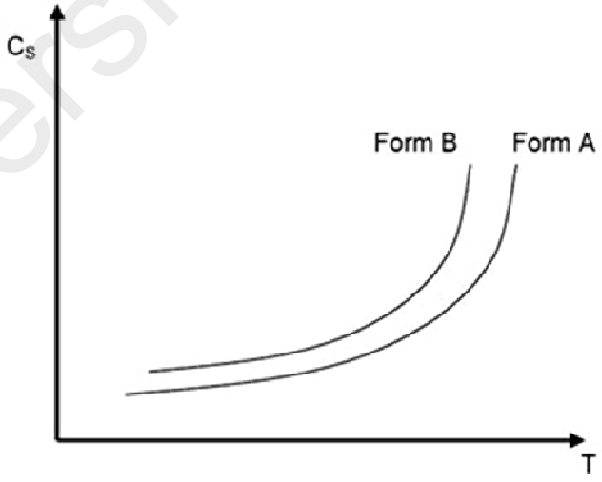

Figure 2.6
Solubility versus temperature curves for a monotropic system
(Perry and Green, 1984).

The term pseudopolymorphism characterizes substances incorporating solvent in their crystal lattice. These substances are also called solvates or hydrates, if water molecules are part of the crystal structure. Like polymorphs, different pseudopolymorphs of one substance can have different physical properties. However, due to the incorporation of solvent, pseudopolymorphs are chemically not identical, and therefore not only the physical properties may be different, but also the chemical ones.

2.4. MICRONIZATION PARTICLE ENGINEERING

2.4.1. Mechanical Techniques

Mechanical methods for particle size redistribution are crushing and grinding, which for some applications are carried out at cryogenic temperatures, by ball milling with or without milling aids and by air micronization (also called jet impingement or fluid energy milling). The disadvantages of conventional methods for size reduction are:

• Due to heat generation during size reduction; not feasible for thermolabile drugs.

• Not appropriate for drugs capable of degrading on exposure to atmosphere.

• Electrostatically charged particles are obtained after fluid energy grinding.

• Difficult to obtain mono-disperse particles.

• The formation of particles below 1μm is a challenge due to aggregation of high surface area materials.

Until now, two mechanical processes were commercialized for nanoparticle preparation. First, the wet milling technique, NanoCrystals® technology, was developed and patented in 1992 by Liversidge *et al.* and formerly owned by Sterling Drug Inc., later acquired by Elan Corporation (Merisko-Liversidge *et al.*, 2003; Muller *et al.*, 2001; Liversidge and Conzentino, 1995).

The second process is a high pressure homogenization process, DissoCubes® technology, which was developed and patented by Müller *et al* in 1994 and formerly owned by the Drug Delivery Services GmbH in Germany and now owned by SkyePharma PLC (Muller *et al*., 1999).

The advantages that nanoparticles have in vitro focusing on:

1. Dissolution enhancement of poorly water soluble APIs
2. Increase in solubility with a decrease in particle size.
3. Improved physical stability occurs through addition of nonionic surfactants to the surface of the particles in order to reduce electrostatic attraction.
4. Less agglomeration due to physical separation by Brownian motion is minimized in nanoparticle dispersions.

However, those advantages have little consequence if there is little or no improvement to in vivo properties including increased API absorption and efficacy and reduced variability and toxicity. It is essential to understand the role of particle size and surface modification in API absorption through a variety of biological membranes.

The advantages that nanoparticles have in vitro focusing on:

1. Nanoparticles as carrier systems are more easily absorbed across biological membranes because of their smaller size. Likewise, permeation can be facilitated by modifying the surface properties which is of particular importance to APIs which display poor absorption characteristics like proteins and peptides.
2. Targeting specific sites within the body to deliver treatment is possible using surface modified nanoparticles especially on the cellular level.
3. Nanoparticles also have the ability to avoid clearance by the immune system or adhering onto mucous membranes thereby increasing the residence time allowing more time for treatment to occur.
4. Encapsulated nanoparticles offer protection to APIs susceptible to degradation mechanisms.

5. Nano-particulate systems can be designed to facilitate transport across biological membranes,
6. Target specific tissues or sites within the body.
7. Avoid uptake by the immune system.
8. Increase residence time within the body.
9. Protect against premature degradation or metabolic processes.
10. It is hypothesized that localized delivery of the chemotherapeutic agent to the tumor site should increase efficacy thereby reducing the required amount needed for tumor size reduction.

2.4.1.1. Wet Milling

Wet milling is an attrition process in which large micron size drug crystals are wet milled in the presence of grinding media and a surface modifier. The rigid grinding media is typically spherical in form, having an average size less than about 3 mm. The grinding media used in the process include zirconium oxide, such as 95% ZrO stabilized with magnesia, zirconium silicate, and other media, such as glass grinding media stainless steel, titania, alumina, and 95% ZrO stabilized with yttrium (Muller *et al*., 1999).

The surface modifies include various polymers, low molecular weight oligomers, natural products and surfactants, such as polyvinylpyrrolidone, pluronic F68, pluronic F108, and lecithin. The particle size of the starting materials is typically less than 100 μm and was micronized by a jet milling process. The particle size of the final products is less than 400 nm (Merisko-Liversidge *et al*., 2003; Muller *et al*., 2001; Liversidge and Conzentino, 1995).

In the wet milling process, the poorly water soluble drug is first dispersed in an aqueous-based surfactant solution, and then the resulting suspension is wet milled with the grinding media. High-energy-generated shear forces and the forces generated during impaction of the milling media with the solid drug provide the energy to fracture drug crystals into nanometer-sized particles (Merisko-Liversidge *et al*., 1996).

Processing temperatures commonly are less than 40°C (Liversidge and Conzentino, 1995) and processing pressures are up to about 20 psi. Milling efficiency is dependent on the properties of the poorly water soluble drug, medium and stabilizer. Liversidge reported that a significant reduction particle size was observed within 24 hours wet milling. Routinely, the drug/surfactant slurry was milled to a final size of less than 400 nm and generally this could be achieved over a four-day period (Liversidge and Cundy, 1995).

Poorly water soluble drugs in the nanoparticle suspension are reported to be in a crystalline state due to a low energy used in the milling process. The nanoparticles are typically less than 400 nm and are physically stabilized with a polymeric excipient. A physically stable nanosuspension is obtained when the weight ratio of drug to stabilizer was 20:1 to 2:1. Liversidge *et al* reported that poorly water soluble drug, naproxen, was reduced average particle size from 20-30 μm to 270 nm over 5 days wet milling. The PVP K-15 was used as a stabilizer in the suspension and the ratio between naproxen and PVP K-15 in the nanosuspension was 5:3.

The naproxen nanosuspension did not aggregate and remained physically and chemically stable for up to 4 weeks at 4°C. The nanosuspension containing 2% paclitaxel and 1% pluronic F127 was prepared by wet milling for 7 days and had

average particle size about 280 nm. It was found that the higher molecular weight polymeric stabilizer was optimal for effective particle size reduction and shelf stability.

NanoCrystals® particles can be used for oral delivery. In the study of preparaing a nanosuspension of naproxen, the bioavailability of NanoCrystals® naproxen was compared to that of the marketed products: Naprosyn® (suspension) and Anaprox® (tablet). The time to reach maximal drug concentrations is approximately 50% less for the NanoCrystals® dispersion, while maintaining a 2.5 – 4.5-fold increase in the AUCs during the first hour of the study.

NanoCrystals® suspensions are also a suitable dosage form for poorly-water soluble injectable products. The nanoparticles produced by wet milling process provided a significantly higher level dosing than using a traditional approach.

Harsh solvent or co-solvent used in the formulation of poorly water soluble drugs are dose limiting due to the toxicity of solvent or excipients. In the comparison of the performance of paclitaxel in the marketed product (Taxol®) using Cremophor EL/ethanol mixture and NanoCrystals® nanosuspension, the maximum tolerated dose of the nanoparticle paclitaxel formulation is greater than that of the commercial product. This advantage could improve the delivery efficacy of the poorly water soluble drugs (Merisko-Liversidge *et al*., 1996).

A limitation of the wet milling process is that the contamination of the product by grinding material has been reported. During the wet milling process, erosion of grinding materials occurs and leads to contamination of the product and the grinding media, such as glass and zirconium oxide are insoluble in the fluid of the GI tract. In addition, wet

milling is a batch process. There is batch-to-batch variation detected in the quality of dispersion, processing time, crystallinity degree of drugs, and particle size distribution. These variations will affect drug particle stability, powder flow properties, and efficiency of delivery system. Milling over a few days also brings the risk of microbiological problems, especially when performing the milling at 30°C or having dispersion media providing nutrition to bacteria.

2.4.1.2. High Pressure Homogenization

High pressure homogenization is another mechanical process to prepare nanometer size particle in suspension containing poorly water soluble drugs. The principle of forming nanosuspensions is the cavitation forces created in high pressure homogenizer like piston-gap homogenizer. In the process, the poorly water soluble drug is first dispersed in an aqueous surfactant solution by high speed stirring and the suspension is then passed through a high pressure homogenizer applying a typical pressure of 1500 bar and 3 to 20 homogenization cycles.

The suspension passes a very small homogenization gap in the homogenizer, typically having a width of 25 μm at 1500 bar. Due to the narrowness of the gap, the streaming velocity of the suspension increases and the dynamic fluid pressure also increases. In addition, the static pressure on the fluid decreases below the boiling point of water at room temperature. In consequence, water starts boiling at room temperature and gas bubbles are formed which implode (=cavitation) when the fluid leaves the homogenization gap. These cavitation forces are strong enough to break the drug microparticles into drug nanoparticles (Muller *et al*., 1999).

Nanosuspension particles have an average particle size ranging from 40 nm to 500 nm, the proportion of particles larger than 5 μm in the total population being less than 0.1%. The particle size of nanosuspension depends on the hardness of the drug substance, processing pressure and number of cycles applied.

For the poorly water soluble drug, budesonide, a pressure of 1500 bar and 10 cycles led to a mean diameter of 511 nm, increasing the cycle numbers to 15 reduced the size to 462 nm, and increasing the pressure to 2500 bar and 10 cycles led to particles with a mean diameter of 363 nm (Liversidge *et al.*,1992). The particle size of poorly water soluble drug can be produced in a controlled way by adjusting the production parameters pressure and cycle accordingly. Changes in drug crystallinity have been reported for high pressure homogenization process. A fraction of poorly water soluble drugs in the particles was amorphous in some cases, while the drugs were found to be completely amorphous in other cases. The application of high pressures in the process was found to promote the amorphous structure. The variation in crystallinity level might be a challenge for quantity control and long term stability (Merisko-Liversidge *et al*., 2003).

The stabilization against aggregation and coalescence is a main challenge for forming nanosuspensions. The stability of nanosuspensions can be determined by the zeta potential. For a physically stable nanosuspension solely stabilized by electrostatic repulsion, a zeta potential of ±30 mV is required as a minimum (Liversidge and Conzentino, 1995).

In addition, Ostwald ripening is also used to determine the stability of highly dispersed systems. The absence of Ostwald ripening indicates long-term physical stability as an

aqueous suspension. It was observed that there was no Ostwald ripening in the nanosuspensions produced by high pressure homogenization process. This was attributed to the uniform particle size created by the homogenization process (Liversidge *et al.*, 1992). The concentration differences in the nanosuspension system were sufficiently low to avoid the ripening effect.

The ability for large-scale production of a drug delivery system is the essential prerequisite for the current nanoparticle engineering processes to be introduced into the pharmaceutical market.

High pressure homogenizers are available with different capacities from a few hundreds to a few thousands liters per hour. In addition, instead of passing a few times through one homogenizer, several homogenizers can be placed in series to produce the product in a continuous mode.

In addition, there are also homogenizers used on a laboratory scale, which can have a minimum batch volume of 20 ml and a maximum of 40 ml, thus allowing the cost-effective processing of expensive drug materials or small amount of experimental compounds.

The disadvantage of high pressure homogenization process is that the high pressures used can cause changes in the crystal structure, and as a result, the amorphous fraction in the particle increases in some cases. The batch to batch variation in crystallinity level might be an issue for quantity control. The stability of partially amorphous nanosuspensions will also present a challenge in pharmaceutical industry applications.

2.4.2. Supercritical Fluid Technology

Cagniard de la Tour is the first researcher to describe the supercritical fluids (SCFs) phenomenon in 1822 (Cagniard, 1822). In spite of this early proposal of SCFs, their industrial application starts only in the late ’70s. The first industrial scale plant for the decaffeination of coffee beans was built 1976 by the HAG Corporation.

In the 1980’s many industrial applications were studied, including chemical reactions, purification of surfactants and pharmaceuticals, polymerization and fractionation of polymers. In the same period, interest in using supercritical fluids for precipitation and crystallization process was developing for pharmaceutical materials and this activity has steadily increased over recent years (McHugh *et al*., 1994).

Industries commonly used carbon dioxide (CO_2) as solvent due to its critical parameters are simple to be obtained in an industrial apparatus, cheap, nonflammable and nontoxic. However, ammonia, alcohols, light hydrocarbons and water have been proposed, among the others, for nanomaterials production at supercritical conditions.

When gas-liquid coexistence curve the density of liquid phase gradually decreases owing to the thermal expansion while density of the gas phase increases owing to its high compressibility and increased pressure (**Figure 2.7**).

The densities of the two phases converge and become equal in the critical point. Beyond the critical point the substance exists as a single phase, called supercritical fluid. The critical point is defined by the critical pressure (P_c) and the critical temperature (T_c); their values are specific to each compound.

Extreme changes in some important properties like density, viscosity, thermal conductivity, surface tension and constant-pressure heat capacity of a pure substance near the critical point (**Figure 2.8**). Similar behavior can be observed for liquid mixtures as they approach the critical loci, as well.

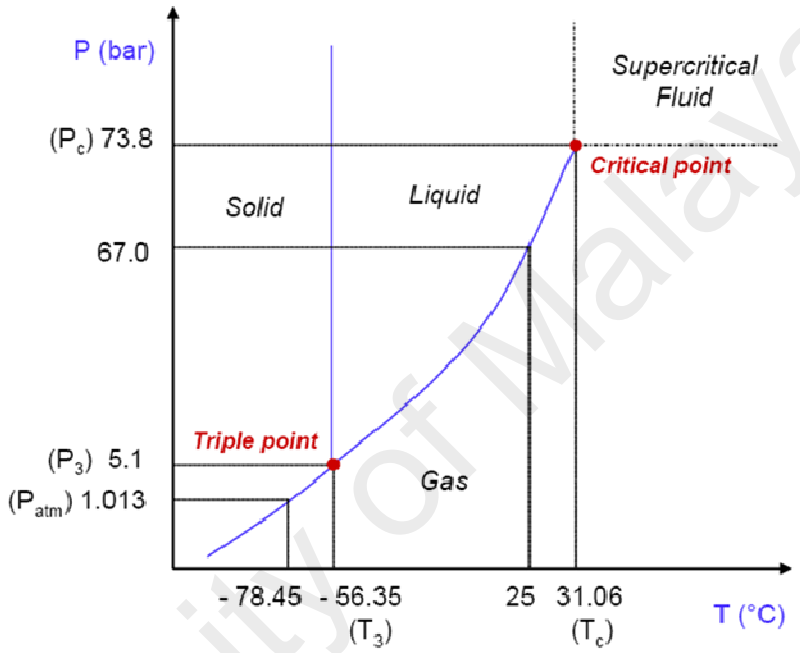

Figure 2.7
Phase diagram of CO_2
(Perry and Green, 1984).

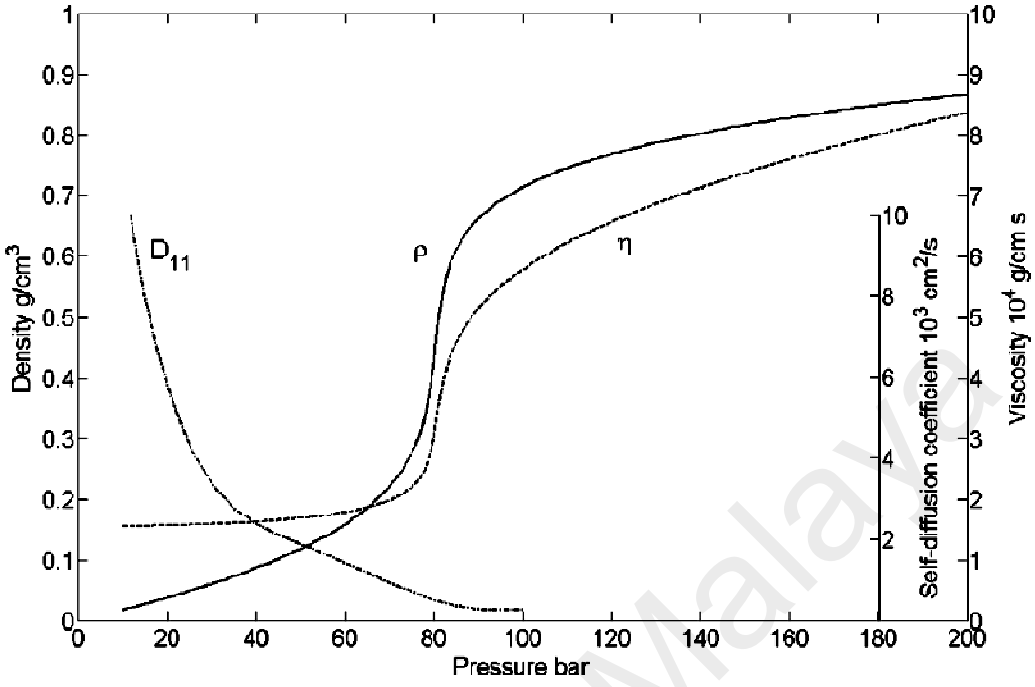

Figure 2.8
Density (ρ), viscosity (η) and self-diffusion coefficient (D11) of CO_2 at 35 °C. (Huang, 1985; Fenghour, 1998; O'Hern, 1955)

In the critical region, fluids are highly compressible; their densities vary between liquid-like and gas-like values as a function of pressure and temperature. Most of the processes using SCFs exploit their enhanced transport properties due to their gas-like viscosity, liquid-like solvent power and intermediate diffusivity as well as the possibility to tune these properties by controlling the pressure and temperature (**Table 2.4**).

Table 2.4
Diffusion coefficient, density and viscosity of gases, liquids and SCFs (Perry and Green, 1984).

	D_{12} [cm^2/s]	ρ [g/cm^3]	η [g/cm s]
Gas	10^{-1}	10^{-3}	10^{-4}
SCF	10^{-3}	0.2 – 1	10^{-4}-10^{-3}
Liquid	10^{-6}	1	10^{-2}

In addition, SCFs exhibit almost zero surface tension, which allows easy penetration into microporous materials. As a result of advantageous combination of physicochemical properties, the extraction process can often be carried out more efficiently with supercritical than with organic liquid solvent. SCF's nanoparticles generation process generally classified according to the SCF acting in the process as **solvents**, **solutes**, **anti-solvents** and **reaction media**. (See **table 2.5**)

Table 2.5
Classification of SCF-based micronization techniques according to act of SCF in the process. (Reverchon and Adami, 2006)

CO_2 ROLE	APPLICATION	PROCESS	ACRONYM	CHARACTERISTICS
Solvent	compounds soluble in SC-CO_2	Rapid Expansion of Supercritical Solutions	RESS	supercritical solution sprayed into atmospheric pressure
		Rapid Expansion of a Supercritical solution into a Liquid Solvent	RESOLV	supercritical solution sprayed into a liquid
		Rapid Expansion of a Supercritical Solution-Solid Cosolvent	RESS-SC	solid co-solvent added to SC-CO_2
Antisolvent	compounds with almost zero-solubility in SC-CO_2, soluble in a solvent that has a good affinity with SC-CO_2	Gas AntiSolvent	GAS	batch operation
		Supercritical AntiSolvent	SAS	semi-continuous operation
		Supercritical AntiSolvent with Enhanced Mass transfer	SAS-EM	semi-continuous operation, vibration added to precipitation vessel
		Solution Enhanced Dispersion by Supercritical fluids	SEDS	semi-continuous operation, SC-CO_2 and solvent mixed in a tube-in-tube injector
		Aerosol Solvent Extraction System	ASES	semi-continuous operation
		Precipitation by Compressed Antisolvent	PCA	semi-continuous operation, CO_2 at subcritical conditions
		Supercritical Fluid-drying	SCF-drying	solvent used water and CO_2 modified with polar solvent
Solute	compounds in which SC-CO_2 is soluble	Particles from Gas Saturated Solution	PGSS	semi-continuous operation
		Supercritical Melting Micronization	ScMM	semi-continuous operation
Co-Solute	compounds with almost zero-solubility in SC-CO_2, soluble in a solvent in which SC-CO_2 is soluble	Carbon dioxide Assisted Nebulization-Bubble Drying	CAN-BD	low volume mixer for SC-CO_2solution
		Depressurization of an Expanded Liquid Organic Solution	DELOS	compressed CO_2 used to homogenous cooling of the solution with solid particle precipitation
		Supercritical Assisted Atomization	SAA	enhanced solubilization mixing SC-CO_2 solution

2.4.2.1 Rapid Expansion of Supercritical Solutions (RESS)

This process first proposed by Matson *et al.* known as supercritical fluid nucleation (SFN) (Matson *et al.*, 1987). In this process the saturation of the supercritical fluid with a solid substrate; then, the depressurization of the solution through a heated nozzle into a low pressure chamber produces a rapid nucleation of the substrate in form of very small particles that are collected from the gaseous stream (**Figure 2.9**).

The morphology of the resulting solid material, crystalline or amorphous, depends on the chemical structure of the material and on the RESS parameters (temperature, pressure drop, impact distance of the jet against a surface, nozzle geometry, etc.) (Jung and Perrut , 2001). Very fast release of the solute in the gaseous medium played crucial role in production of very small particles. This process is particularly attractive due to the absence of organic solvents.

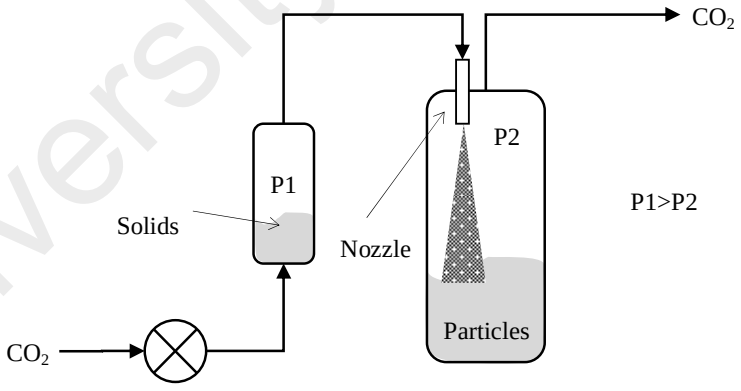

Figure 2.9
A schematic illustration of the Rapid Expansion of Supercritical Solutions (RESS).
(Jung and Perrut, 2001)

2.4.2.2 Supercritical Antisolvent (SAS)

Supercritical anti-solvent precipitation (SAS) has been proposed using various acronyms; but, the process is substantially the same in all the cases. In this process liquid solution contains the solute to be micronized; at the process conditions, the supercritical fluid should be completely miscible with the liquid solvent; whereas, the solute should be insoluble in the SCF. Therefore, contacting the liquid solution with the SCF induces the formation of a solution, producing supersaturation and precipitation of the solute (**Figure 2.10**). The formation of the liquid mixture is very fast due to the enhanced mass transfer rates that characterize supercritical fluids and, as a result, nanoparticles could be produced.

This process has been used by several authors using different process arrangements; however, the most significant differences are related to the way the process operates: in batch or semi-continuous mode (Reverchon, 1999).

In batch operation (GAS: Gas AntiSolvent) the precipitation vessel is loaded with a given quantity of the liquid solution and, then, the supercritical antisolvent is added until the final pressure is obtained. In the semi-continuous operation (SAS), the liquid solution and the supercritical anti-solvent are continuously delivered to the precipitation vessel in co-current or counter-current mode. An important role is also played by the liquid solution injection device (Dehghani and Foster, 2003).

The injector is designed to produce liquid jet break-up and the formation of small droplets to produce a large mass transfer surface between the liquid and the gaseous phase. Several injector configurations have been proposed in the literature and patented (York *et al.*, 1995; Gupta and Chattopadhyay, 2002; Subramaniam *et al.*, 1997).

High pressure vapor-liquid equilibria (VLEs) and mass transfer between the liquid and the SCF also play a relevant role in SAS. Particularly, VLEs of the ternary system solute-solvent-SC antisolvent and the position of the operating point in SAS processing with respect to these VLEs can be decisive for the success of the process. The formation of a single supercritical phase is the key step for the successful production of nanoparticles (Reverchon and Caputo, 2003).

The washing step with pure supercritical antisolvent at the end of the precipitation process is also fundamental to avoid the condensation of the liquid phase that otherwise rains on the precipitate modifying its characteristics. As a rule SC-CO_2 has been used in this process.

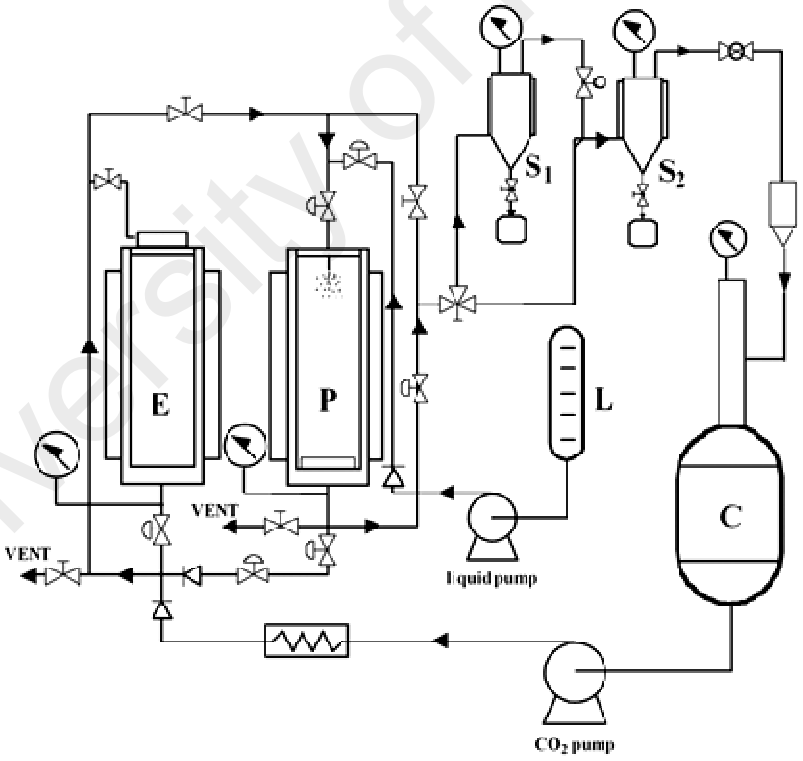

Figure 2.10
Schematic representation of SAS semi-industrial scale apparatus:
C) CO_2 storage vessel; L) liquid solution; E) extraction vessel; P) precipitation vessel; S1, S2) liquid separators

2.4.2.3 Supercritical Assisted Atomization SAA

Supercritical assisted atomization (SAA) is a recent process in which the SCF acts as atomizing medium. The process (**Figure 2.11**) is recently developed process based on the solubilization of supercritical CO_2 in the liquid solution formed by the solvent and the (solid) solute, and on its subsequent atomization using a thin wall nozzle (Reverchon and Spada, 2004).

Polymethylmethacrylate (PMMA) nanoparticles have been producing by SAA, using acetone as solvent. To producing particles with a mean diameter of 120 nm of PMMA feed solution concentration (10 mg/mL) of PMMA in acetone and at a mixing temperature of 80 °C and a mixing pressure of 76 bar.

Process temperatures and the chemical characteristics of the solid solute play important roles on the forming of particles Amorphous or crystalline. Two atomization processes take place in this process (Reverchon and Spada, 2004):

- Primary droplets production at the exit of the nozzle by pneumatic atomization.
- Destroys these droplets by the fast release of CO_2 from the internal of the droplet (decompressive atomization).

The limit of this process is that the smallest particles produced depend on the dimensions of the smallest droplets generated (one droplet-one particle process). These dimensions are connected to the classical parameters that control droplet dimensions during atomization: surface tension, viscosity and quantity of SCF dissolved in the liquid.

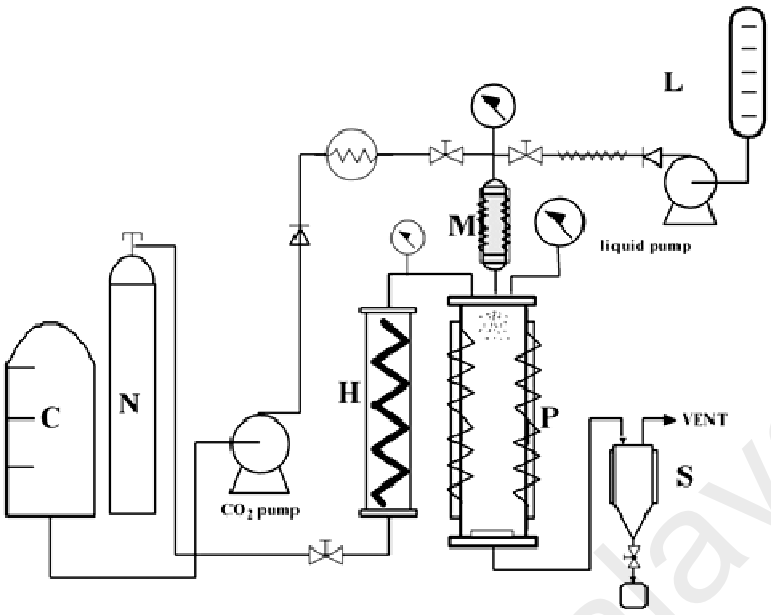

Figure 2.11
Schematic representation of the SAA apparatus:
C) CO_2 cylinder; L) liquid solution; N) N_2 cylinder; H) heat exchanger; M) saturator; P) precipitator; S) condenser.

2.4.2.4 Sol/gel Drying

Using of SCFs is well founded in gels drying since it allows the drying process with zero surface tension, avoiding the gel collapse. In this process, the SCF is only used to recover the produced nanoparticles. Hu *et al.* proposed the preparation of gels in aqueous solution, the replacement of water in the precipitate with a mixture of n-propanol and benzene and, then, the elimination of the organic solution using SC-CO_2 (Hu *et al.*, 1999).

In this case the process was finalized to the production of copper borate nanoparticles. Hu *et al*. proposed the formation of TiO_2 nanoparticles by sol preparation and the replacement of water in the precipitate with n-butanol and subsequent supercritical drying. Particle sizes ranging between 10 and 20 nm and surface areas up to 166.8m^2/g were obtained.

The same research group (Hu *et al*., 2001) also performed the supercritical drying of a beryllium borate aerogel to produce nanoparticles. In this case the replacement of water in the precipitate was obtained with a mixture of n-butanol and ligroin; then, supercritical drying was obtained using CO_2.

In a subsequent work they (Hu *et al*., 2002) used supercritical ethanol as the drying medium to recover magnesium borate nanoparticles. A sort of SC-drying process used to produce nanometric particles has also been patented (Weber, 2000). In this case a liquid colloidal suspension is first formed, and then it is introduced into a supercritical fluid that extracts the liquid solvent.

2.4.2.5 Synthesis in SCFs

Powders producing from gas phases can be occurred by reaction of precursor gases, the products have sharp particle size distribution and non-porous particles (Pratsinis and Vemury, 1996). In analogy with the classical methods, nanoparticles can also be the product of a reaction in which a SCF is used as the reaction medium.

2.4.2.5.1 Hydrothermal synthesis in supercritical water (HTS-SCW)

Hydrothermal synthesis (HTS) is used to produce synthetic materials mimic the natural geothermal processes (Dawson, 1988). The reaction equilibrium of metal salt aqueous solutions changes with temperature and results in the formation of metal hydroxides or metal oxides.

Supercritical water (SCW) provides an excellent reaction medium for hydrothermal synthesis, since it allows changing reaction rate and equilibrium by shifting the dielectric constant and solvent density with pressure and temperature. One of the expected benefits is higher reaction rates and smaller particles. The reaction products have to be not soluble in SCW.

The HTS-SCW process is usually operated as follows: a metal salt aqueous solution is prepared, pressurized and heated. The pressurized metal salt solution and a supercritical water stream are combined in a mixing point, which leads to rapid heating and subsequent reaction. After the solution leaves the reactor, it is rapidly quenched and in-line filters remove larger particles. Cooling water is directly fed to the reactor to quench the reaction.

Two different process modes have been proposed: the first uses a batch reactor and is characterized by a long reaction time; the second uses a flow reactor that assures continuous operation.

2.4.2.5.2 Reduction

Shah *et al*. demonstrated that it is possible to stabilize Ag nanocrystals in SC-CO_2 using appropriate surfactants (alkanethiols). The process, called by the authors arrested growth, consists of the reduction with H_2 in a batch reactor of SC-CO_2 soluble organo-metallic precursors in the presence of a stabilizing perfluoro-octanediol ligand that binds to the surface of metal nanoparticles and arrests particle growth. The key characteristics of this process are: (a) precursors soluble in SC-CO_2 (b) polar products not soluble in SC-CO_2 (Shah *et al*., 2000). Using the same process, they synthesized

stabilized nanocrystals of Ag In and Pt with diameters ranging between about 2 and 12 nm.

Moreover, analyzing the arrested precipitation of Ag nanocrystals in SC-CO_2, they studied the influence of the process parameters on particles diameter and polydispersity (Shah *et al.*, 2000), concluding that CO_2 density is the major parameter affecting particle size and distribution in this process. At higher solvent densities they obtained crystals of about 2 nm in diameter due to the strong barrier formed by the surfactant; whereas, at lower CO_2 densities, larger Ag crystals of about 4 nm were obtained with higher polydispersity, since particles grew to a larger size before the coverage of surfactant was sufficient to prevent their further coagulation. Precursor concentration, thiol/precursor ratio and reaction time do not appreciably affect the crystals size, though they can affect their polydispersity.

Korgel *et al*. synthesized by arrested precipitation Ag nanoparticles in SC-CO_2 by reduction of silver acetilacetonate in presence of organic ligands that acted as stabilizers of the nanoparticles. Using the same technique silicon nanocrystals ranging between 2 and 20 nm were also synthesized in SC-hexane (Korgel *et al*., 2002).

2.4.2.5.3 Hydrolysis

Ziegler *et al*. synthesized copper oxide (Cu_2O) nanoparticles from copper nitrate by hydrolysis in SCW. They performed the reaction with and without ligands. Cu_2O polydisperse particles with diameters ranging from 10 to 35 nm were obtained by hydrolysis when they did not use alkanethiol ligands; when 1-hexanethiolwas added in the reactor, Cu nanocrystals of about 7 nm in diameter were obtained (Ziegler *et al*., 2001). The alkanethiol ligand stabilized the synthesis of nanocrystals and controlled

their oxidation by reduction to Cu nanoparticles. Ligands that bind on the nanoparticles surface can block the growth of nanoparticles, with a stabilization process analogous to the arrested growth discussed in the reduction process (Shah *et al.*, 2000). The authors also studied different precursors, obtaining particles with different morphologies.

2.4.2.5.4 Thermal decomposition

The thermal decomposition of a precursor is a classical process used to induce high supersaturations in a fluid phase which leads to the nucleation of nanoparticles. A classical thermal decomposition process is the spray pyrolisis. The precursor material is atomized and carried by a gas into a high temperature zone, the solvent evaporates from the droplets and the porous dried particles obtained sinter to form dense particles.

The use of the same process in a supercritical medium can lead to higher nucleation rates because of the very high supersaturation of metal atoms. Nucleation generates metal clusters composed by few atoms. These clusters grow by binary contact and coalescence to give nanoparticles. Depending on the main process parameters (pressure, temperature, residence time, metal precursor concentration), these nanoparticles can grow to larger crystalline particles or aggregates to produce nanostructured particles.

Cansell *et al*. proposed the thermal degradation of metallic precursors dissolved in a supercritical fluid (ammonia). They used as precursors Cu and Fe acetylacetonates that show a good solubility in ammonia; then, they increased the temperature of the reactor thus inducing the decomposition of the precursors and the precipitation of the corresponding oxides and nitrites (Cansell *et al*., 1999).

Aggregates of about 50 nm were obtained, for example, in the case of Fe compounds, consisting of very small subunits <10 nm in diameter. The same research group (Desmoulins-Krawiec *et al.*, 2004) subsequently proposed the thermal decomposition process to produce nanostructured particles of several other compounds: Cr, Co, Cu, Ni, Al, Ti and Ga using supercritical ammonia-methanol mixtures.

Holmes *et al.* prepared organic-passivated Si nanocrystals by thermally degrading diphenylsilane in mixtures of supercritical octanol and hexane (Holmes *et al*., 2001). The nanocrystals were relatively monodisperse and sterically stabilized. The smallest nanocrystals exhibited also a discrete optical transition, characteristic of quantum confinement effects for crystalline nanocrystals with a narrow size distribution (Holmes *et al*., 2001).

2.4.2.5.5 Dispersion polymerisation

Dispersion polymerisation in SC-CO_2 is a process that has been used by various authors to produce microparticles of polymers (DeSimone, 1994). A stable dispersion in SC-CO_2 is produced using a co-polymer with CO_2-phobic and CO_2-philic groups and each cell of the dispersion acts as a nanoreactor in which the polymerisation takes place.

Lee *et al*. used dispersion polymerization in presence of a triblock copolymer stabilizer (surfactant) in SC-CO_2 to produce aromatic polycarbonate (PC) nanoparticles (Lee *et al*., 2002). Spherical particles ranging between 30 and 140 nm were obtained depending on the process conditions.

2.4.2.5.6 Reverse micelles

Water-in-oil (w/o) microemulsions are thermodynamically stable aggregates formed by a nanometric sized water core in an apolar continuous phase. They are generated by amphiphilic surfactants with a hydrophilic head group surrounding the water core and a hydrophobic tail that extends into the apolar continuous phase (Johnston, 1999). The oil-surfactant interactions form a large variety of structures to avoid the direct water/oil contact.

Micelles are the simplest structure: they are spherical or cylindrical objects formed by surfactant molecules separating oil and water. Drops of oil in water are called micelles, reverse micelles are drops of water in oil. Reverse micelles are widely used as nanoreactors to synthesize organic and inorganic nanoparticles.

A reactant is, as a rule, contained in the aqueous core and the other in the continuous organic phase. As the reaction is confined in the water core, whose dimensions are controlled by thermodynamic conditions, the diameter of the produced nanoparticles can be controlled by the core size.

Traditional recovery methods have a relevant effect on the increase of particle size and particle size distribution, due to aggregation phenomena. A large amount of the surfactant remains on the nanoparticles.

Supercritical CO_2 has a large affinity with many organic solvents; therefore, it can be used in the recovery step as an antisolvent, or solvent-catcher, to extract all the liquid solvent (and most of surfactant) producing dry non-coalescing nanoparticles in a single process step.

Using selected surfactants that can stabilize water droplets in near critical or supercritical CO_2, an elegant process, is also possible in which water-in-CO_2 (w/c) microemulsions are formed. In this case no organic solvents are required for the continuous phase and particles collection can be performed by simple decompression.

2.4.3. Cryogenic Technology

2.4.3.1 Freeze dryer

Freeze-drying or "lyophilization" is a drying process where the solvent, is first frozen and then removed by sublimation under low pressure, typically in the range of 6.6 Pa to 66 Pa (Pikal, 2003).

The process consists of three main stages: freezing, primary drying and secondary drying (**Figure 2.12**). After complete solidification in the first stage, the shelf temperature is then slightly increased to supply heat for the sublimation of ice. The secondary drying phase includes removal of water from the solute phase by desorption usually at temperatures above room temperature (Oetjen, 1999).

The freeze-drying process shows several advantages over other drying techniques:-

(1) Chemical decomposition is minimized due to the low drying temperatures. This improves the stability of heat sensitive drugs (e.g. biological substances).

(2) Fast and complete dissolution of the dried product is maintained by the very high specific surface area of the product.

(3) The freeze-drying process allows better sterile operations compared with dry powder filling. Sterile filtration of solutions can take place immediately before filling of vials (Nail *et al*., 1993).

(4) Lyophilization results in a better long-term stability of protein drugs.

(5) Freeze-dried formulations provide easy handling (shipping and storage) (Nail and Gatlin, 1993).

Technically freeze dryer is commonly constructed with two main parts (Pikal, 2002): a "drying" chamber holding temperature controlled shelves is connected by a valve to a

"condenser" chamber, which contains coils capable to achieve very low temperatures between -50°C and -80°C (Christ, 2003).

One or more vacuum pumps in series are connected to the condenser to obtain very low pressures in the entire system. With this, the sublimed water of the primary drying stage is reconverted to ice by the condenser and thus removed from the system. However, the multitude of variables inherent in a large batch of individual vials in a complex chamber setup makes process control difficult (Rambhatla *et al*., 2003).

Understanding of the product, the thermodynamic behavior of formulations and principles of the different drying stages are of fundamental importance to avoid product damage.

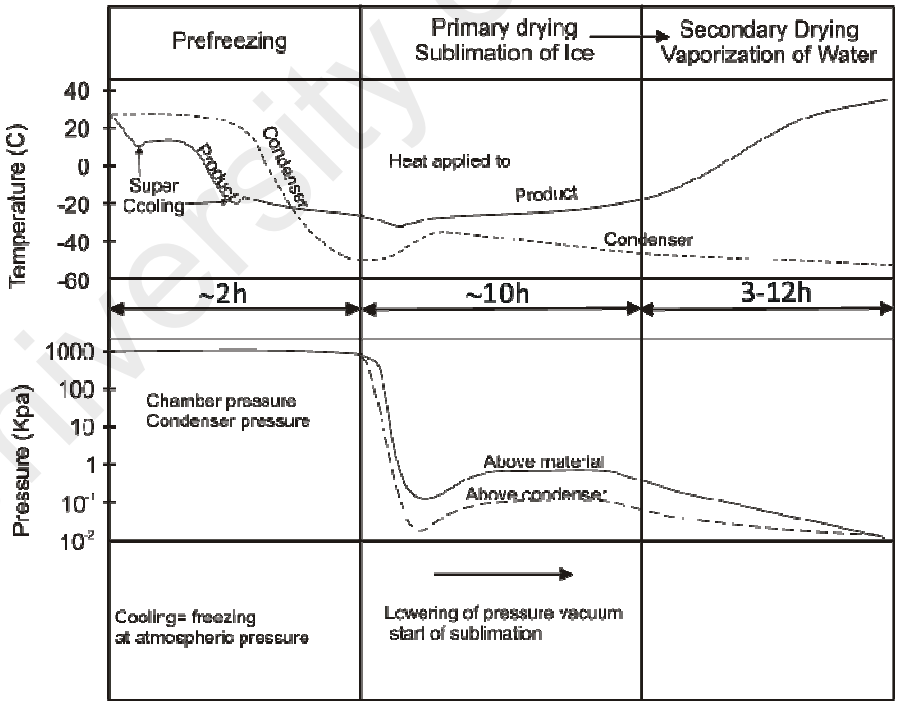

Figure 2.12
Freeze dryer stages.
(Oetjen, 1999).

2.4.3.1.1 Freezing

Freezing step is to convert liquids or viscous solutions into solids so that the sublimation of solvent could be started. Ice formation is initiated by homogeneous or heterogeneous nucleation after a certain degree of supercooling of the solution (MacKenzie, 1976). Heterogeneous nucleation is caused by suspended impurities or by the walls of the container. Spontaneous ordering of solvent molecules leads to homogeneous nucleation.

Usually, nucleation in water base solutions for freeze drying is heterogeneous, since homogeneous nucleation of pure water takes place only at very low temperatures (about -40°C) (Nail and Gatlin,1993). The freezing process has a deep impact on APIs aggregation, primary drying and secondary drying rates, extent of product crystallinity, and surface area of the freeze-dried product (Searles *et al*., 2001).

In general, a fast freezing rate leads to small ice crystals (Willemer, 1992; Wisniewski, 1998). This is because water is super-cooled and crystallization occurs rapidly, generating small ice crystals (House and Mariner, 1996). In contrast, a slow cooling rate produces large ice crystals. The pore size created after subsequent drying depends on the former size of the ice crystals.

Large ice crystals produce large pores, causing rapid water sublimation during primary drying. Unfortunately, the secondary drying rate may decrease, owing to smaller surface areas which limit water desorption during the secondary drying step (Bindschaedler, 1999). Therefore, ice crystal morphology and size distribution play an important role in the freezing step, influencing several critical parameters.

During freezing most of the water is transferred to ice, and the solutes are either converted to crystalline or amorphous solids below their eutectic temperature, Te, or their glass transition temperature on maximal freeze concentration, Tg'. Following the time scale of freezing of a solution (**Figure 2.13**), a sudden increase in temperature indicates the crystallization of ice (Tf), owing to the release of energy.

Further cooling causes more liquid water to convert into ice and all interstitial fluids in the vicinity concentrate ultimately until they (1) crystallize or (2) the viscosity of the system is so high to transform into a solid amorphous system (Nail and Gatlin, 1993).

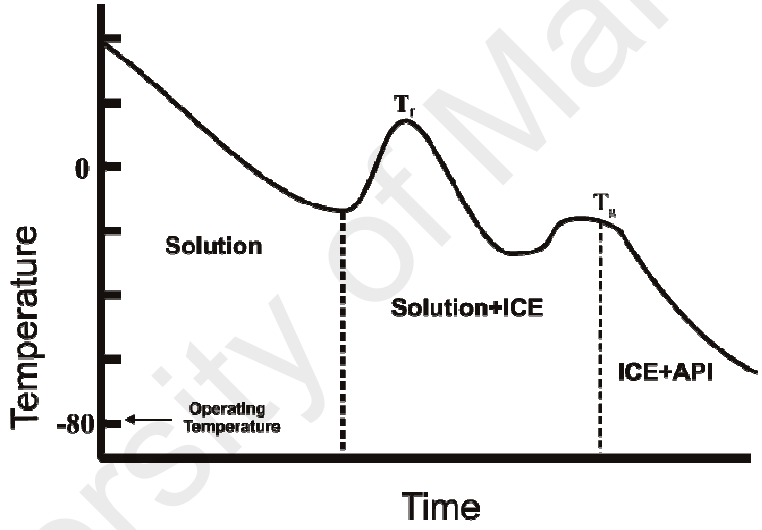

Figure 2.13.
Temperature vs. time for freezing of sodium chloride/water.
(Nail and Gatlin, 1993)

Proteins and other excipient do not crystallize during the freezing step, but are converted from highly viscous syrup to a rigid amorphous solid ("glass") which contains about 10-30% water (Hatley *et al*., 1996). The temperature of this reversible transition for the maximally freeze-concentrated solution is termed glass transition temperature, Tg'.

A solid amorphous system during freezing is generated by reducing the temperature below Tg' (Franks, 1998). Prior to drying crystallizing solutes, the product temperature must be lowered below Te of the system to carry out complete freezing.

When the temperature of an aqueous protein formulation is further lowered after crystallization of the least soluble excipient, this excipient (as shown in **table 2.6.**) and water crystallize out at the same time as a mixture (Christ, 2003). Because of component interaction(s), many multicomponent protein formulations do not show a clear Te (Hatley *et al*., 1996). The relationship between Te and Tg' is shown in **Figure 2.13.** (Wang, 2000).

Franks illustrated the freezing behavior of a sucrose-water system (**Figure 2.14**). Here, the solute phase has been concentrated from an initial solid content of 5% to about 80%, which delineates that most of desiccation in the freeze-drying process occurs during freezing, but still a high fraction of unfrozen water exists (Hatley, 1996; Franks, 1998).

Table 2.6
Examples of commonly used excipients in freeze-drying of pharmaceutical products. (Abdelwahed *et al*., 2006)

Type	Function	Substance
Bulking agents	Provide bulk to the formulation specially when the concentration of product to freeze dry is very low	Hydroxyethyl starch, trehalose, mannitol, lactose, and glycine
Buffers	Adjust pH changes during freezing.	Phosphate, tris HCl, citrate, and histidine.
Stabilizers	Protect the product during freeze-drying against the freezing and the drying stresses.	Sucrose, lactose, glucose, trehalose, glycerol, mannitol, sorbitol, glycine, alanine, lysine, polyethylene glycol, dextran, and PVP.
Tonicity adjusters	Yield an isotonic solution and control osmotic pressure.	Mannitol, sucrose, glycine, glycerol, and sodium chloride.
Collapse temperature modifiers	Increase collapse temperature of the product to get higher drying temperatures.	Dextran, hydroxypropyl-β-cyclodextrin, PEG, poly (vinyl pyrrolidone).

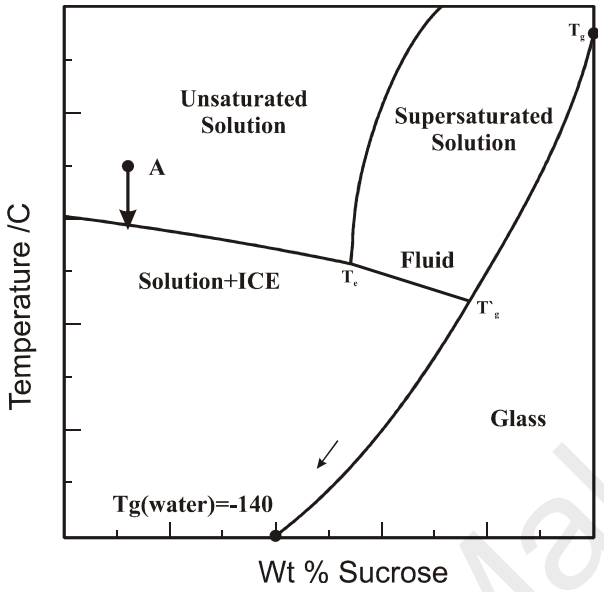

Figure 2.14
Solid-liquid state diagram for the sucrose-water system (Franks, 1998; MacKenzie, 1976).

The sucrose system does not precipitate as a crystal phase when the solution is cooled to the eutectic point, but remains in a thermodynamically unstable supersaturated solution. Beneath Tg´ the system behaves like a solid, which is also indicated by a sharp decrease in electrical resistance of the frozen system (Pikal *et al*., 1990).

2.4.3.1.2 Primary drying

Primary drying starts with the reduction of the chamber pressure and the shelf temperature is raised to supply the heat removed by ice sublimation. The chamber pressure (P_c) is well below the vapour pressure of ice, and ice is transferred from the product to the condenser by sublimation and crystallization onto the cold plates in the condenser (Tang and Pikal, 2004). P_c impacts on both heat and mass transfer in primary drying.

Process control is related to control of the product temperature vs. time profile during this section without exceeding the maximum allowable temperature during drying, which is determined either by the T_{eut} or T_c of the product (Nail and Gatlin, 1993).

To maintain a constant product temperature, about 2720 J of heat per gram of ice must be supplied from a shelf to the product. A given product temperature results from a balance between heat transfer rate to the product and the drying rate or mass transfer of water vapour and thus the primary drying phase is a problem in coupled heat and mass transfer (Pikal, 2003).

2.4.3.1.3 Secondary drying

During secondary drying water is desorbed from the cake produced by primary drying. Some secondary drying takes place during primary drying as ice is removed from a region. However, the main part of secondary drying is performed after primary drying is over and the product temperature has been elevated (Tang and Pikal, 2004).

The product temperature is commonly raised to about 25°C-35°C. Protein denaturation in the relatively dry solid state is thought not to be a problem until temperatures reach 100°C (Christ, 2003). To prevent collapse, the product temperature must not be increased before all of the ice (and some unfrozen water) has been removed. Drying is executed rapidly during the initial part of secondary drying caused by the high water content, but slows greatly as drying continues (Pikal, 1994).

It is advantageous to run a high shelf temperature for a short period rather than a low temperature for a long time (Pikal *et al*., 1990). The reason is that the water desorption

rate decelerates dramatically with time at a defined temperature, and times longer than 3-6 h at a given temperature reduce the moisture content only marginally (Tang and Pikal 2004).

The shelf temperature is increased during secondary drying. In addition, chamber pressure is decreased to the lowest achievable level. This practice is based on the idea that the product can withstand higher heat input because ice is no longer present in the formulation and there is no concern about cake collapse. Furthermore, the water left during secondary drying is more strongly bound, resulting in more energy for its removal (Nail and Gatlin, 1993).

The chamber pressure for secondary drying was found, however, to have no measurable influence on drying rate provided that the vapor pressure of the product at the given product temperature is higher than the vapor pressure of the chamber (Oetjen, 1999). Therefore, chamber pressure adjustment (to higher pressures) during secondary drying should lead to better heat transfer and faster drying.

Secondary drying is the removal of unfrozen water. The water is either bound at the surface of the crystals in a crystalline product or embedded in the highly viscous amorphous matrix (Oetjen, 1999). Therefore, the amount of residual water to be removed during secondary drying is influenced by the freezing behaviour of the solutes.

For a crystalline solute, essentially all of the water is present either as eutectic ice or pre-eutectic ice. The only water left after complete sublimation of ice is water adsorbed to the surface of the solute crystals, unless water of hydration is present within the

matrix. As a result, the product is essentially dried after the primary drying step and secondary drying takes only a short time.

In contrast, an amorphous solute is existant in a glassy matrix containing perhaps as much as 40% water. The process of drying takes place by molecular diffusion, because there are few, if any, open channels for vapor transfer from the interior of the glass phase to the product surface. Because of the large amount of water to be removed and the slow mechanism of vapor transfer, secondary drying can highly affect the overall drying time (Nail and Gatlin, 1993).

The secondary drying conditions are also influenced by the solute concentration. At higher solute concentration, the dry product shows a smaller specific area. This leads to slower reduction of the adsorbed water; thus longer times and/or higher temperatures are needed to finish secondary drying (Tang and Pikal, 2004).

To prevent loss of product quality, the product temperature should be kept below its glass transition temperature during secondary drying. Normally, this is not a problem because drying sharply increases the glass transition temperature, retaining the product in a glassy state.

Secondary drying is carried out until target moisture content is reached. The optimum moisture content is evaluated by stability studies. Over drying and therefore damage of proteins must be prevented (Pikal, 1994). The main target of secondary drying is to minimize the residual moisture content to a level optimal for stability, which is usually less than 1% (Tang and Pikal, 2004).

2.4.3.2 Atmospheric spray-freeze-drying

Micronized powders can be generated with the atmospheric spray-freeze-drying technique. In general, the liquid feed is an aqueous or cosolvent solution or suspension containing an Active Pharmaceutical Ingredient (API) and various pharmaceutical excipients.

The possibility of freeze-drying at atmospheric pressure was first suggested by Meryman. The partial pressure of water vapor, rather than the total pressure in the drying chamber, determines the water mass transfer. Meryman proposed convective freeze-drying with a circulated cold and dry air stream (Meryman, 1959). Freeze drying at a reduced particle size was also shown to be comparable to vacuum freeze-drying (Woodward, 1963; Heldman and Hohner , 1974).

The principle of this technology is as follows: the liquid feed is sprayed into a fluidized bed containing dry ice and dry air or alternatively only predried cryogenic air (Rogers, 2001). **Figure 2.15** shows the spray-freeze-drying apparatus described by Leuenberger.

A two-fluid nozzle with heating facilities nebulizes the solutions or dispersions into the stream of cryogenic air (-60°C; top spray) (Leuenberger, 2002). As a result, frozen droplets are formed. The cryogenic air stream then sublimes the frozen solvent(s). A filter maintains the fine product within the drying chamber. The water vapor is driven to the cooling system where it condenses on the refrigerated surfaces. To lower the relative humidity and to deliver sufficient energy for sublimation, the cryogenic air passes through a heater.

The resulting drying air temperature must, however, be kept below the eutectic temperature, Te, or the glass transition temperature, Tg, of the frozen product. Further sublimation takes place when the recycled air reenters the drying chamber.

This SFD-device contains two cooling systems working alternately: while one is cooling, the other is de-icing. A bypass connecting tube makes it possible to open the drying chamber without effecting the drying air's temperature or humidity. To protect sensitive drug formulations from oxidation, nitrogen as an inert drying medium can be used.

Aggregation of the individual particles of the frozen powder during the drying step is prevented by the bed fluidization. The particle agitation also increases the sublimation rate, giving drying times that are below those required for standard lyophilization. Thus, the drying process was actually accomplished at the surface of the filter system via a thin powder layer in a matter of hours (Malecki *et al*., 1970).

In fluidization processes with an unprotected solid wall, contamination of particles on the wall is unavoidable. In most powder fabrication processes, collection efficiency is a concern. Unprotected walls may cause large losses, which are undesirable when producing pharmaceutical agents.

Furthermore, for inhalational lung drug delivery, the powder should typically have a mass median aerodynamic diameter smaller than 5 μm. Particles at such a small size are normally very cohesive and are thus difficult to convey using a simple fluidization method after deposition.

Geldart classified powders into four types according to their fluidization behaviors and particle properties (Geldart, 1973). Group A (aeratable), Group B (bubbly ready or sand-like) and Group D (spoutable) all have good flowability and can be fluidized on their own without fluidization aids. Group C powders, however, are cohesive and channel consistently during fluidization.

Therefore a uniform gas–solid suspension is difficult to achieve without fluidization aids such as the addition of coarse particles (excipients) or external forces. Vibration fluidized beds have been successfully used in small scale application for fabricating composite materials, but apparently give rise to manufacturing concerns in the scale-up design since such an application in large scale has not been reported in the literature to the uthors' knowledge.

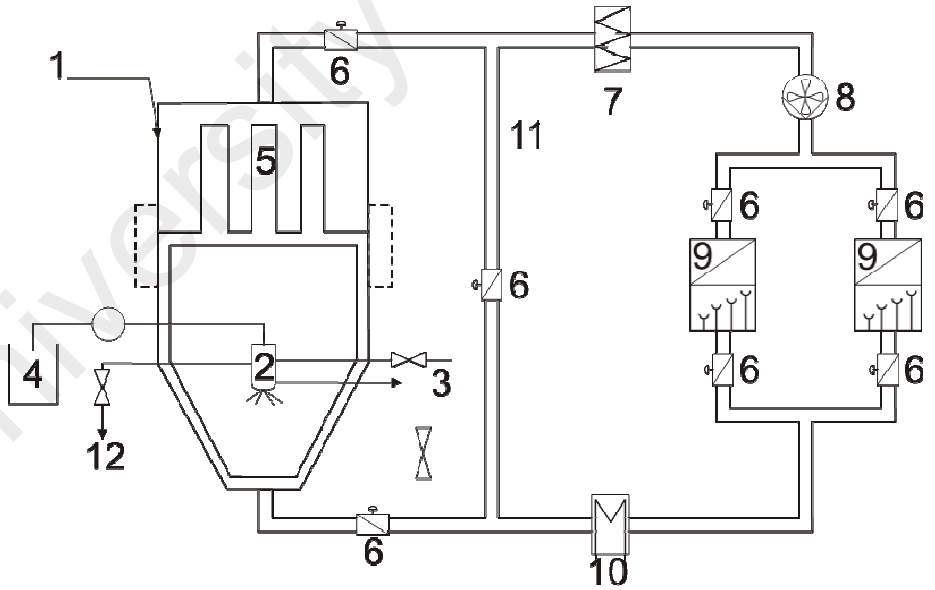

Figure 2.15
Schematic diagram of atmospheric spray-freeze-drying apparatus [Leuenberger, 2002]. (1) Spray tower, (2) Spray nozzle, (3) Nozzle heating device, (4) Liquid feed, (5) Filter system, (6) Flap, (7) Airfilter, (8) Fan, (9) Refrigerator and condensers, (10) Heating system, (11) Bypass pipe, (12) Compressed air for spray nozzle.

2.4.3.3 Spray freezing into vapor over liquid (SFV/L)

Briggs and Maxwell invented the first process of spray freezing onto cryogenic fluid. The patent dates back to 1973, wherein the authors described a process of blending a solid biological product with sugars (Briggs and Maxwell, 1973; Briggs and Maxwell, 1975; Briggs and Maxwell, 1976).

The API and the carrier (mannitol, maltose, lactose, inositol or dextran) were dissolved in water and atomized above the surface of a boiling agitated fluorocarbon refrigerant. To enhance the dispersion of the aqueous solution a sonication probe was placed in the stirred refrigerant.

Solid particles were sieved and lyophilized. Freon 12 (dichlorodifluoromethane) was found suitable for this purpose because its boiling point (Tb = -30 °C) is sufficiently low to cause instantaneous freezing, but not enough low to form an extensive "vapor barrier" around the droplets which would hinder fast freezing.

Several APIs were blended in this manner including proteins and enzymes (luciferase, hexokinase, glucose-6-phosphate dehydrogenase (G-6-PDH), lactate dehydrogenase (LDH), pyruvate kinase; luciferin, bovine albumin, morpholinopropane sulfonic acid (MOPS), 2,6-dichlorophenol indophenol (DIP), nicotinamide-adeninine-dinucleotide (NAD) and its reduced derivative (NADH).

In the following two patents, the authors completed the above list of APIs with blood serum, red blood cells, bacitracin, polymyxin B, tetracycline, chlorpromazine, maltase enzyme, testosterone, Vitamin C, cholesterol and gelatin (Briggs and Maxwell, 1973;

Briggs and Maxwell, 1975; Briggs and Maxwell, 1976). Processed materials exhibited high biological activity, high homogeneity and adequate stability.

In 1980, Adams *et al*. patented a method similar to the one of Briggs and Maxwell with the slight difference that they used capillary nozzles to disperse the solution or suspension onto the surface of stirred halocarbon refrigerant (Adams *et al*., 1980; Adams *et al*., 1982) (**Figure 2.16**). Blood plasma particles processed in Freon 12 ranged from 0.84 to 1.68 mm in diameter.

Hebert *et al*. prepared microparticles of controlled release device by spraying the solution containing the pharmaceutical ingredients into cold nitrogen gas (**Figure 2.17**.). Particles were frozen partially in the gaseous phase and collected in the liquid phase at the bottom of the vessel where they solidified completely. In a second vessel liquid nitrogen was evaporated and residual organic solvent was removed by extraction (Hebert *et al*., 1999).

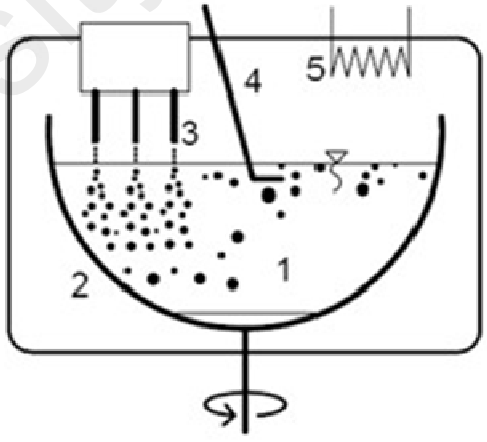

Figure 2.16
Schematic diagram of the apparatus invented by Adams *et al*.
1. Refrigerant; 2. Rotated vessel; 3. Nozzles; 4. Wire screen; 5. Condenser.
(Adams *et al*, 1980).

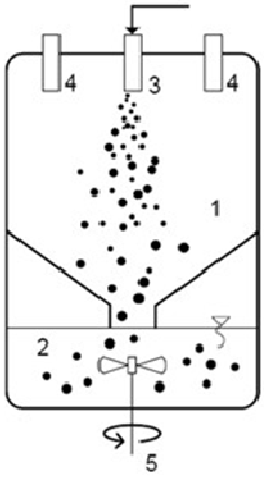

Figure 2.17
Schematic diagram of the apparatus invented by Hebert *et al.*
1. Freezing vessel; 2. Extraction vessel; 3. Nozzle;
4.Liquified gas inlet; 5. Mixing device.

Gombotz *et al.* patented a similar process to prepare microparticles of biodegradable polymers wherein the solution of API is atomized directly into liquid non-solvent or in liquefied gas containing frozen non-solvent at a temperature below the melting point of the solution (Gombotz *et al*., 1990).

The solvent in the microspheres then thaws and is slowly extracted by the non-solvent. However, it can be difficult to find a good solvent, which extracts exclusively the organic solvent, and residual organic traces are hard to remove. Previously, Gombotz *et al*. published another process, which consisted in atomizing the solution or suspension of API into a liquefied gas and lyophilizing the frozen particles (Gombotz *et al*., 1991).

Gombotz *et al.* have described the formulation of zinc insulin, catalase, heparin, hemoglobin, dextran, superoxide dismutase (SOD), horse radish peroxidase (HRP), bovin serum albumin (BSA), glycine and testosterone. Particles ranged from 10 to 90 μm in diameter and kept 70 – 95 % of their initial biological activity. To achieve a mean diameter smaller than 10 μm, which is desirable in the case of injectable controlled drug delivery device, the lyophilized product was suspended in a non-solvent and exposed to

ultrasonic energy. Owing to the porous structure and the great specific surface area of lyophilized products, particles were easy to disintegrate and micronize to the size range of 0.1-10 μm (Gombotz *et al*., 1991).

2.4.3.4 Spray Freezing into Cryogenic Fluids

More intense atomization can be achieved by submerging the nozzle into the cryogenic substance. Due to the liquid-liquid collision, atomization beneath the surface of the cryogen results in smaller droplets which freeze much faster.

In 1969, Harold A. Sauer patented the first method using submerged atomization device. Solution was injected in liquid refrigerant through a heated nozzle at the bottom of the vessel (**Figure 2.18**). At the end of the atomization process, frozen droplets floating on the surface were collected in a spherical screen and dried in cold air or nitrogen gas. Residual moisture was removed under reduced pressure. (Sauer, 1969).

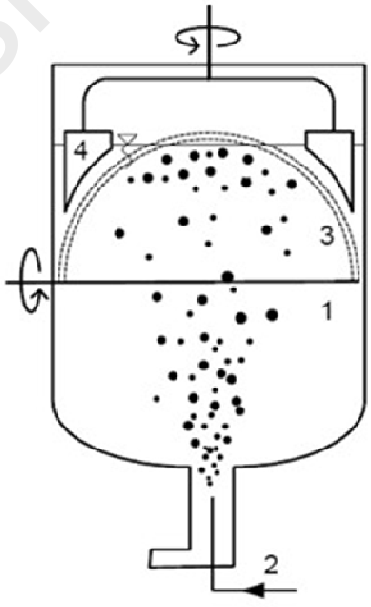

Figure 2.18
Schematic diagram of the apparatus invented by Harold A. Sauer.
1. Freezing and drying vessel; 2. Nozzle;3. Screen hemisphere; 4 .Mixer paddle.
(Sauer, 1969).

The method developed by Dunn involves two immiscible halocarbon refrigerants. The boiling point of the denser refrigerant must be slightly above the melting point of the solvent while that of the lighter one is lower. Solution is dispersed through a heated nozzle in the denser phase from which rising solution droplets step in the lighter refrigerant and solidify (**Figure 2.19**).

Frozen particles floating on the surface of the upper refrigerant are collected and freeze-dried. The authors described the precipitation of aluminum sulphate in various Freon-based cryogenic systems (Dunn *et al.*, 1972).

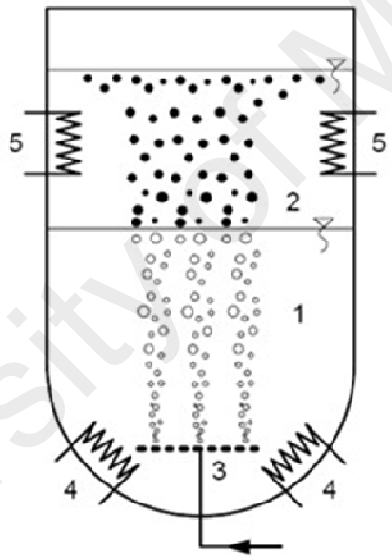

Figure 2.19
Schematic diagram of the apparatus invented by Dunn *et al.*
1. Denser refrigerant (Injection zone);2. Lighter refrigerant (Freezing zone); 3. Atomization device; 4 Heating coil; 5. Cooling coil.
(Dunn *et al.*, 1972).

In a more recent patent Williams *et al*. describe a method called Spray Freezing into Liquid (SFL) which, due to an insulating nozzle, enables injection into extremely cold liquids or liquefied gases without any nozzle blockage (Williams *et al.*, 2002) (**Figure 2.20**).

Unlike the process of Dunn *et al*., in SFL process, atomization and freezing occur simultaneously in the same cryogenic liquid which results in smaller droplet size and faster freezing. Small droplet (particle) size not only increase dissolution rate of processed powders but increase the rate of freezing during the preparation.

Ultra rapid freezing hinders the phase separation and the crystallization of the pharmaceutical ingredients leading to intimately mixed, amorphous drug-carrier solid dispersions and solid solutions.

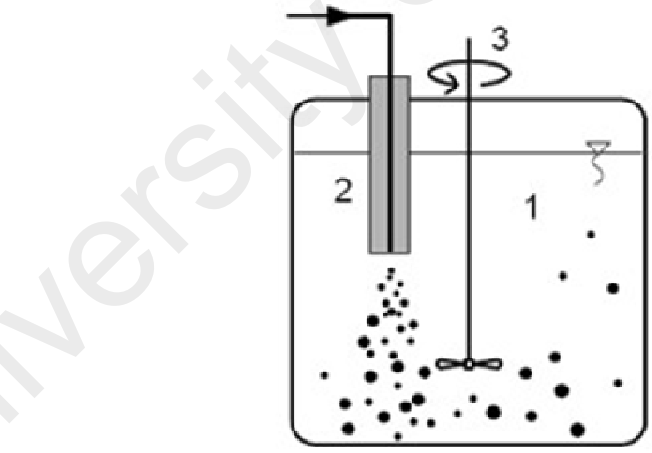

Figure 2.20
Schematic diagram of the apparatus invented by Williams *et al*.
1. Liquified gas; 2. Insulating nozzle; 3. Propeller stirrer.
(Williams *et al*., 2002).

In addition to the small particle size (10 nm – 10 μm) and the glassy state, SFL prepared solid dispersions exhibited several advantageous properties including great specific

surface area (>100 m^2/g), porous structure, improved wettability, low residual solvent content and high biological activity (Rogers *et al*., 2002; Rogers *et al*., 2003; Yu *et al*., 2004; Hu *et al*., 2003).

2.4.3.5 Ultra Rapid freezing (URF)

URF was recently developed as a particle engineering technology designed to enhance the dissolution rates and bioavailability of poorly water-soluble APIs (Evans *et al*., 2006).

Briefly, the process involves freezing an API contained in a polymer solution onto the surface of a cryogenic substrate with a thermal conductivity k between 10 and 20 W/ (m K), collecting the frozen particles and removing the solvent.

Because of rapid conductive heat transfer, resulting in high supersaturation and nucleation rates, the URF technology has the potential to create powders with superior physico-chemical properties, similar to those produced by other rapid freezing technologies. As in other freezing technologies, the rapid freezing of the API/polymer composition is critical in preventing phase separation during freezing, allowing for the active to be molecularly dispersed with the polymer. Recrystallization of the active is avoided by the inclusion of high glass-transition temperature (T_g) polymers such as polyvinylpyrrolidone (PVP) or hypromellose (HPMC). Additionally, URF process is continuous, allowing for improved scale-up applications. A reservoir of boiling cryogenic liquid is not required, allowing for lower operating costs and more convenient operation.

Numerous citations report solvent/ drug/ excipient compositions being frozen in liquid or gaseous nitrogen or other cryogenic fluids. All of these approaches face the same challenge in transferring the heat necessary to cool and freeze the solution forming the drug particle domains. The heat transfer is forced to pass through a gas film at the surface of the particle. This imparts a rate-limiting step in the heat transfer and defines the maximum freeze rate (Hall *et al*., 1969). URF technology overcomes the limitation of transferring heat through a gas film by eliminating the gas interface element and using direct contact with the cryogenic substrate (Gottfried *et al*., 1966).

Drug solutions that come into direct contact with a boiling liquid cryogenic substrate transfer heat through a gas bubble film until the temperature of the particle comes into thermal equilibrium with the liquid at its boiling point (Gottfried *et al*., 1966). Note that conduction is improved by using a cryogenic material with a high thermal conductivity, density, and mass relative to the solution being frozen so as to maintain the surface temperature and heat transfer rate while the solution is being frozen. With URF technology, the thickness of the freezing solution may be controlled to fix its minimum freezing rate since the freezing rate drives the particle formation and determines the freezing solution's characteristics and, hence, drug particle formation.

2.5. CHAPTER SUMMARY

Several useful micronization techniques to produce nano-particles by generate dry powders comprised of either API alone or API in combination with pharmaceutical excipients (bulking agents, stability and absorption enhancers, etc.) were discussed.

Recently, nano-particle research directed to pharmaceutical applications has resulted in many effective delivery systems which have improved the absorption and bioavailability of many poorly water soluble APIs. The in vitro properties inherent to nanoparticles are becoming more fully understood through the development of more accurate analytical techniques and equipment such as the TEM and AFM. At the same time, new particle engineering technologies are being developed to control the physicochemical properties of nanoparticles to develop systems with superior in vitro properties.

These technologies include those designed to reduce the particle size of existing particles such as milling, as well as technologies designed to nucleate and stabilize nanoparticles.

Significant research in formation and delivery of nanoparticles has been accomplished particularly in the areas of enhancing the properties of poorly water soluble APIs. This includes the effect of size on dissolution rate enhancement as well as addition of surface modifiers for dissolution enhancement, stabilization, and drug targeting. Only now are researchers beginning to understand how these nanoparticles, with their enhanced physico-chemical properties in combination with human physiology, are able to enhance absorption and bioavailability of these particles.

3.0 METHODOLOGY

3.1. MATERIALS USED

In this work, two APIs, namely Isoniazid and Griseofulvin, are chosen with Polyvinylpyrrolidone as polymer and Sodium dodecyl sulphate (SDS) as surfactant.

3.1.1. Isoniazid (INH):

INH (99% purity), iso-nicotinic acid hydrazide, abbreviate (INH) is efficient in the treatment of pulmonary tuberculosis on the other hand, possible poisoning accidents, leading to death, have sometimes happened due to over dosage with INH (Russell, 2001).

Therefore, the assay of INH level in human body fluids is vital for clinical purposes and the relatively small concentration difference between effectively therapeutic and toxic dosages makes it very necessary to develop new drug delivery method to reduce effective therapeutic dosage. At present, the accepted treatment of tuberculosis is achieved by drugs involving a combination of isoniazid, pyrazinamide, ethambutal, rifampicin, etc.

There are three main properties of antituberculosis drugs: bactericidal activity, sterilizing activity and the ability to prevent resistance. The essential antituberculosis drugs possess these properties to different extents. Isoniazid (INH) and rifampicin are the most powerful bactericidal drugs active against all populations of TB bacilli (O'Hara and Hickey, 2000).

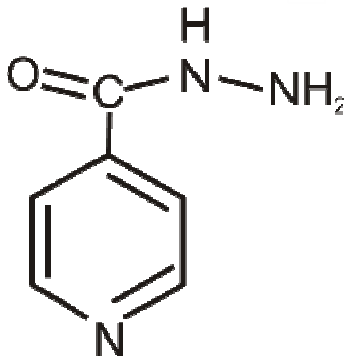

Figure 3.1
Structure of isoniazid.

INH molecule can form complexes through its nitrogens and oxygen as a ligand (see **Figure 3.1**). The NH_2 group hydrogens behave as donors and nitrogen and oxygen behave as acceptors.

3.1.2. Polyvinylpyrrolidone (PVP):

PVP K16-K18 is a water-soluble non-ionic synthetic polymer. Improved stability and dissolution properties of hydrophobic drugs prepared with PVP have been proven for several kinds of drugs (Gohel and Patel, 2003). It is an amphiphilic large molecular weight compound containing highly polar amide groups in conjunction with a polar methylene and methane (CH) moieties (see **Figure 3.2**). The molecule exists as a loose random coil in solution and is soluble in a wide range of organic solvents. It is now classically used in a pharmaceutical context as a binder, although more novel formulations include the polymer as a taste masking additive, controlled release excipient and transdermal penetration enhancer.

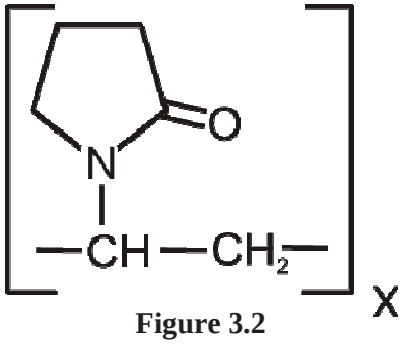

Figure 3.2
Structure of Polyvinylpyrrolidone (PVP)

3.1.3. Sodium dodecyl sulphate (SDS):

SDS has been used as an emulsifying agent in pharmaceutical formulations (See **Figure 3.3**). Because of intrinsic toxicity problems, SDS is often used in combination with other excipients to obtain enhanced solubility and dispersion stability of drug particles.

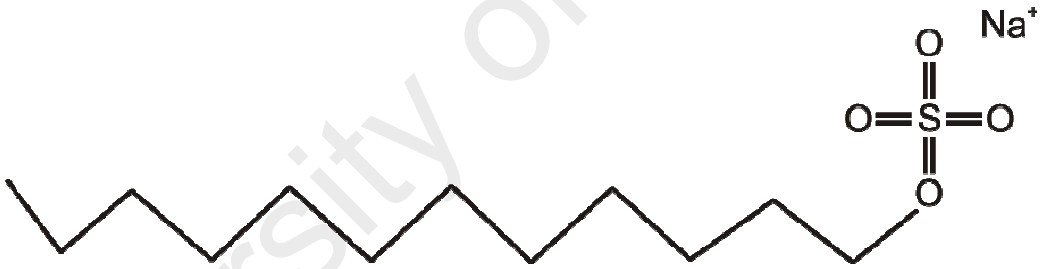

Figure 3.3
Structure of Sodium dodecyl sulphate (SDS)

3.1.4. Griseofulvin (GF):

GF (99% purity) is an antibiotic and antifungal drug used in an oral dosage form. GF is one of the antifungal drugs with systemic effect; it has been used since 1958. Perhaps, this drug has appeared so frequently in the literature of pharmaceutical sciences owing to its incomplete and erratic absorption after oral administration of conventional or micronized forms. The slow dissolution rate is the dominating factor in producing irregular and incomplete absorption of this drug.

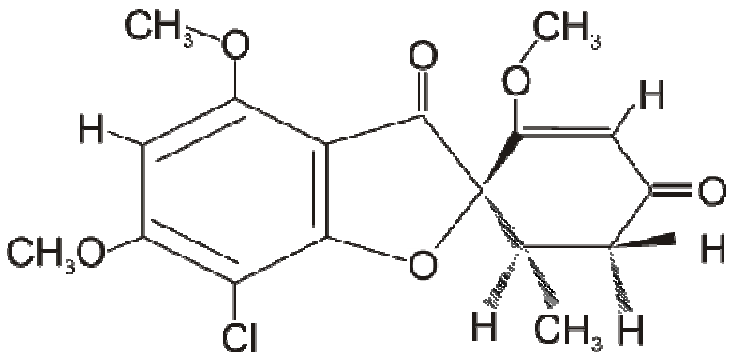

Figure 3.4
Structure of Griseofulvin (GF)

Griseofulvin (**Figure 3.4**) contains 6 proton-accepting oxygen atoms, comprising 2 keto groups and 4 ether groups. Since these groups are capable of forming hydrogen bonds with the proton-donating groups, such as the hydroxyl groups of phenols (Higuchi *et al.*, 1969) and the carboxyl group of fatty acids (Grant and Abougela, 1982), the solubility behaviour of griseofulvin in these solvents is much higher than in hydrocarbon solvents, on account of the specific solute-solvent interactions, and is more difficult to predict.

Besides that, High Performance Liquid Chromatography (HPLC) grade acetonitrile (ACN) and methanol were purchased from Fisher Scientific USA, as solvent to dissolve GF and INH, respectively.

3.2. EXPERIMENTAL SETUP

3.2.1. URF apparatus:

Figure3.5.A. shows a schematic diagram of cryogenic surface setup. Mainly, it consists of liquid Nitrogen storage connected by isolated tube stainless steel (type 304) to cryogenic surface. Cryogenic surface built from vessel covered with stainless steel cover thermal conductivity of the stainless steel is 16 W/m K.

Outlet tube directed to the cryogenic surface to decrease time consuming for reaching specific temperature and reduce liquid (N_2) emission. When liquid (N_2) drop forming on cryogenic surface start manually measuring the temperature with water proof thermometer include K type thermocouple probe and slightly reduce outlet valve to prevent release (N_2) in liquid form and let the gas release.

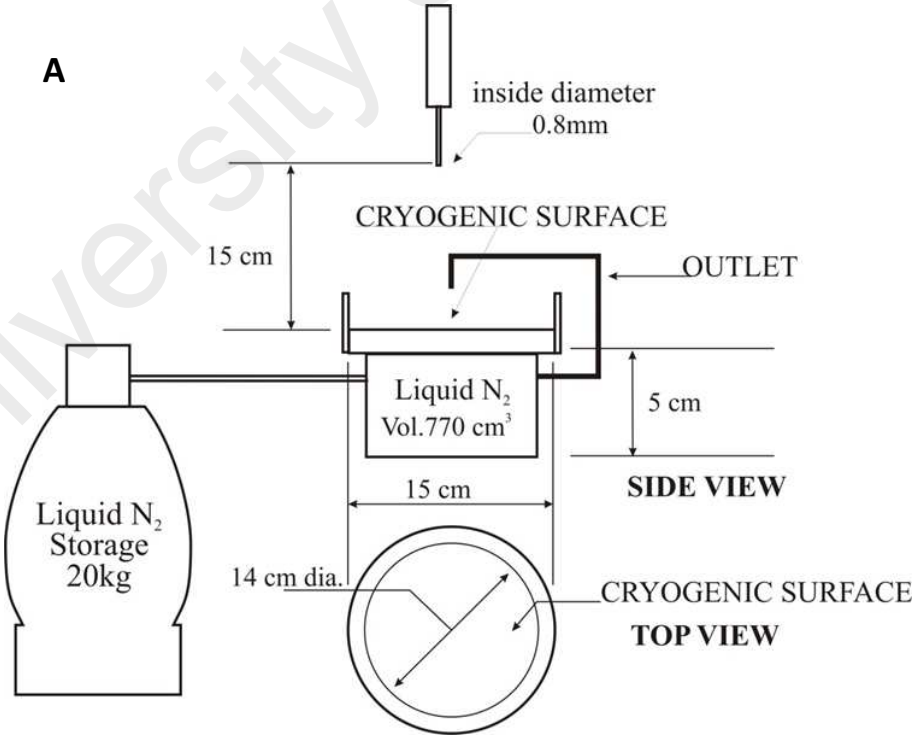

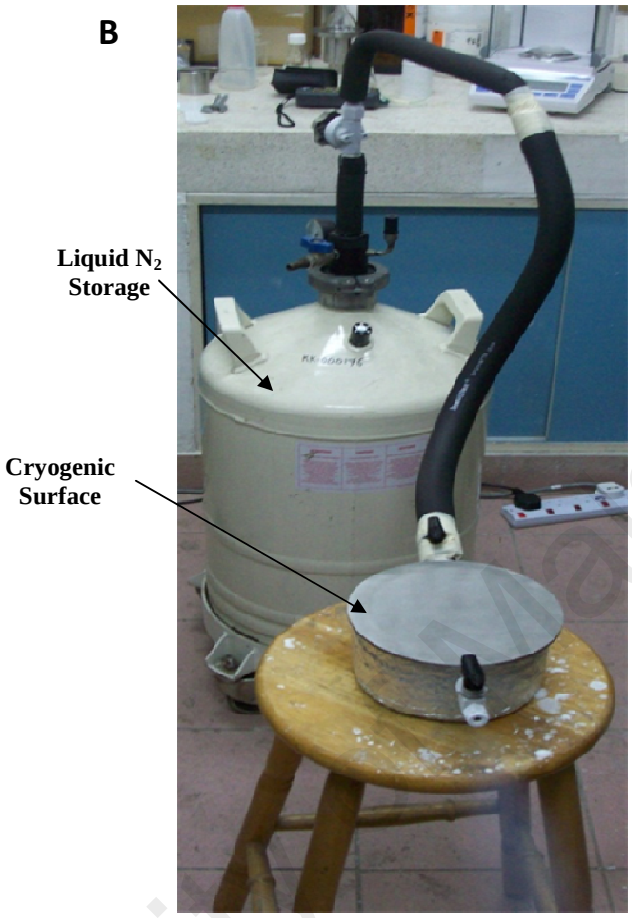

Figure 3.5
A. Schematic of experimental setup for cryogenic surface.
B. Photograph of experimental setup for cryogenic surface.

3.2.2. Experimental planning:

In order to produce nano-particle, INH with varies composition with polymer were tested. This further elaborated in section 3.2.2.1 is to overcome the dissolution rate of GF, different composition of GF with polymer and surfactant were used (see Section 3.2.2.2.)

3.2.2.1. Production of nanoparticles for INH

The URF compositions investigated in this study are described in **Table 3.1.** The compositions were prepared by dissolving API and PVP K16-K18 into an appropriate volume of water. The ratio of the URF compositions were chosen as recommended in the literature values (Rogers et al., 2002; Rogers et al., 2003; Yu et al., 2004; Hu et al., 2003).

Table 3.1
Summary of URF Formulations*

Formulation	Composition	Ratio
URF A	API* : PVP	3:1
URF B	API : PVP	2:1
URF C	API : PVP	1:1
URF D	API : PVP	1:2
URF E	API	100%
FD E	API	100%
FD A	API : PVP	3:1
FD B	API : PVP	2:1
FD C	API : PVP	1:1
FD D	API : PVP	1:2

*URF indicates ultra-rapid freezing, FD indicates freeze dryer.
*API refers to active pharmaceuticals ingredient (isoniazid and griseofulvin).

The feed solutions were applied on a cryogenic surface by using pipette, where the injected mixture with predetermined composition, frozen rapidly on the cryogenic surface. The surface temperature range was -90°C to -80°C. The freezing droplet was collected by filling freeze dryer container with liquid (N_2) to prevent defrost, weighted and lyophilized using freeze dryer (FDU-2100, EYELA) (see **Figure 3.6 and Figure 3.7**) at -80°C to remove the solvent. Micronized powders were stored at room temperature for characterization.

Figure 3.6
FDU-2100, EYELA freeze dryer.

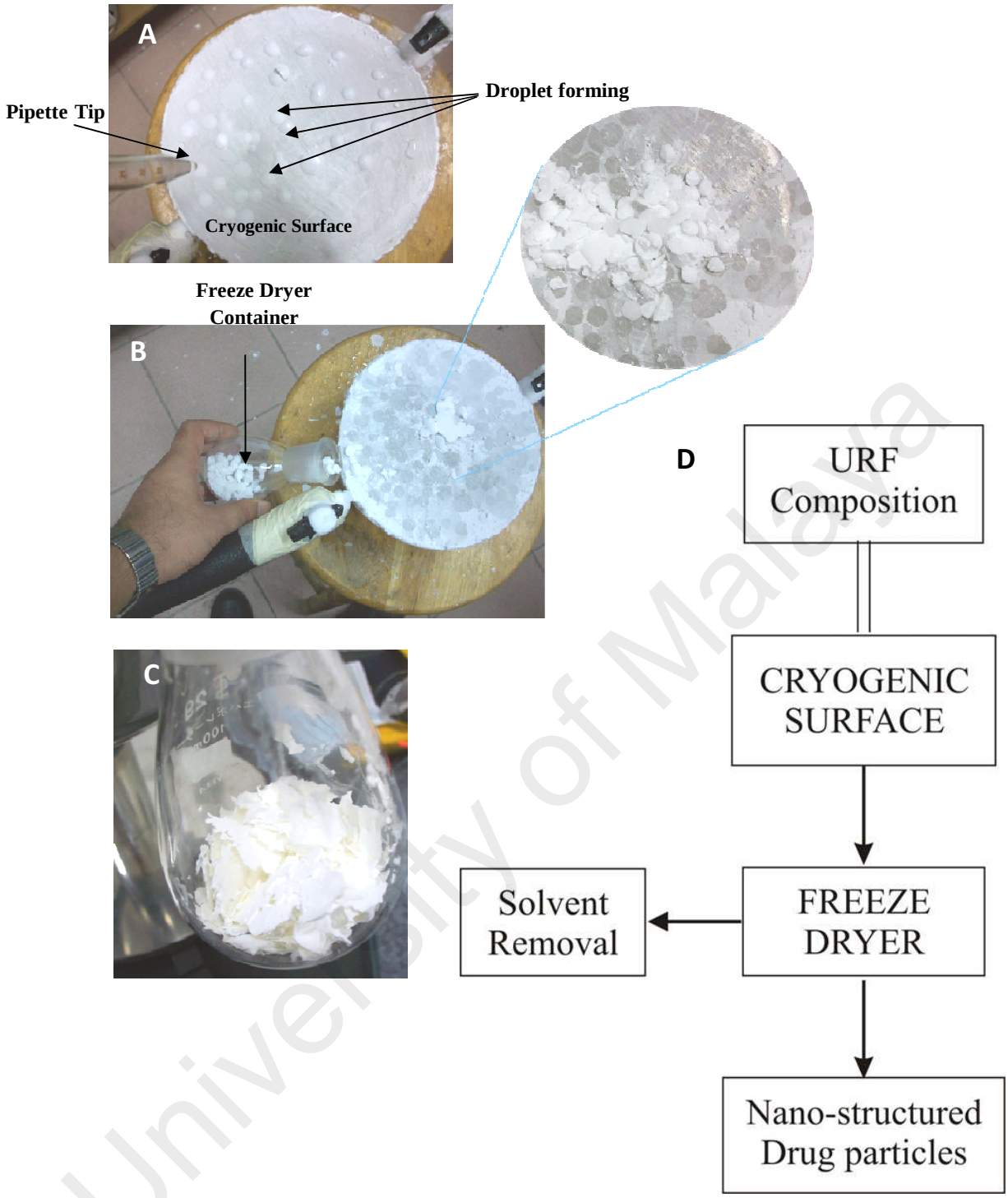

Figure 3.7
Photographs represent URF process:
A. Droplets applied on a cryogenic surface by using pipette.
B. Collecting freezing droplets.
C. Attached container to Freeze Dryer.
D. Flow diagram represented the Process.

3.2.2.2. Enhance Dissolution Rates of GF

URF feed solutions were prepared according to the following procedure. Griseofulvin was dissolved in acetonitrile (ACN). Polyvinylpyrrolidone (PVP) K16-K18 and/or SDS were dissolved in distilled water. The aqueous and organic solutions were then mixed (refer **Table 3.2.**) to obtain GF feed solutions. Frozen particles formed instantaneously. The frozen particles were collected and lyophilized in an EYELA freeze dryer (FDU-2100, EYELA, Japan) of API and excipient frozen at -80°C and lyophilized for 48 hours. Analysis of dissolution rate and determination of amorphousity are done respectively (see section 3.3.2)

Table 3.2
*Summary of GF Formulations**

Sample	PVP	SDS	GF	Composition	Ratio
GF	0	0	100%	GF	100%
GF 2	75%	0	25%	GF:PVP	3:1
GF 3	0	50%	50%	GF:SDS	1:1
GF 4	60%	20%	20%	GF:SDS:PVP	3:1:1
GF 5	0	33%	66.7%	GF:SDS	2:1
GF 6	67%	11%	22%	GF:SDS:PVP	2:1:6
GF 7	60%	0	40%	GF:PVP	3:2

*GF indicates Griseofulvin, SDS indicates Sodium dodecyl sulphate, PVP indicates Polyvinylpyrrolidone

3.2.2.3. Droplet size forming into cryogenic Surface

In the process of dissolution rate, ACN was used. As the freezing of ACN is rather low (-45°C), water was added to increase the freezing point of the mixture, to set sufficient freezing rate. By determine the droplet size; the rate of freezing can be monitored.

Droplets of URF composition were released from a syringe without piston with a 0.8 mm diameter tip 15 cm above cryogenic surface and allowed to impinge on the surface. The spread droplet thickness was easily determined with the assumption that the droplet impacting on the cold substrate deformed into a cylinder with an equivalent volume to the original droplet volume before impact.

Droplet volume was determined by dropping 10 droplets into a graduated cylinder and measuring the total volume. Frozen spread droplet diameters were measured with a ruler across two directions and averaged for 10 droplets. Droplet thicknesses were then calculated from the known volume of the falling droplet and the diameter of the frozen spread droplet.

$$Mean\ Drop\ Area = \left(\frac{1}{2} Diameter\right)^2 \times PI$$

$$Mixture\ Density = \frac{Mass}{Volume}$$

$$Drop\ Volume = Drop\ Area \times Thickness$$

$$Drop\ Thickness = \frac{Drop\ Mass}{Mixture\ Volume \times Drop\ Area}$$

Average Diameter=7.7 mm

Average Drop Weight =0.00589 g

Drop Area (mm^2) = 46.566 mm^2

Mixture Density= 0.9059 g/ml

Thickness of the Drop = 0.139 mm

3.3. ANALYSIS AND CHARACTERIZATION

3.3.1. Nano Particles Analysis

3.3.1.1. Quantitative Determination of Nanoparticles Drug

The suspended solutions are prepared by dispersing 80mg from each sample as mention in **Table 3.1.** into 30ml of chloroform and sonicated for (5mintute). The suspension was later filtered using 0.2 μm membrane filter (PTFE filter, sartorius®), and then the filtrate was mixed with 30 ml methanol.

UV/Vis Spectrophotometer (Lambda35, PerkinElmer®) was used to determine the isoniazid concentration in nanoparticle fractions. The calibration curve (**Figure 3.8**) was prepared by using standard concentrations of Isoniazid (8.00×10^{-2}, 5.60×10^{-2}, 4.39×10^{-2}, 3×10^{-2}, 1.2×10^{-2}, 1.08×10^{-2}) mg/ml in mixture of chloroform and methanol (50/50, V/V).

It is worth to mention that the Isoniazid showed peaks at 263 (nm) (**Figure 3.9)**, this is good agreement with (Becker *et al.*, 2007). The following correlation was obtained to represent the relationship between isoniazid concentration and absorbance peak.

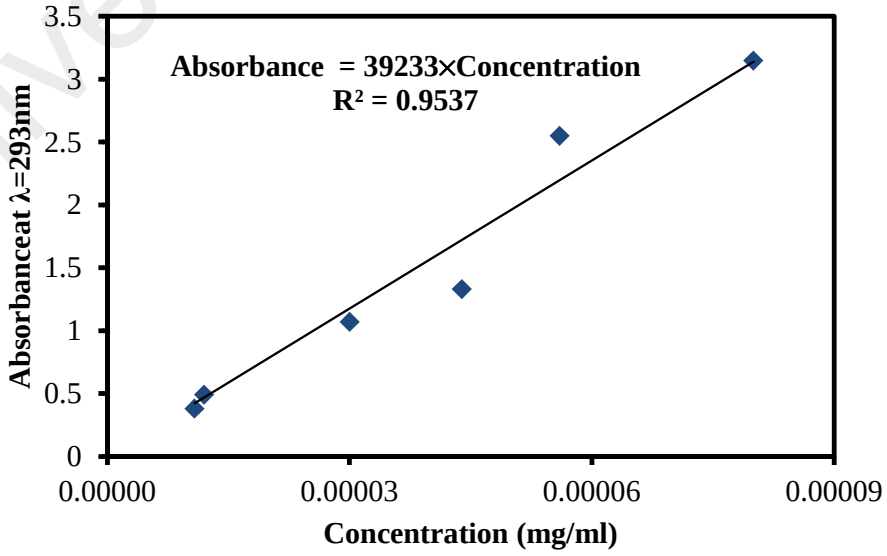

Figure 3.8
Calibration curve of the relation between INH concentration and absorbance.

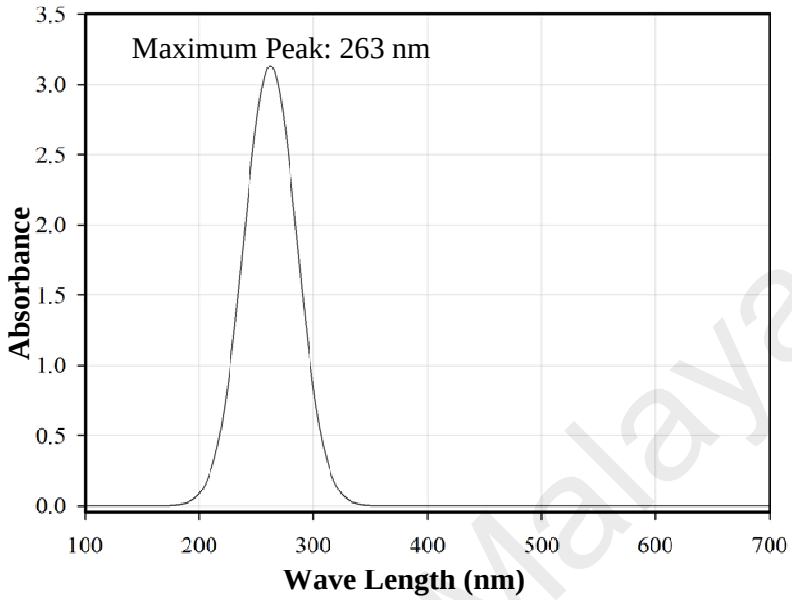

Figure 3.9
UV/vis spectrum of INH in mixture of chloroform and methanol (50/50, V/V)

Overlay peak with the polymer have been avoided by created background solution with same concentrations of polymer in chloroform and diluted with the same ratio. Each measurement was taken in triplicate.

3.3.1.2. Characterization

3.3.1.2.1. Particle size analysis

The volumetric particle size distribution for each suspension was determined by a dynamic light scattering method using Mastersizer 2000 (Malvern Instruments Ltd., USA). The Mastersizer2000 possesses a detection range of 0.2-2000 μm.

The particle size distribution was measured after sonication for 5min, Chloroform was used a dispersant media in order to determine size of API particles without excipient due to its ability to dissolve PVP without intact API Particles.

Span index is used to describe the polydispersity in a given particle size distribution and is defined as (D90-D10)/D50, where D10, D50, and D90 are the respective particle size at 10, 50, 90% cumulative percent undersize (Lefebvre, 1989). The particle diameters are reported based on volume.

3.3.1.2.2. Surface morphology

Visualization and evaluation surface morphology of the particles where conducted by using Hitachi Model S-4500 field emission scanning electron microscope (SEM) (Hitachi Instruments, Irvine, CA) .

3.3.1.2.3. Powder X-ray diffraction (PXRD)

The X-ray diffraction patterns of all powder samples were analyzed using a Philips X'Pert MPD system equipped with a graphite monochromator, operating at 40 kV and 30 mA and employing nickel-filtered CuKa radiation (l¼ 0.1542 nm). The leveled powder was measured from 5 to 45 2θ degrees using a step size of 0.02 2θ degrees and a dwell time of 1 s.

3.3.2. Dissolution Improvement studies

3.3.2.1. Determination of the Griseofulvin concentrations in water

The calibration curve (**Figure 3.10**) was prepared by using standard concentrations of GF (0.1, 0.35, 0.4, 0.53, 0.74, and 0.8) mg/100ml. It is worth to mention that the GF showed peaks at 295 (nm) (**Figure 3.11**) this is good agreement with (Knoblauch and Zimmermann, 2007). The following correlation was obtained to represent the relationship between GF concentration and absorbance peak.

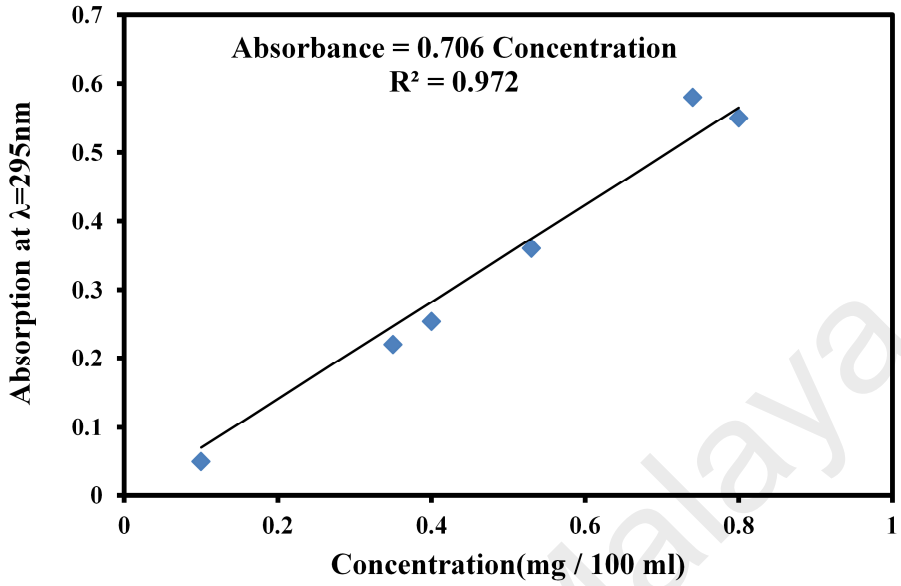

Figure 3.10
Calibration curve of the relation between GF concentration and absorbance.

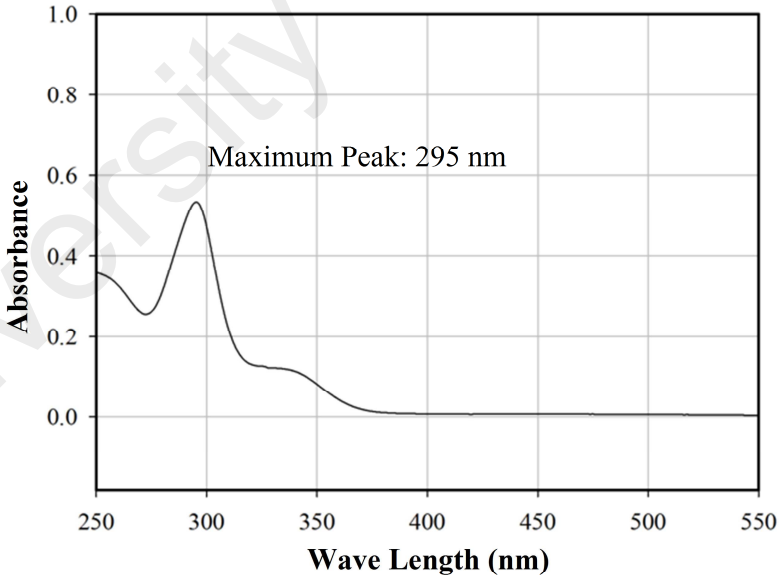

Figure 3.11
UV/vis spectrum of GF in distilled water.

3.3.2.2. Characterization

3.3.2.2.1. Dissolution Test

After freeze drying, dry powders containing ~20 mg GF were added to 1000 ml dissolution medium (distilled water). Bath temperature and paddle speed were set at 37 ± 0.5 ℃ and 75 rpm. Samples (5 ml) were withdrawn at predetermined time intervals and immediately replaced with equal volumes of dissolution medium. Samples were filtered (0.45 Millipore filter) and then their concentrations were determined using UV/Vis. Spectrophotometer (Lambda35, PerkinElmer®) at 295 nm.

3.3.2.2.2. Differential scanning calorimetry (DSC)

Thermograms of processed compounds were recorded on a Differential Scanning Calorimeter (DSC) using Mettler Toledo Mettler STAR® system. The temperature axis and cell constant of DSC were previously calibrated with indium standard materials. Powder sample was accurately weighed into an aluminum pan and an empty aluminum pan was used as a reference. Usually a heating rate of 5 ℃/min was used up to a maximum temperature of 300℃.

DSC was utilized to determine Phase separation occurrence in different rate of freezing. The same procedure mentioned above was used with one different, feed solution samples are cooled from 25℃ to -80℃ with two freezing rates 1.5min and 21min (equivalent to 70 and 5 ℃/min freezing rate respectively) and the amount of energy is quantified.

4.0 RESULTS AND DISCUSSION

4.1. Solid-liquid Phase separation

Phase separation is the separation of a one phase mixture into two or more phases. In this study, solid-liquid separation phase was the main concerned.

DSC was utilized to identify the quantity of energy absorb or release. **Figure 4.1 and Figure 4.2** show the DSC profile of GF 4 (see **Table 3.2** for composition), feed solution with different rate of freezing. Area under the curve represents the amount of heat. The values of heat (485.78 J/g, 55.94 J/g) were measured with the rate of freezing of 21 min and 1.5 min respectively. The amount of exothermal heat is inversely proportional to the freezing rate.

This different in exothermal heat contributed to phase separation which induces nucleation. Nucleation in which fresh particles are formed, generally by phase separation start to grow until the solution is vitrified.

Great reduction in exothermal heat in high rate freezing sample reflects the risk of phase separation is minimized as soon as the solution is vitrified. Minimized phase separation of solutes within the solution and promotion of the high energy amorphous product morphology was identified.

This study supported the hypothesis that; if the freezing rate is sufficiently fast, phase separation between the API and stabilizing agents can be prevented, this lead to the formation of nanoparticles molecular dispersed in the stabilizing agents.

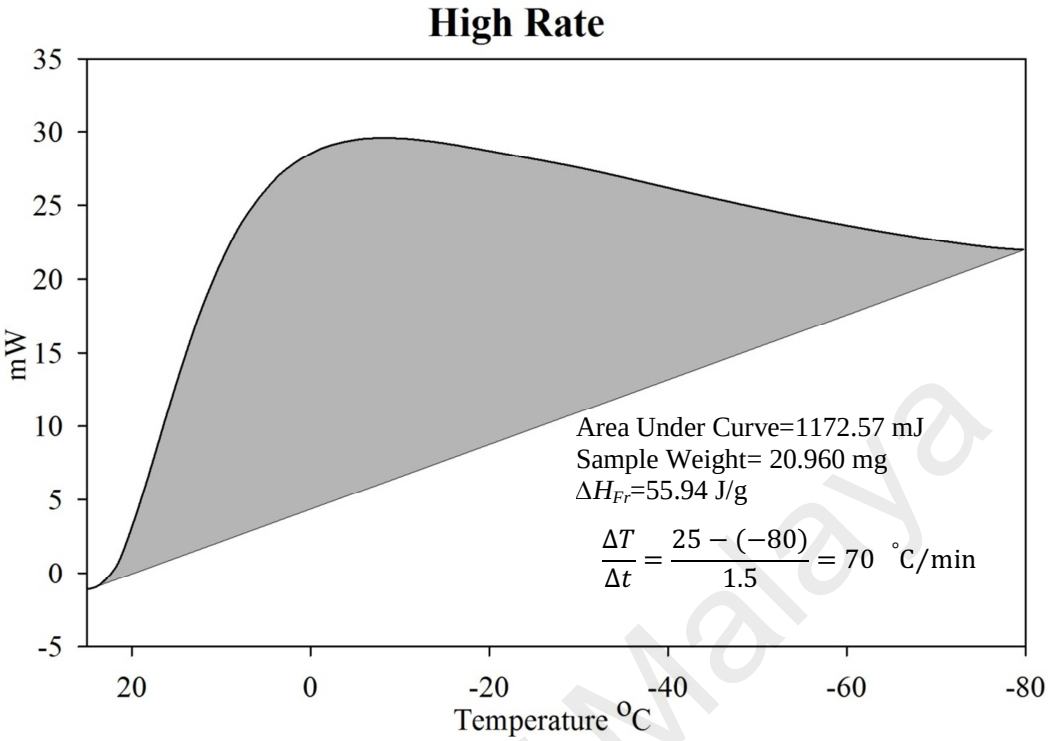

Figure 4.1

DSC profile represents the quantity of energy absorbs or release with high rate of cooling.

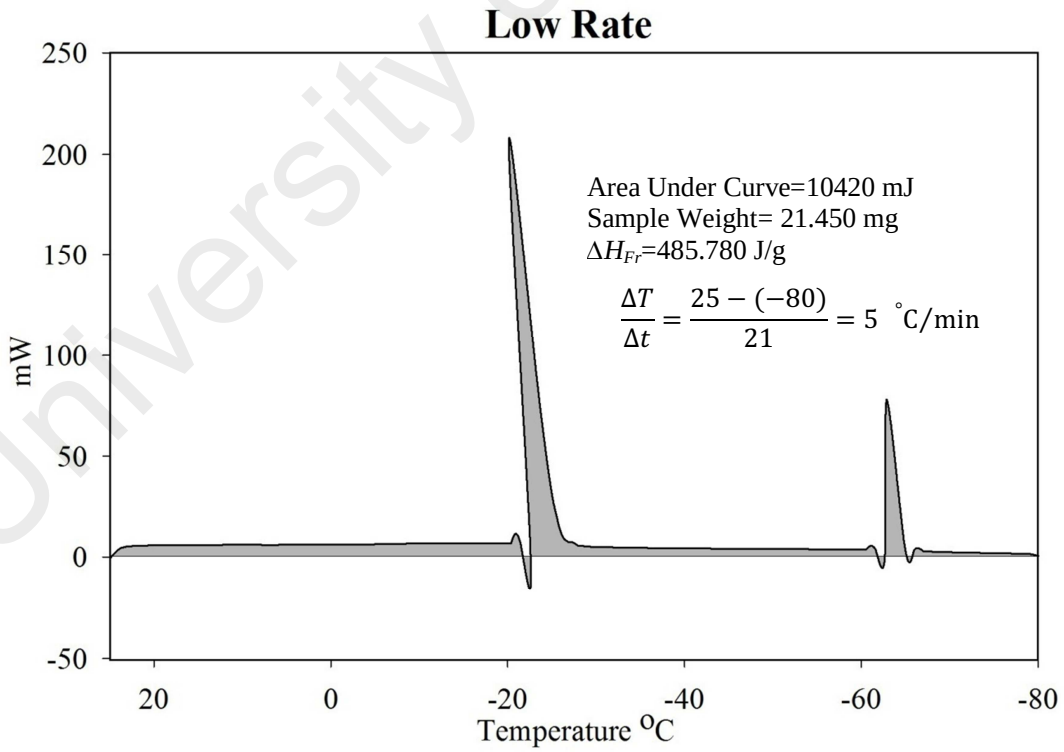

Figure 4.2

DSC profile represents the quantity of energy absorbs or release with low rate of cooling.

4.2. Production of nanoparticles for INH

4.2.1. Quantitative determination of nanoparticles drug

The quantitative determinations of nanoparticles were conducted by creating nanoparticles suspension. Chloroform was chosen due to its properties as good solvent for polymers, this mixture is then sonicated to create a homogenous suspension. Filtration was performed with 200nm membrane filter (PTFE filter, sartorius®) to separate out particles ≤200nm and the filtrate is further dissolved in equivalence volume of methanol. The amount of the drug existed as nanoparticles in the suspension was determined by Uv/Vis Spectrophotometer. The yield was determined by comparing the measured drug concentration and the amount of initial concentration as seen in **Table 3.1**.

Quantitative determination revealed that the percentage of nanoparticles formation increase proportionally with the ratio of PVP (see **Figure 4.3**). The difference in the percentage yield of nanoparticles formation between URF and FD are mainly due to the different in rate of freezing at the same composition. The difference in yield between URF and FD in term of PVP ratio was summarized (see **Table 4.1).** It is observed that the maximum difference in yield is at 25% polymer ratio, where the difference recorded is 16.81%. The difference in the values might occur due to the effect of solvent volume on the polymer chain formation (length, shape) under high rate of freezing which led to increase possibility of API molecular attach to polymer chain.

Sixty seven percentages (67%) is the maximum PVP ratio tested with nanoparticles formation 98.47%, 90% for URF and FD respectively. In pharmaceutical industries excipient loading is sensibly added due to cost, storage and healthy limitations.

Table 4.1
The difference between FD and URF in nanoparticles formation with the ratio of PVP.

%PVP	% Yield (FD)	% Yield (URF)	Difference
0	23.21%	26.67%	3.46%
25	34.49%	51.30%	16.81%
33	81.96%	84.53%	2.57%
50	83.13%	86.00%	2.87%
67	90.00%	98.47%	8.47%

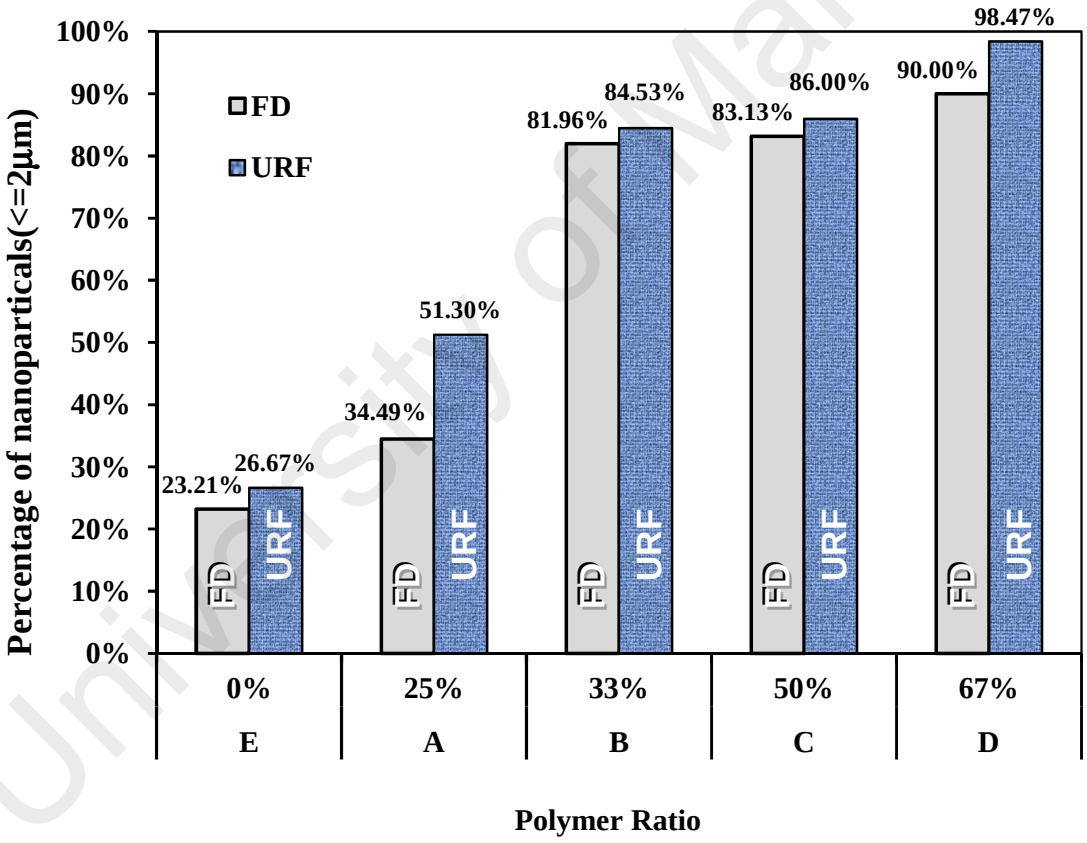

Figure 4.3
Percentage of drug nanoparticles (<0.2 µm) in the suspensions obtained from FD mixtures and URF mixtures.

4.2.2. Characterization

4.2.2.1. Particle size analysis

The particle size distribution for the URF powders (**Table 3.1.**) was determined by laser light diffraction equipment called Malvern Mastersizer 2000.

The mean particle diameter (M50) of the URF INH/PVP ratio 3:1, 2:1, 1:1, 1:2 powders was 885, 788, 135, 94 nm respectively. The size reduction was significant after URF processing compared to the starting material, micronized bulk INH, which had an M50 of 1,310,882 nm (1,310.882µm).

Interestingly, size distribution of nanoparticles URF D (94 nm) was found to be very narrow, as indicated by a span index of 0.844. In contrast, URF A (885 nm) was found to be high, with a span index of 1.584. The narrow span index of URF D reflects increasing in nanoparticles percentage see **Figure 4.3.**

Significant increase in surface area was observed with increase in PVP ratio contribution to inhabitation effect of PVP during URF process. Detailed results of the size analysis can be found in appendix A1-A6.

Table 4.2
Particle size distribution and surface area measurements of the dry micronized URF powders and control formulations.

Formulation	D10(nm)	D50(nm)	D90(nm)	Span index*	Specific surface area (m^2/g)
Bulk INH	990,642	1,310,882	1,645,472	0.500	0.00473
URF E	234,470	507,225	1,093,322	1.693	0.0144
URF A (3:1)	454	885	1,856	1.584	7.59
URF B (2:1)	515	788	1,379	1.097	7.85
URF C (1:1)	63	135	1,147	8.055	49.7
URF D (1:2)	62	94	141	0.844	64

*The span index is (D90 - D10)/D50

(A)

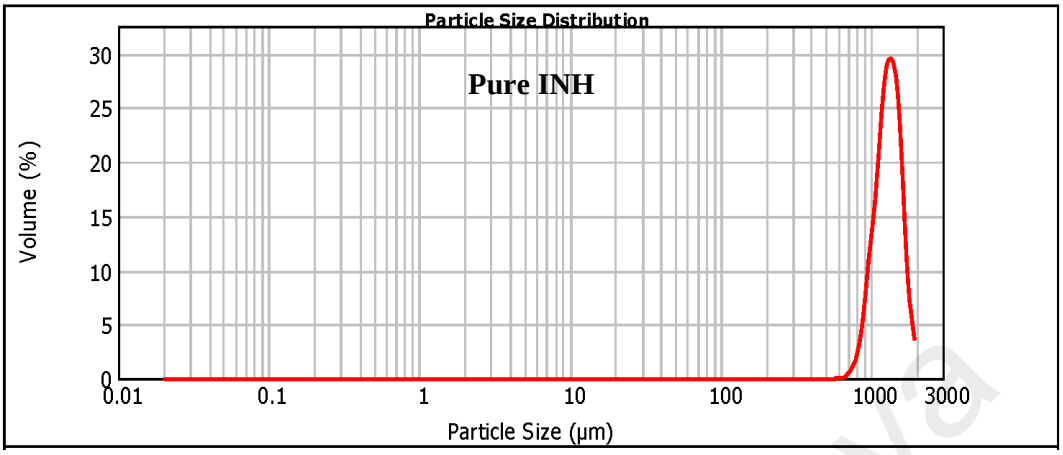

(B)

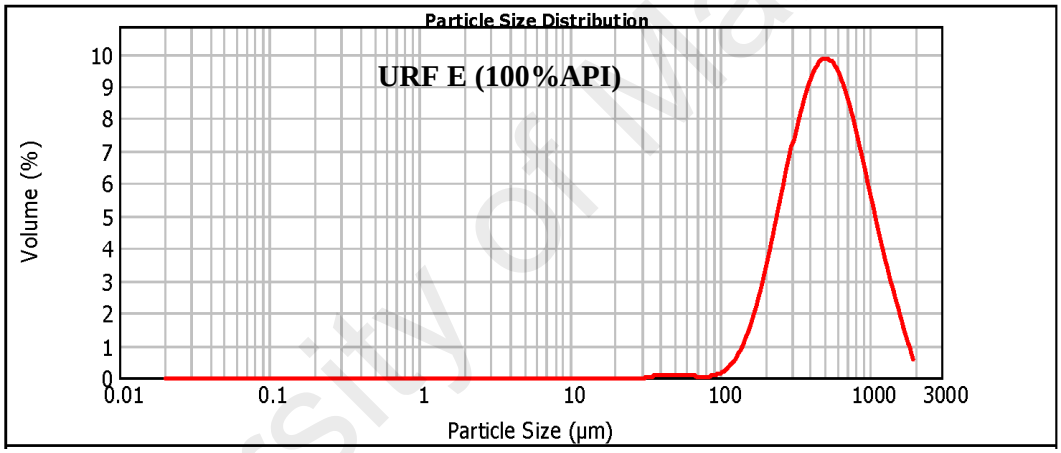

(C)

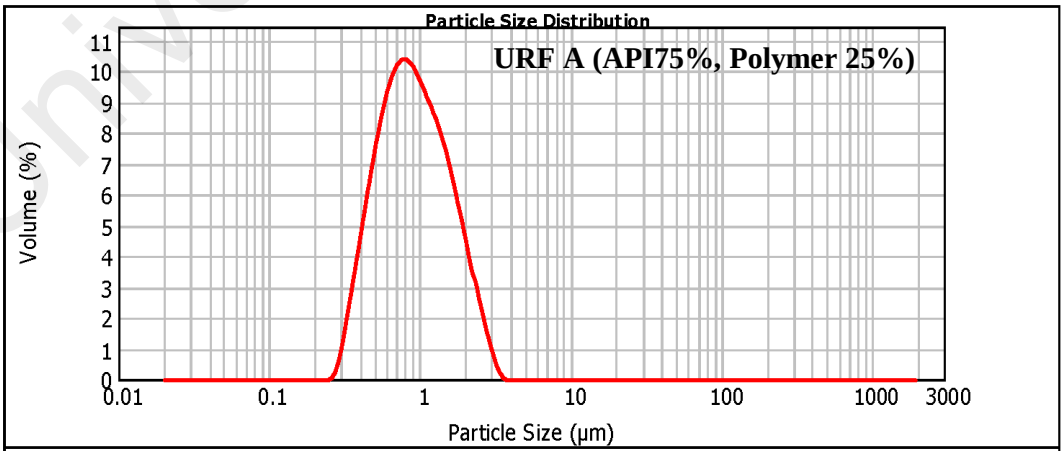

(D)

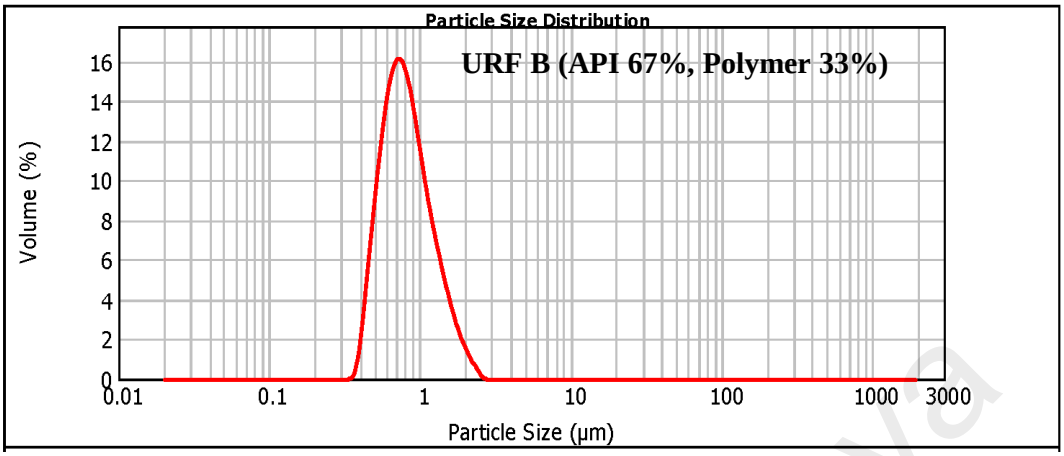

(E)

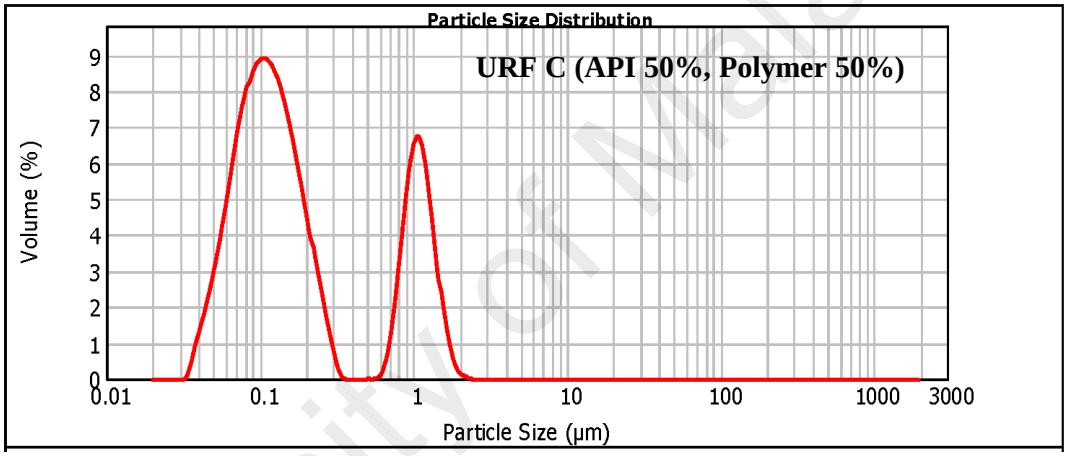

(F)

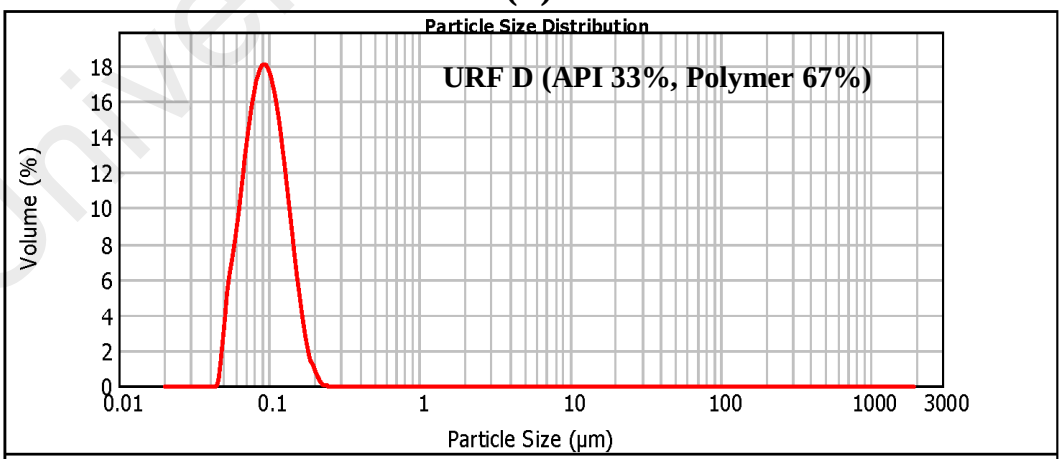

Figure 4.4

Particle size distribution patterns of INH mixing with different ratio of PVP produce by FD and URF after dispersing into distilled water.

(A) Pure INH, **(B)**URF(100%API), **(C)**URF A(API 75%, Polymer 25%), **(D)**URF B (API 67%, Polymer 33%), **(E)**URF C (API 50%,Polymer 50%), **(F)**URF D (API 33%,Polymer 67%).

4.2.2.2. Surface morphology

SEM micrographs revealed needle shape with sharp edge for pure INH produce by FD and for URF. The needle shape became shorter and wider with rounded edge for URF in comparison with FD. **(See Figures 4.5(a), 4.5(b))**

By increasing the polymer ratio to 25%, micrographs in FD process shows particles existed in rectangular shape **(See Figure 4.5(c)).** In contrast for the URF process, the sizes of particles are smaller and randomly disordered due to the increasing rate of freezing. **(See Figure 4.5(d))**

The tendency to forming rectangular shape was still dominant in FD process at polymer ratio of 33% and 67% (**See Figure 4.5(e), 4.5(g))**. This phenomenon could be due to the effect of interaction between INH and PVP on crystal forming.

In contrast, the URF micronized powders growth change to irregular broken particles with non-uniform shapes at polymer ratio 33% (**Figure 4.5(f))**. High agglomerated smooth particles appeared at polymer ratio of 67%, these smooth agglomerated particles may be formed fully coated with polymer (**Figure 4.5(h))**.

The SEM images clearly show reduction in particle size induced by increasing rate of freezing. Furthermore, particles shape morphing was inhibited due to the effect of polymer ratio, where the particles shape change from needle shape with sharp edge to rectangular shape.

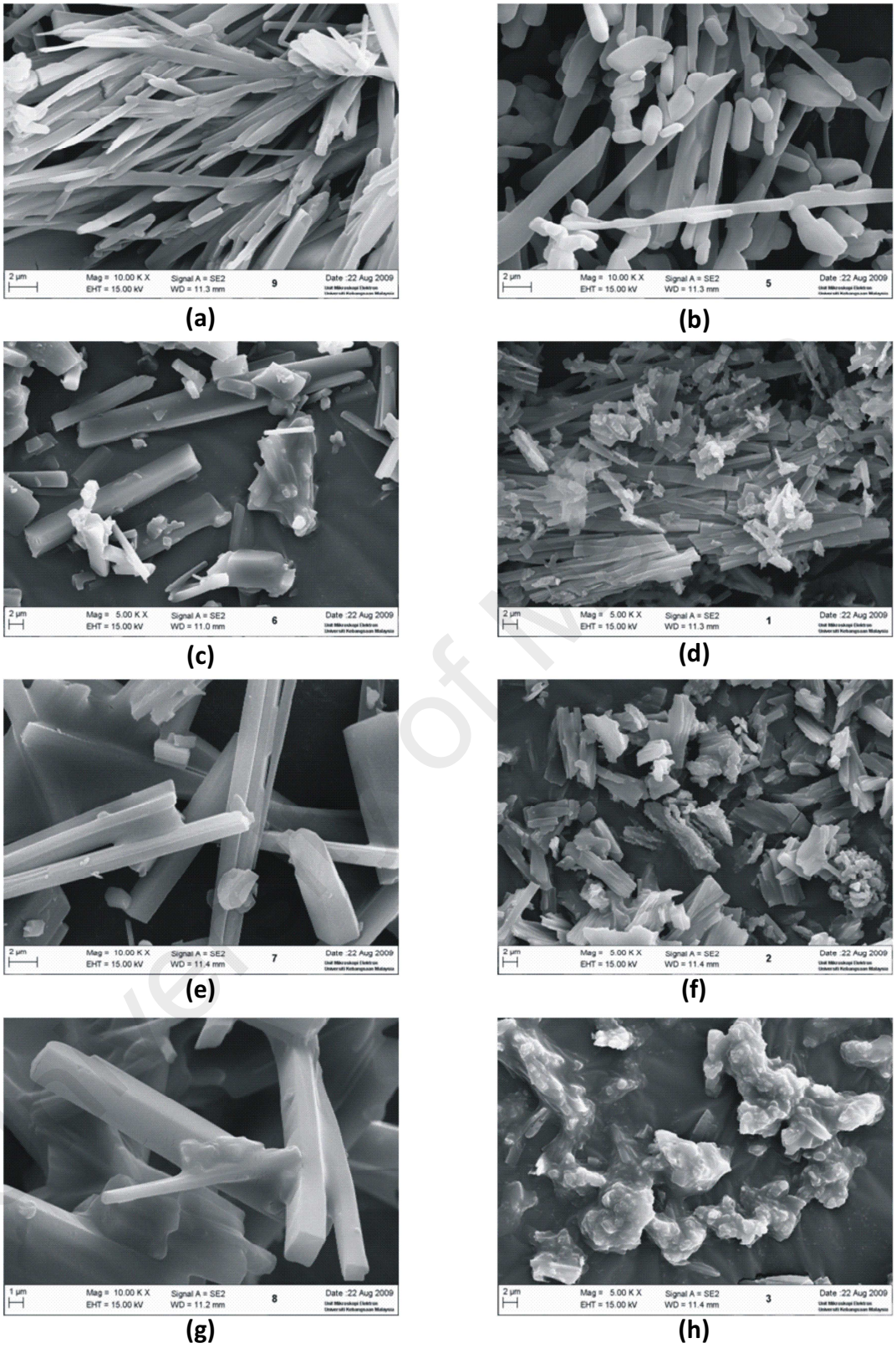

Figure 4.5

SEM micrographs of INH mixing with different ratio of PVP producing by FD and URF, **(a)** FD E (API 100%), **(b)** URF E (API 100%), **(c)** FD A (API 75%, Polymer25%), **(d)** URF A (API 75%, Polymer25%), **(e)** FD B (API 67%, Polymer33%), **(f)** URF B (API 67%, Polymer33%), **(g)** FD D (API33%, Polymer67%), **(h)** URF D (API33%, Polymer67%).

4.2.2.3. Powder X-ray Diffraction (PXRD)

To confirm the crystalline state of selected URF powders and FD powders, X-ray diffraction was performed. The peak intensities indicated a high degree of crystallinity.

The X-ray pattern of the URF INH/PVP powders with 33% INH concentration exhibited a significant reduction in peak intensity of INH. The characteristic diffraction peaks of INH at 16.8, 15.3 and 14.0 (2θ) degrees exhibited a significant reduction in peak intensity of INH/PVP powder indicating that the INH was in an amorphous state. Similarly, a lack of crystallinity was also found for the URF INH/PVP powders with higher concentration PVP (50, 67%). XRD of different URF formulations, however, shows crystalline as well as amorphous character, depending on stabilizers concentration (**Figure 4.6**).

In contrast to URF processed INH, freeze dryer samples of INH displayed peaks characteristic of crystalline Isoniazid. Freezing rate, therefore, has a direct impact on the formation of crystalline INH. Since URF feed solution is atomized directly into cryogenic surface, there is not sufficient time for the INH molecules to crystallize prior to freezing. Freeze dryer INH samples, however, Freeze dryer allow for the organization of the INH molecules into their thermodynamically favored crystalline habit. The organized crystalline lattice structure formed during crystallization of the slowly frozen formulations must be broken in order for dissolution to occur, whereas amorphous formulations have a higher chemical potential and thus may form supersaturated solutions.

(A)

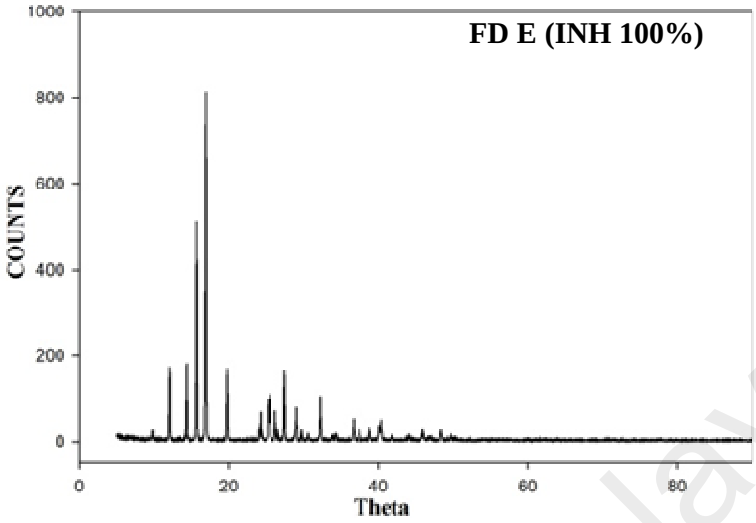

(B)

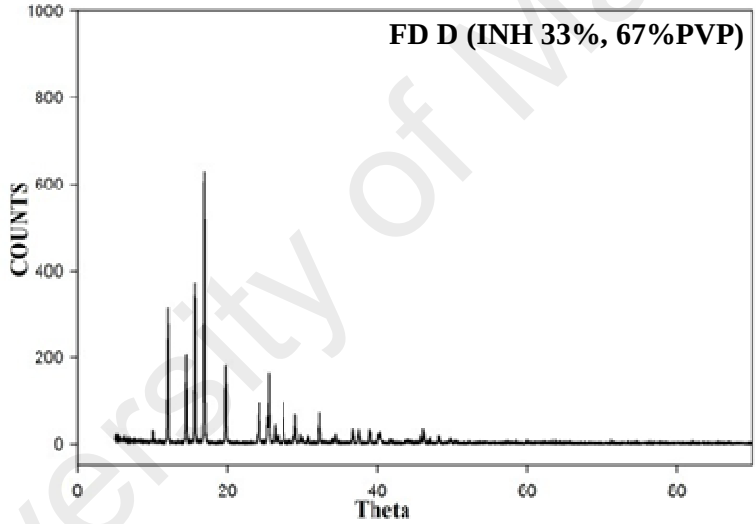

(C)

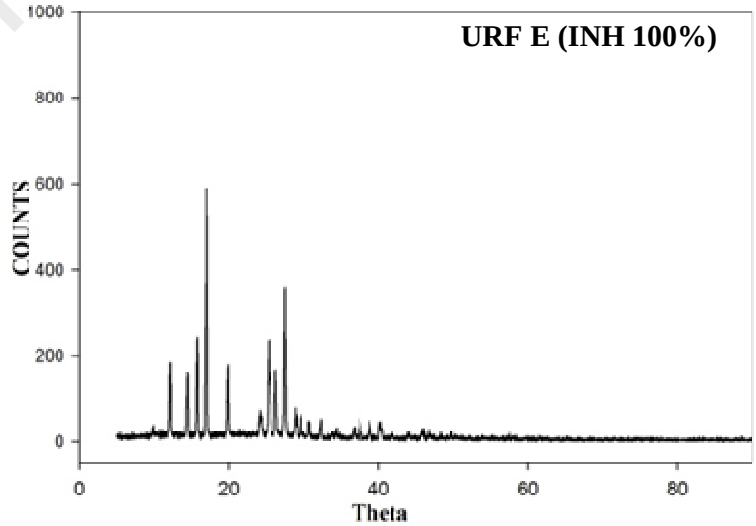

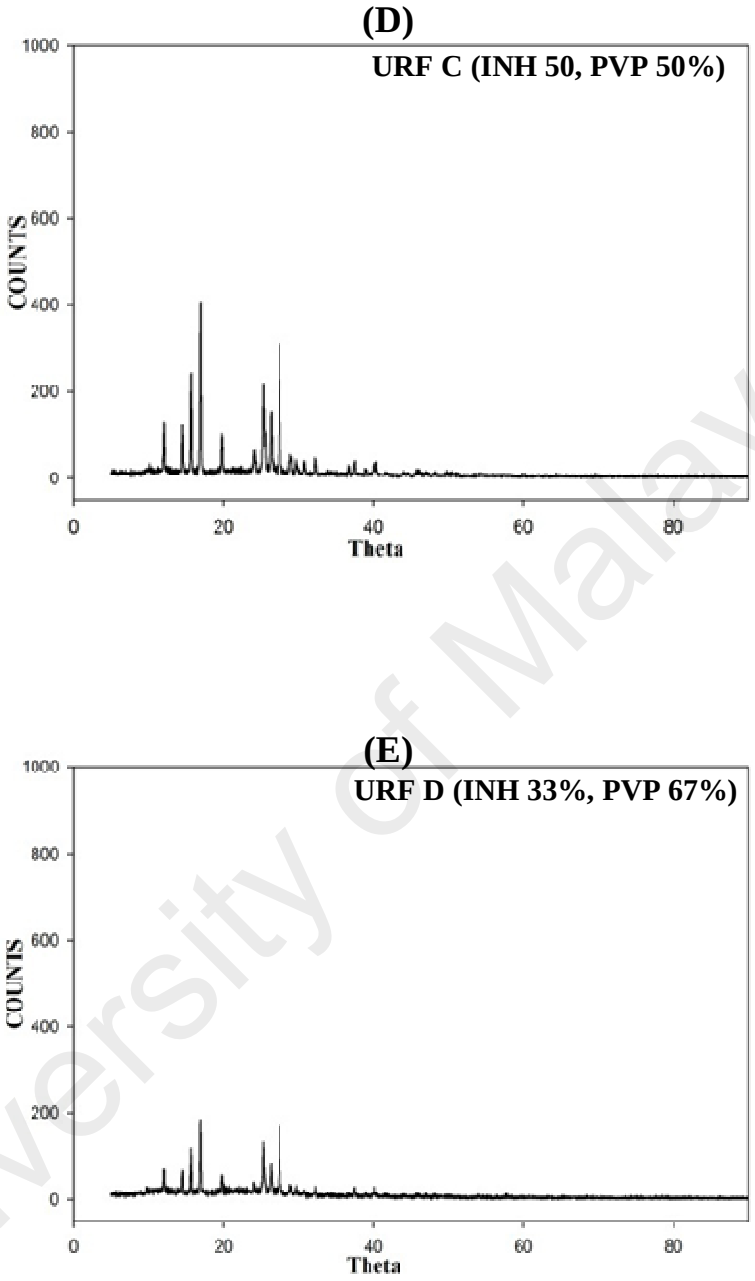

Figure 4.6
The X-ray diffraction pattern of INH/PVP powder producing by FD and URF, **(A)** FD E (INH100%), **(B)** FD D (INH33%, PVP67%), **(C)** URF A (INH100%), **(D)** URF C (INH50%, PVP50%), **(E)** URF D (INH33%, PVP67%).

4.3. Dissolution Improvement studies

4.3.1. Dissolution Test

The amount of GF dissolved, as a function of time, was determined and the profiles presented in **Figure 4.7** illustrate the dissolution of the URF prepared formulations.

Dissolution studies were carried out on GF formulations from distilled water. Approximately 20% of raw drug pure GF (GF1) was dissolved within 60 min, the amount dissolved increase to 35% after 80 minutes, this value further increased to 40 % after three hours.

As expected, the dissolution of GF from the URF composition into the dissolution media was instantaneous, occurring within the first two minutes of the experiment. Rapid dissolution was observed by all GF processed powders showing greater than 30% dissolution within 60 minutes.

However, differences were seen within the first 2 minutes between the URF composites powders. GF 6 appeared to dissolve instantaneously on contact with the surface of the dissolution media and shows the fastest dissolution of all GF processed powders. From the dissolution profile, the GF 6 powder is 48% dissolved within the first two minutes.

GF2 and GF7 started almost identically, but after 150 mint dissolution of GF2 increased slightly. GF3 instantaneously dissolved in comparison with GF5, which is slightly higher in dissolution rate.

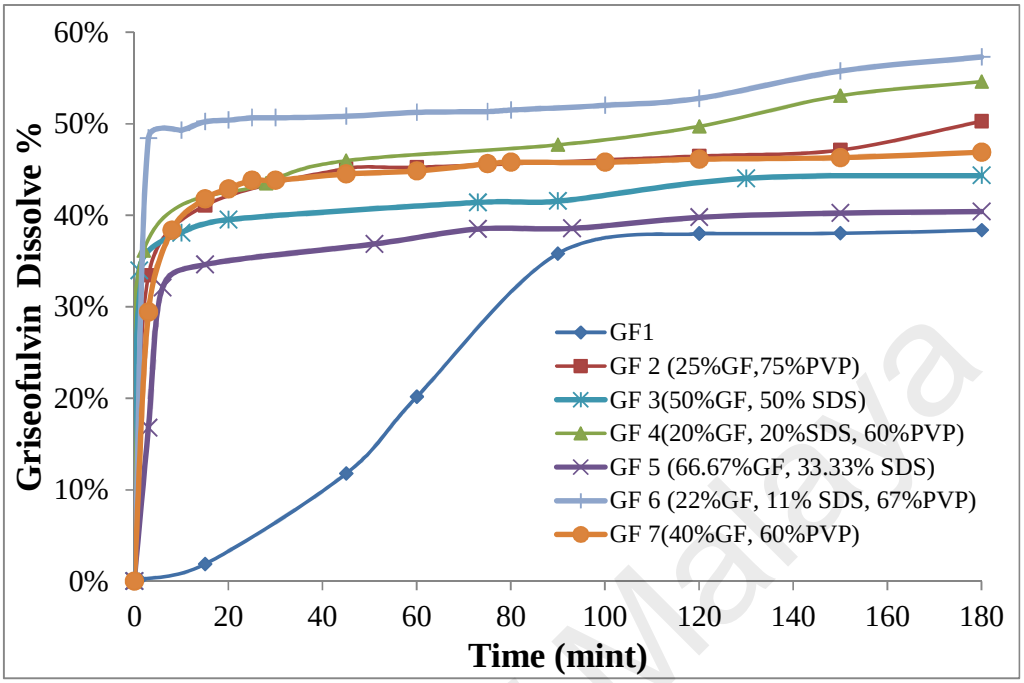

Figure 4.7
Effect of API and excipients (PVP, SDS) ratio on drug dissolution rate of GF.

The overall interaction effects are displayed in **Figure 4.8**; a 3D representation of the polynomial is obtained from the experimental data. The dissolution rate increase proportionally to PVP ratio, as expected, conform the inhibiter effect of PVP which led to reduce particle growth. Increasing SDS concentration above 10% has little effect on dissolution rate due to the aggregate structure for mixtures of PVP (homopolymers) and ionic surfactants (SDS). The interaction between PVP and SDS possibility were proposed by Shirahama (Shirahama, 1974), the interaction forming a pearl-necklace with surfactant aggregates along the polymer chain. As for surfactant aggregation it is the tendency to avoid water contact that drives the surfactant to the polymer, which often also is interpreted as a hydrophobic attraction between the polymer, containing hydrophobic domains, and the surfactant that accounts for the main contribution to the free energy of association in the mixtures (Lindman et al., 1993). Generally, all surfactants bind to hydrophobically modified polymers, with stronger binding with

decreased polarity of the polymer. For the polymer PVP, it is claimed that adsorption occurs by hydrophobic interactions (Ishimaru, 1994).

However, the effect of SDS and PVP the dissolution rate can also be represented in 2D contour as in **Figure 4.9.**

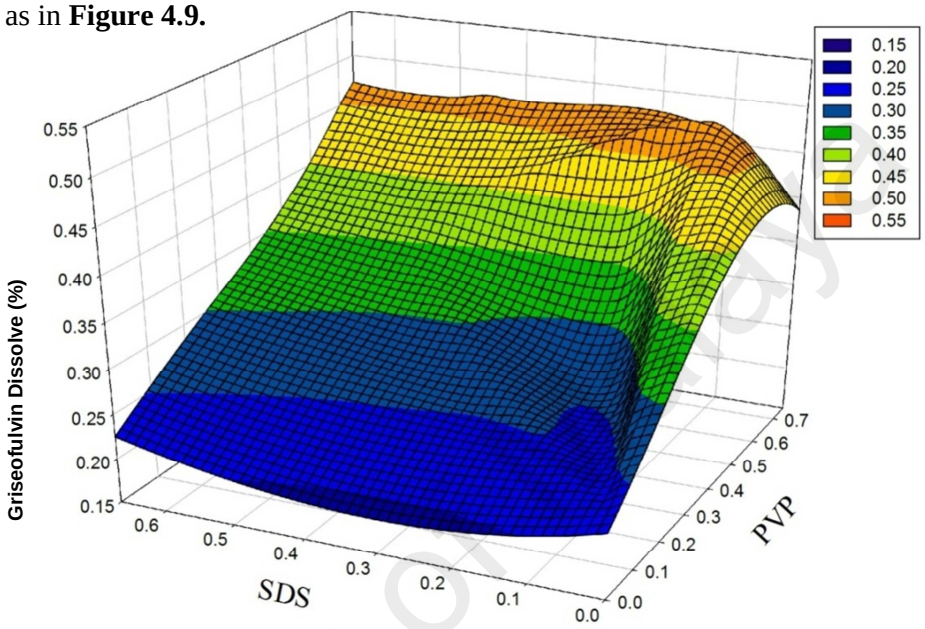

Figure 4.8

3D response surface graph for GF dissolve%: SDS concentration vs PVP concentration.

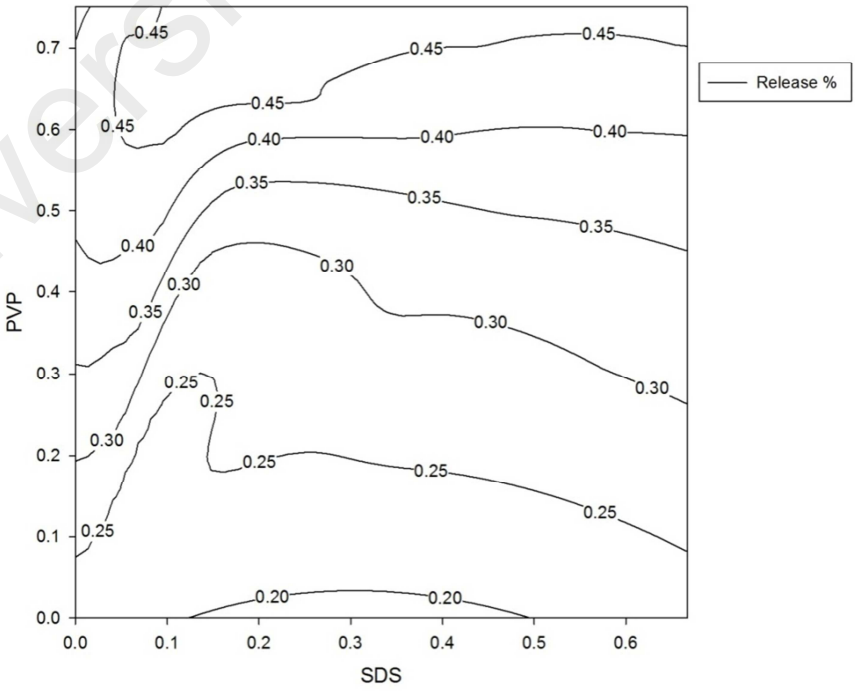

Figure 4.9

Contour plot for GF dissolve%: SDS concentration vs PVP concentration.

4.3.2. GF Amorphisity Measured in URF Micronized Powders

The crystallinity greatly influence on solubility and dissolution rate of poorly water soluble APIs (Shibata et al., 1983).

The chemical potential of amorphous metastable high energy state can be noticeably larger than that of an equilibrium crystal. This higher chemical potential can lead to a substantially greater local solubility of the API near the interface and thus a faster mass transfer rate into the dissolution media. Therefore, the crystallinity of an API can be reduced in order to enhance the dissolution rate. (Kaushal et al, 2004).

Differential Scanning Calorimetry (DSC) is a technique which measures the temperatures and heat flows associated with transitions in materials as a function of temperature or time in a controlled atmosphere. Therefore, DSC provides a direct indication of the crystalline and amorphous structure in API mixture. In the case of GF sample, DSC can be used to measure the degree of crystallinity by rationing the heat of melting (fusion) for a specific sample versus that for a 100% crystalline standard pure GF (see **Figure 4.10**). The figure reveals that the melting point of pure GF1 is 215°C with heat of melting (-118.9 J/g), and this value was used as reference point in all other mixture composition for amorphosity and crystallinity determination.

Where the heats of melting ΔHf for GF2- GF7 are respectively measured from **Figures 4.11- 4.16**, and are summarized in **Table 4.3**.

Thermal analysis of the GF compositions powder was performed and compared to the raw material. The GF powders investigated were obtained by URF process. The results of thermal analysis by DSC were summarized in **Table 4.4.**

Table 4.3

The degree of crystallinity of griseofulvin based on the above expression is shown table.

Sample	Sample weight (mg)	GF %	SDS %	PVP %	GF in sample	Enthalpy (mJ)	ΔH_m (j/g)	Crystallinity	Amorphosity
GF1	14.93	100%	-	-	14.93	-1770.55	-118.59	100.00%	0.00%
GF2	3.11	25%	-	75%	0.777	-37.37	-48.0952	40.56%	59.44%
GF7	1.76	40%	-	60%	0.704	-18.3	-24.474	20.64%	79.36%
GF3	1.91	50%	50%	-	0.955	-67.92	-71.1204	59.97%	40.03%
GF5	1.63	67%	33%	-	1.087	-35.13	-32.3183	27.25%	72.75%
GF4	3.19	20%	20%	60%	0.638	-50.29	-78.8245	66.47%	33.53%
GF6	2.32	22%	11%	67%	0.510	-37.96	-74.4314	62.76%	37.24%

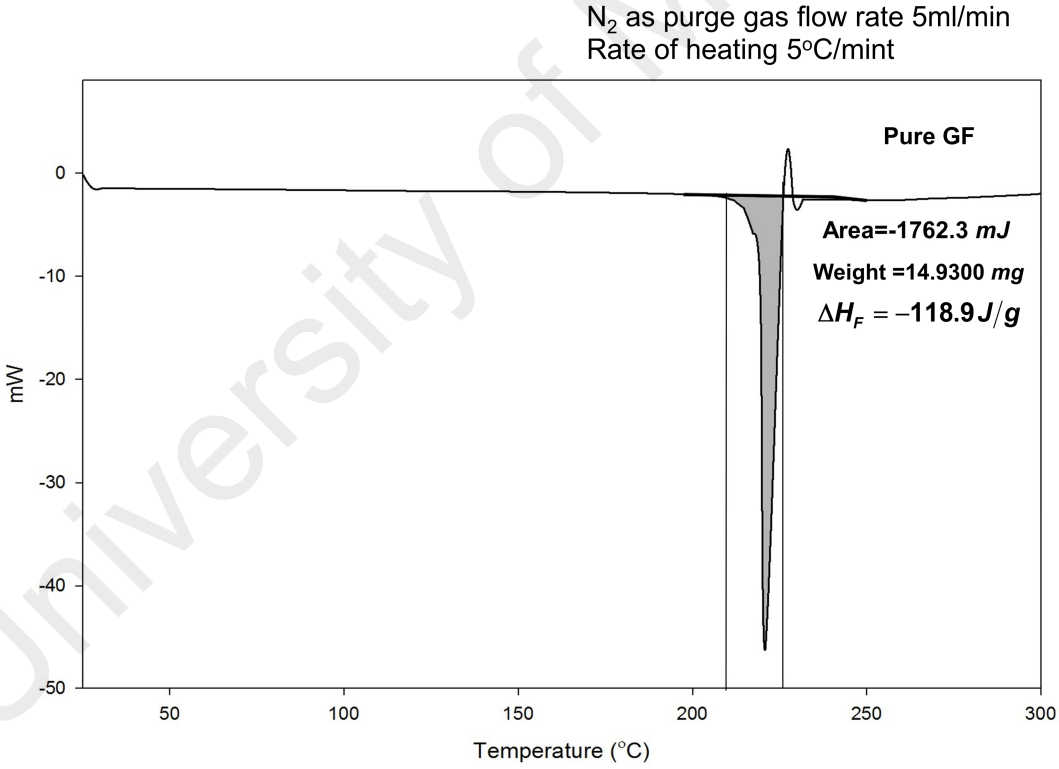

Figure 4.10

Total heat flow (DSC profile) for GF1 micronized powder (assume 100% crystalinity).

DSC GF1 samples curve revealed three main peaks represent dehydration, glass transition temperature and fusion respectively. The values of dehydration peak increasing with samples contained PVP; in contrast, with samples contained SDS this variance occurred due to mechanism of water absorption for PVP and SDS.

Amorphosity values for (GF3, GF5) were measured and found to be 39.82% and 72.62% respectively, where the difference is rather significant. Increasing in amorphosity can be interpreted as GF tendency to make ionic interaction with SDS.

In contrast with; GF2 and GF7 amorphosity values (59.34%, 79.26%), where the difference is insignificant, and this could be due to the much lessees ionic interaction with PVP in ratio.

However, amorphosity values for GF4 and GF6 are 33.12% and 38.83% respectively, the small increase in amorphosity could be attributed to increase in ionic bond between GF and SDS rather than non-ionic bond between GF and PVP.

In consistency with dissolution rate profile in **Figure 4.7**, amorphosity values contributed to increase of dissolution rate. But the amorphosity contribution was hinder with the presence of SDS due to interactions between the hydrophilic head group in SDS and the PVP chain (Chari, 1992). In contrast, PVP hydrophilic head group stay free were contributed to enhance dissolution rate.

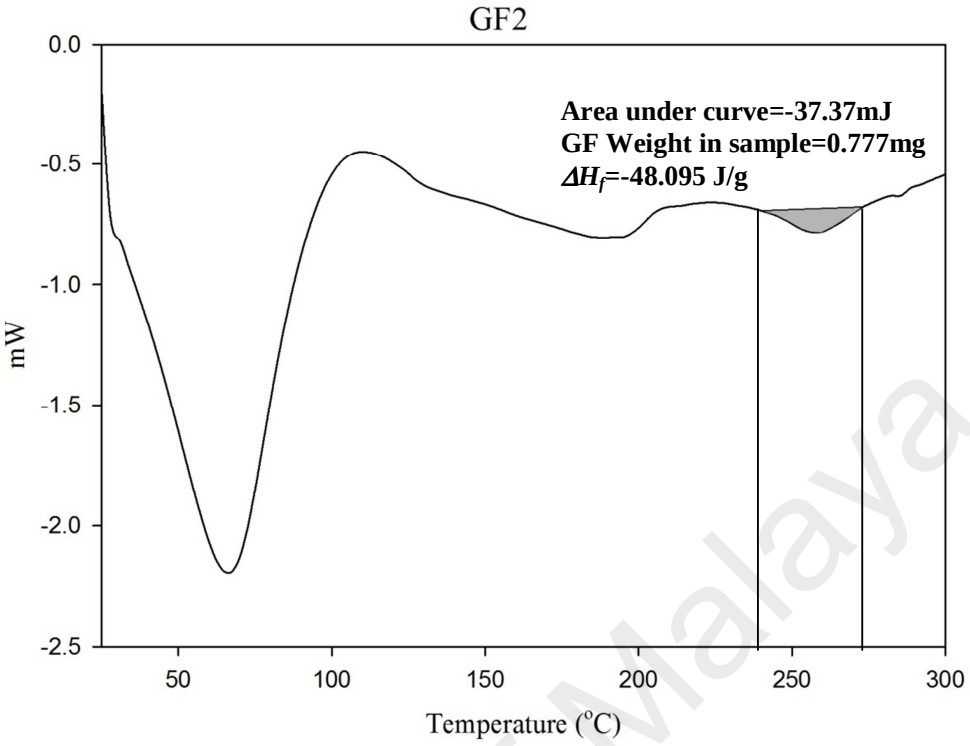

Figure 4.11
Total heat flow (DSC profile) for GF2 micronized powder.

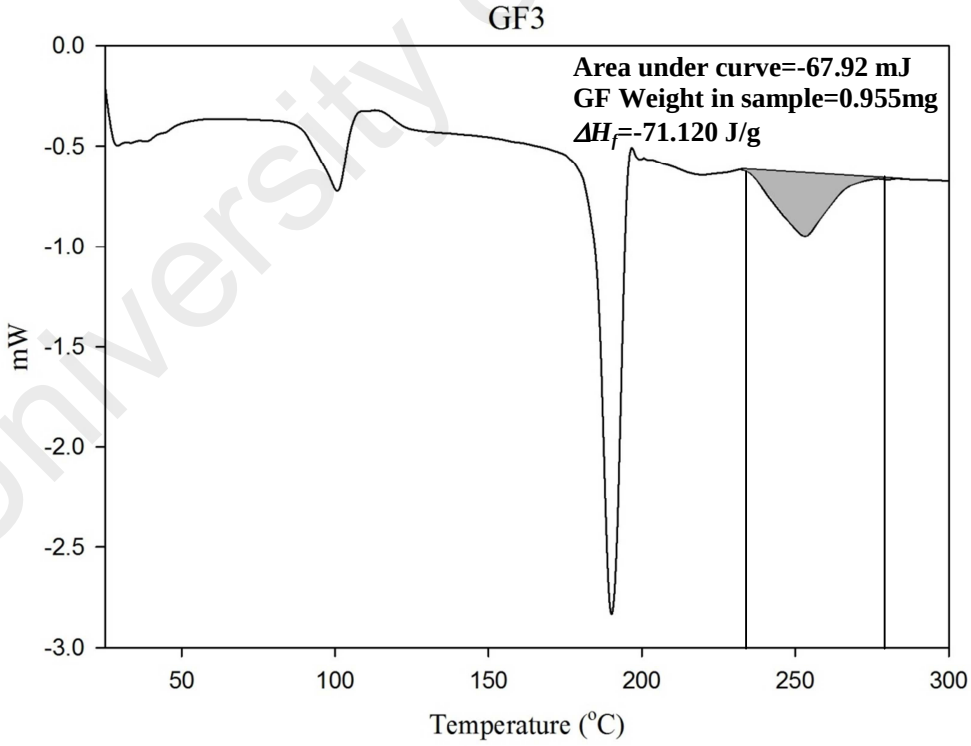

Figure 4.12
Total heat flow (DSC profile) for GF3 micronized powder.

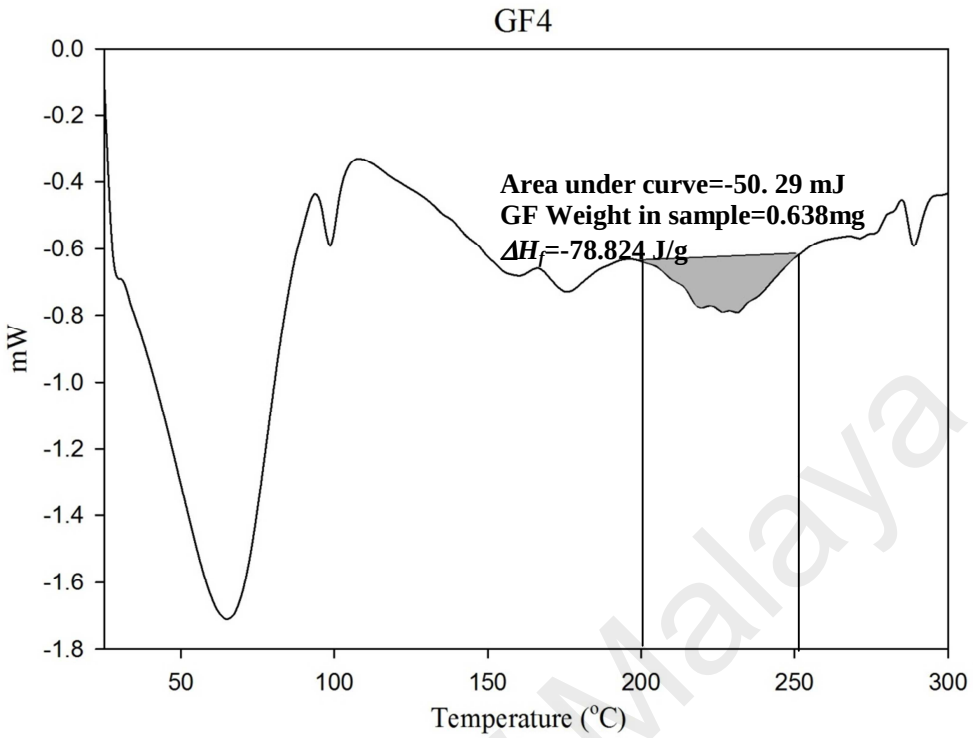

Figure 4.13
Total heat flow (DSC profile) for GF4 micronized powder.

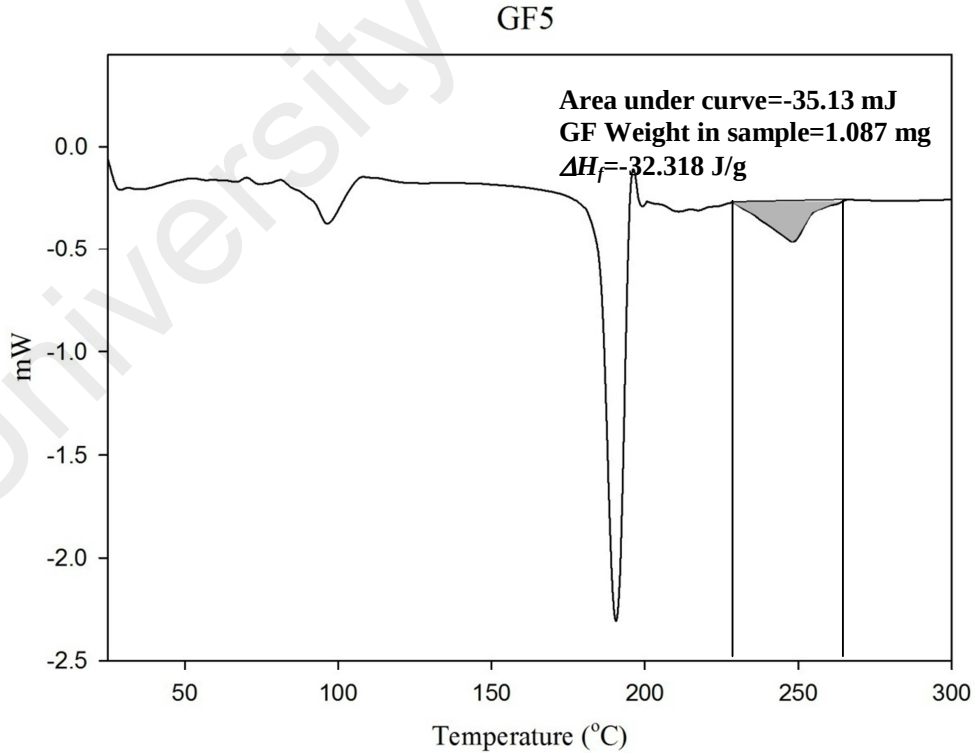

Figure 4.14
Total heat flow (DSC profile) for GF5 micronized powder.

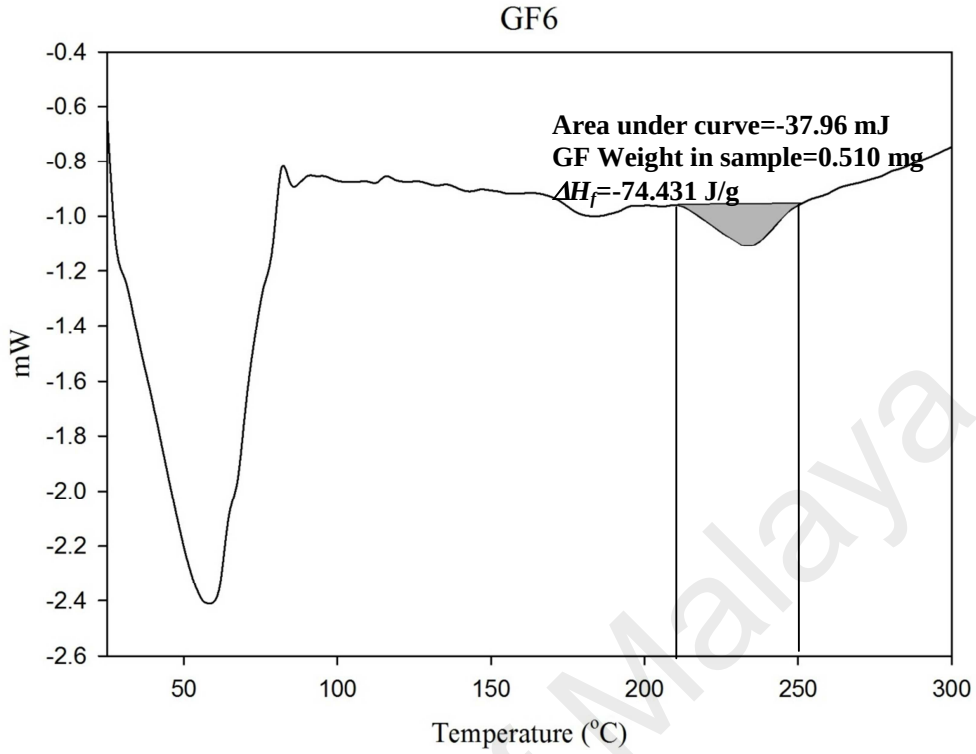

Figure 4.15
Total heat flow (DSC profile) for GF6 micronized powder.

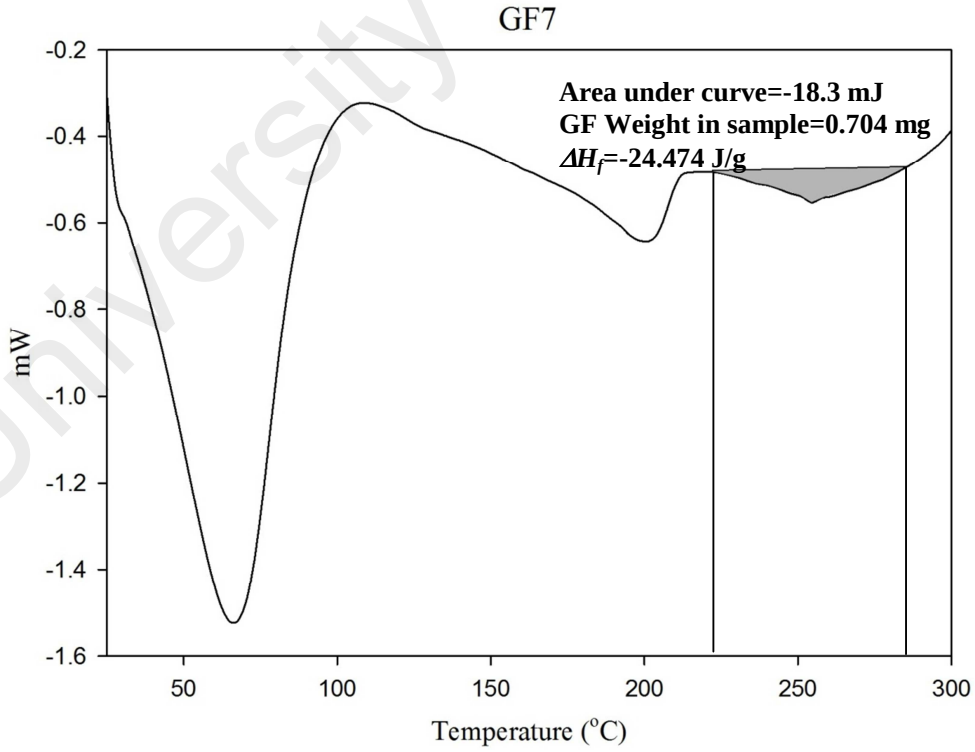

Figure 4.16
Total heat flow (DSC profile) for GF7 micronized powder

5.0 CONCLUSIONS AND RECOMMENDATIONS FOR FURTHER STUDY

5.1. Conclusions

The conclusions that we can drawn from this research work on cryogenic surface can be summarized as follows:-

1. The results obtained from Cryogenic surface showed that the yield of nano particles is higher compared to FD and the difference in yields attributed to the increase in rate of freezing.

2. Increasing in rate of freezing led to reduction in the possibility of phase separation were investigated in term of amount of energy absorb or release with different rate of freezing 70 °C/min and 5 °C/min, it observed that the values of heat (485.78 J/g, 55.94 J/g) respectively. This reduction in heat values interpreted to energy consumed activities of the system such as prevent phase separation and crystal growth inhabited which played important role in controlling crystal size to forming nano-size crystal.

3. Different polymer (PVP) ratios (0%, 25%, 33%, 50%, 67%) were examined with URF and FD. Quantitative determinations of nanoparticles revealed significant increase in the yield of nanoparticles percentage production in URF (26.67, 51.30, 84.53, 86.00 and 98.47%) in comparing with FD (23.21, 34.49, 81.96, 83.13 and 90.00%). The particle size distribution for URF powders showed reduction in size in consistency with nanoparticles quantitative studies i.e., the particle size distribution for M50 values were 507225nm, 885nm, 788nm, 135nm and 94nm for PVP ratios 0, 25, 33, 50 and 67% respectively.

4. Characterization of the samples produced by URF and FD using SEM clearly showed reduction in particle size induced by increasing rate of freezing. Furthermore, particles shape morphing was inhibited due to the effect of polymer ratio, where the particles shape change from needle shape with sharp edge to rectangular shape.

5. Characterization of the samples produced by URF and FD using XRD clearly showed reduction in peak values due to the effect of increasing in rate of freezing. Furthermore reduction in peak values proportionally with increasing PVP ratio due to the effect of rate on crystal growth and proved its reduction in particles size.

6. The URF technology was demonstrated to enhance dissolution rate for GF in term of amorphosity values. Enhancing dissolutions rate were observed in six compositions manufactured using URF process due to influence of ionic and non-ionic surfactants on the enhancing dissolution rate of GF. 3D response surface revealed that the effect of PVP on API release is significantly high in compare with the effect of SDS. Forming amorphouse powders were investigated using DSC to elucidate the change in dissolution rate. The results of DSC and disolution profile showed evidence in interaction between hydrophilic parts of SDS and let hydrophobic parts free which led to reduction in dissolution rate despite of increasing in amorphousity.

7. It can be concluded convincingly, that developed technique is an effective particle formation process for pharmaceutical development (particularly Isoniazid & Griseofulvin) and manufacturing to improve dissolution rates of poorly water soluble APIs.

5.2. Recommendations for future work

The research can be further developed by expanding the scope of studies. From the difficulty encountered and observations made during the research work, the following recommendations are proposed as a guide for further investigation.

- It is recommended to study the aerodynamic characteristic of powders produced by URF. In order to understand the process of inhalation and intake of drug by patient.
- It is recommended to investigate the benefits of URF powders in vivo studies. The workers in the field of pharmacology can further work on this.
- URF should be carried on Different APIs which fallen into Class 2, 3 and 4, with different permeability and solubility characteristics.
- It is recommended to modify the design with one stage process (atomization and drying) by atomization in cold vacuum chamber. The current stage where the process of transferring of the droplet from cryogenic surface to the freeze dryer could lead to deforestation.

REFERENCES

Abdelwahed, W., Degobert, G., Stainmesse S., Fessi H. (2006). Freeze-drying of nanoparticles: Formulation, process and storage considerations. *Advanced Drug Delivery Reviews.* **58.**1688–1713.

Adams, T.H., Beck J.P., Menson R.C. (1980). Method and apparatus for making novel particulate compositions. *Patent US* **4**.211-015.

Adams, T.H., Beck J.P., Menson R.C. (1982). Novel particulate compositions. *Patent US* **4**.323-478.

Amidon, G. L., Lennernäs, H., Shah, V. P., Crison, J. (1995). A Theoretical Basis for a Biopharmaceutic Drug Classification: The Correlation of in Vitro Drug Product Dissolution and in Vivo Bioavailability. *R. Pharm. Res.* **12**.413-420.

Barrow, E. L., Winchester, G. A., Staas, J. K., Quenelle, D. C., and Barrow W. W. (1998). Use of microsphere technology for targeted delivery of rifampin to Mycobacterium tuberculosis-infected macrophages. *Antimicrob. Agents Chemother.* **42**. 2682–2689.

Bayomi, M.A., Abanumay, K.A., and Al-Angary, A.A. (2002). Effect of inclusion complexation with cyclodextrins on photostability of nifedipine in solid state. *Int. J. Pharm.* **243(1-2)**. 107-117.

Becker, C., Dressman, J.B., Amidon, G.L., Junginger, H.E., Kopp, S., Midha, K.K., Shah V.P., Stavchansky S., Barends D.M. (2007). Biowaiver Monographs for Immediate Release Solid Oral Dosage Forms: Isoniazid. *J. of pharm. Sci.* **96.** 522-531.

Bindschaedler, C. (2004). Lyophilization process validation. J. *Drugs and the Pharmaceutical Sciences,* **137**. 535-574

Briggs, A.R., Maxwell, T.J. (1973). Process for preparing powder blends. *Patent US* 3.721,725.

Briggs, A.R., Maxwell, T.J. (1975). Lyophilized biological products. *Patent US* 3, 928, 566.

Briggs, A.R., Maxwell, T.J. (1976). Method of preparation of lyophilized biological products. *Patent US* 3,932,943.

Cansell, F., Chevalier, B., Demourgues, A., Etourneau, J., Even, C., Pessey, V., Petit, S., Tressaud, A., Weill, F. (1999). Supercritical fluid processing: a new route for materials synthesis. *J. Mater. Chem.* **9.** 67-75.

Chambers, E., Mitragotri, S. (2004). Prolonged circulation of large polymeric nanoparticles by non-covalent adsorption on erythrocytes. *J. Control Release.* **100(1).** 111–119.

Chari, K. (1992). The structure of the PVP---SDS complex in water. J. Colloid Interf. Sci. 151.294-296.

Chiou, W.L. and Riegelman S. (1971). Pharmaceutical applications of solid dispersion systems. *J. Pharm. Sci.* **60(9)**. 281-302.

Christ M. (2003). Systematical Freeze Drying: The Christ-Seminar. Osterode, Germany.

Constantinides, P.P. (1995). Lipid microemulsions for improving drug dissolution and oral absorption: physical and biopharmaceutical aspects. *Pharm. Res.* **12(11).**1561-1572.

Craig, D.Q.M. (2002). The mechanisms of drug release from solid dispersions in water-soluble polymers. *Int. J. Pharmaceutics.* **231(2).**131-144.

Cussler, E. L. (1986). Diffusion, Mass transfer in fluid systems. Cambridge University Press: NY.

Davda, J., Labhasetwar, V. (2002). Characterization of nanoparticle uptake by endothelial cells. *Int. J. Pharm.* **233(1–2).** 51–59.

Dawson, W.J. (1988). Hydrothermal synthesis of advanced ceramic powders. *Am. Ceram. Soc. Bull.* **67**. 1673-1678.

de Boer, A.H., Molema, G., and Frijlink, H.W. (2001). *Pulmonary drug delivery: delivery to and through the lung. Drug targeting, organ specific strategies.* **12** (eds G. Molema and D. K. F. Meijer), Wiley-VCH Verlag GmbH, Weinheim, FRG.

Dehghani F., Foster N.R. (2003). Dense gas anti-solvent processes for pharmaceutical formulation. *Curr. Opin. Solid State Mater. Sci.***7(4-5).** 363-369.

DeSimone, J.M., Maury, E.E., Menceloglu, Y.Z., McClain, J.B., Romack, T. J., Combes, J.R. (1994). Dispersion polymerizations in supercritical carbon dioxide. *Science.* **265(5170).** 356-359.

Desmoulins-Krawiec, S., Aymonier, C., Loppinet-Serani, A., Weill, F., Gorsse, S., Etourneau, J., Cansell, F. (2004). Synthesis of nanostructured materials in supercritical ammonia: nitrides, metals and oxides. *J. Mater. Chem.* **14(2).** 228-232.

Dirksen, J.A., Ring, T.A. (1991). Fundamentals of crystallization: Kinetic effects on particle size distributions and morphology. *Rev. Chem. Eng. Sci.* **46**. 2389-2427.

Dunn, E.B., Masavage, G.J., Sauer, H.A. (1972). Method of freezing solution droplets and the like using immiscible refrigerants of differing densities. *Patent US* **3**,653,222.

Evans, J.C., Scherzer, B.D., Tocco, C.D., Kupperblatt, G.B., Becker, J.N., Wilson, D.L., Saghir, S.A., Elder, E.J. (2006). Preparation of nanostructured particles of poorly water soluble drugs via a novel ultra-rapid freezing technology, in: S. Svenson (Ed.), Polymeric Drug Delivery – Polymeric Matrices and Drug Particle Engineering, ACS Symposium Series 924, American Chemical Society, Washington, DC, 320–328.

FDA, Draft – Guidance for Industry: Bioavailability and Bioequivalence Studies for Orally Administered Drug Products. U.S. Department of Health and Human Services, Food and Drug Administration, Center for Drug Evaluation and Research (CDER), July 2002.

Fenghour, A., Wakeham, W.A., Vesovic, V. (1998). The viscosity of carbon dioxide. *J. Phys. Chem. Ref. Data.* **27(1).** 31-44.

Foster, K.A., Yazdanian, M., Audus, K.L. (2001). Microparticulate uptake mechanisms of in-vitro cell culture models of the respiratory epithelium. *J. Pharm. Pharmacol.* **53(1).** 57–66.

Fox, W., Ellard, G.A., Mitchison, D.A. (1999). Studies on the treatment of tuberculosis undertaken by the British Medical Research Council Tuberculosis Units, 1946–1986, with relevant subsequent publications. *Int. J. Tuberc. Lung. Dis.* **3(2).** S231-S279.

Franks, F. (1998). Freeze-drying of bioproducts: putting principles into practice. *Euro. J. of pharm. and biopharm.***45**. 3-9.

Geldart, D. (1973). Types of gas fluidization. *Powder Technol.* **7(5).** 285–292.

Gohel, M.C. and Patel, L.D. (2003). Processing of nimesulide-PEG 400-PG-PVP solid dispersions: preparation, characterization, and in vitro dissolution. *Drug Dev. Ind. Pharm.* **29(3).**299-310.

Gombotz, W.R., Healy, H.S., Brown, R.L. (1990). Process for producing small particles of biologically active molecules. *Patent WO* 90/13285.

Gombotz, W.R., Healy, H.S., Brown, R.L. (1991). Very low temperature casting of controlled release microspheres. *Patent US* **5**,019,400.

Gottfried, B.S., Lee, C.J., Bell, K.J. (1966). The Leidenfrost phenomenon: film boiling of liquid droplets. *Int. J. Heat Mass Transfer.* **9.** 1167-1187.

Grotenhermen, F. (2003). Pharmacokinetics and pharmacodynamics of cannabinoids. *Clin. Pharmacokin.* **42(4)**.327-360.

Gupta, R.B., Chattopadhyay, P. Method of forming nanoparticles and microparticles of controllable size using supercritical fluids and ultrasound. *US patent* No. 20020000681, 37.

Hall, R.S., Board, S.J., Clare, A.J., Duffey, R.B., Playle, T.S., Poole, D.H. (1969). Inverse Leidenfrost phenomenon. *Nature.* **224**.266-267.

Hatley, R.H., Franks, F., Brown, S., Sandhu, G., Gray, M. (1996). Stabilization of a Pharmaceutical Drug Substance by Freeze-Drying: a Case Study. *Drug Stability* **1**.2-12.

Hebert P.F., Healy M.S. (1999). Production scale method of forming microparticles. Patent US 5,922,253.

Heldman, D.R., Hohner, G.A., (1974). An analysis of atmospheric freeze drying. *J. Food Sci.* **39.**147–155.

Heyder, J., Gebhart, J., Rudolf, G., Schiller, C.F., Stahlhofen, W. (1986). Deposition of particles in the human respiratory tract in the size range 0.005–15 μm. *J. Aerosol Sci.* **17(8).** 11–25.

Holmes, J.D., Ziegler, K.J., Doty, R.C., Pell, L.E., Johnston, K.P., Korgel, B.A. (2001). Highly luminescent silicon nanocrystals with discrete optical transitions. *J. Am. Chem.* Soc. **123(16).**3743-3748

House, J. A. and Mariner, J. C. (1996). Stabilization of rinderpest vaccine by modification of the lyophilization process. *Developments in biological standardization.* **87.**235-244.

Hu, J., Johnston, K.P., Williams III, O.R. (2003). Spray freezing into liquid (SFL) particle engineering technology to enhance dissolution of poorly water soluble drugs: organic solvent versus organic/aqueous co-solvent systems. *Eur. J. Pharma. Sci.* **20**. 295-303.

Hu, Z.S., Dong, J.X., Chen, G.X., Lou, F. (1999). Preparation of nanometer copper borate with supercritical carbon dioxide drying. *Powder Technol.* **102(2).** 171-176.

Hu, Z.S., Lai, R., Lou, F., Wang, L.G., Chen, Z.L., Chen, G.X., Dong, J.X. (2002). Preparation and tribological properties of nanometer magnesium borate as lubricating oil additive. *Wear.***252 (5-6),** 370-374.

Hu, Z.S., Wang, L.G., Ou, Z.W., Huang, L., Lai, R., He, T., Dong, J.X., Chen, G.X. (2001). Preparation of aerogel beryllium borate with supercritical carbon dioxide drying. *Powder Technol.* **114(1-3)**. 163-167.

Huang, F.H., Li, M.H., Lee, L.L., Starling, K.E., Chung, F.T.H. (1985). An accurate equation of state for carbon dioxide. *J. Chem. Eng. Japan*. **18.** 490-496.

Ishimaru Y. (1994). J. *Appl. Polym. Sci.* **29**:1675.

Johnston, K.P., Jacobson, G.B., Lee, C.T., Meredith, C., Da Rocha, S.R.P., Matt, Z.Y., DeGrazia, J. (1999). Microemulsions, emulsions and latexes. In: P.G. Jessop. W.

Leitner (Eds.). Chemical Synthesis Using Supercritical Fluids. Wiley-VCH. Weinheim. (p. 127).

Jung, J., Perrut, M. (2001) Particle design using supercritical fluids: Literature and patent survey. *J. Supercrit. Fluids.* **20(3).** 179-219.

Kashchiev, D. (2000). Nucleation—basic theory with applications, Butterworth-Heinemann, Oxford.

Kaushal, A.M., Gupta, P., and Bansal, A.K. (2004). Amorphous drug delivery systems: molecular aspects, design, and performance. *Crit. Rev. Ther. Drug Carrier Syst.* **21(3).** 33-93.

Kipp, J.E. (2004). The role of solid nanoparticle technology in the parenteral delivery of poorly water-soluble drugs. *Int. J. Pharm.* **284(1-2).** 109-122.

Knoblauch, J., Zimmermann, I. (2007). Thermochemical analysis of the dissolution process of Griseofulvin. *Euro. J. of Pharmaceutics and Biopharmaceutics.* **67.** 743–751.

Koch, A.M., Reynolds, F., Merkle, H.P., Weissleder, R., Josephson, L. (2005). Transport of surface-modified nanoparticles through cell monolayers. *Chembiochem.* **6(2).** 337–345.

Kucers, A., Bennet, N. M. (1988). The use of antibiotic: A comprehensive review with clinical emphasis, 4th ed. William Heinemann Medical Books: London.1528.

Leach, W.T., Simpson, D.T., Val, T. N., Anuta, E. C., Yu, Z., Williams, R.O., Johnston, K.P. (2005). Uniform encapsulation of stable protein nanoparticles produced by spray freezing for the reduction of burst effect. *J. Pharm. Sci*.**94.** 56–69.

Lefebvre, A. H. (1989). Atomization and Sprays, Hemisphere Publishing Corp., New York.

Lennernäs, H., Ahrenstedt, O., Hallgren, R., Knutson, L., Ryde, M., Paalzow, L. K. (1992). Regional Jejunal Perfusion, a New in Vivo Approach to Study Oral Drug Absorption in Man. *Pharm. Res.* **9(10)**. 1243-1251.

Lennernas, H., Ahrenstedt, O., Ungell, A. L. Br. (1994). Intestinal drug absorption during induced net water absorption in man; a mechanistic study using antipyrine, atenolol and enalaprilat. *J.Clin. Pharmacol.* **37(6)**. 589-596.

Leuenberger, H. (2002). Spray Freeze-drying - The Process of Choice for Low Water Soluble Drugs? *Journal of Nanoparticle Research*. **4(1-2).** 111-119.

Lindman, B., Thalberg, K., (1993). Polymer–surfactant interactions-recent developments, in: E.D. Goddard, K.P. Anathapadmanabhan (Eds.), Interact. Surfactants Polym. Proteins. 203–276.

Liversidge, G. G., Conzentino, P. (1995). Drug particle size reduction for decreasing gastric irritancy and enhancing absorption of naproxen in rats. *Int. J. Pharm.* **125**.309-313.

Liversidge, G. G., Cundy, K. C., Bishop, J. F., Czekai, D.A. (1992). Surface modified drug nanoparticles. *US Patent.* **5.**145-684.

Liversidge, G.G. and Cundy, K.C. (1995). Particle size reduction for improvement of oral bioavailability of hydrophobic drugs: I. Absolute oral bioavailability of nanocrystalline danazol in beagle dogs. *Int. J. Pharm.* **125(1)**. 91-97.

MacKenzie, A.P. (1976). The physico-chemical basis for the freeze-drying process. *Dev. Biol. Stand.***36**. 51-67.

Malecki, G.J., Shinde, P., Morgan, A.I., D.F., (1970). Atmospheric fluidized bed freeze drying. *Food technology.* **24.** 601–603.

Merisko-Liversidge, E., Liversidge, G. G., and Cooper, E. R. (2003). Nanosizing: a formulation approach for poorly-water-soluble compounds. *Eur. J. Pharm. Sci.* **18**.113-120.

Merisko-Liversidge, E., Sarpotdar, P., Bruno, J., Hajj, S., Wei, L., Peltier, N., Rake, J., Shaw, J. M., Pugh, S., Polin, L., Jones, J., Corbett, T., Cooper, E., and Liversidge, G. G. (1996). Formulation and antitumor activity evaluation of nanocrystalline suspensions of poorly soluble anticancer drugs. *Pharm. Res.* **13.** 272-278.

Meryman H.T. (1959). Sublimation Freeze-Drying without Vacuum. *Science*. **130(3376).** 628–629.

Muller, R. H., Becker, R., Kruss, B., and Peters, K., (1999). Pharmaceutical nanosuspensions for medicament administration as systems with increased saturation solubility and rate of solution. *US Patent.* **5.**858.410.

Muller, R.H., Jacobs, C., Kayser, O. (2001). Nanosuspensions as particulate drug formulations in therapy. Rationale for development and what we can expect for the future. *Adv. Drug Deliv. Rev.* **47(1).** 3–19.

Mullin J. W. (2001). Crystallization 4th edition, Butterworth-Heinemann, Oxford.

Mullin, J. W. (1988), Crystallization And Precipitation, Ullmann's Encyclopedia Of Industrial Chemistry,Volume B2 Weinheim,

Nail, S., Gatlin, L. (1993). Freeze Drying: Principles and practice. Pharmaceutical dosage forms. 2. Marcel Dekker, New York.

Noyes, A. A., Whitney, W. R. (1897). The rate of solution of solid substances in their own solutions. *J. Am. Chem. Soc.* **19**. 930-934.

O'Hara P. and Hickey A. J. (2000). Respirable PLGA microspheres containing rifampicin for the treatment of tuberculosis: manufacture and characterization. *Pharm. Res.* **17.** 955–961.

O'Hern, H.A., Martin, J.J. (1955). Diffusion in carbon dioxide at elevated pressure. *Ind. Eng. Chem. Res.***47(10)**. 2081-2087.

Oetjen, G. W. (1999). Freeze Drying. Wiley-VCH, Weinheim.

Overhoff, K. A., Johnston, K. P., Williams III, R.O.(2006). Improvement of dissolution rate of poorly water soluble drugs using a new particle engineering process—spray freezing into liquid. Polymeric Drug Delivery II. Svenson, S. [Ed.], ACS Symposium Series, 924, Am. Chem. Soc. Washington, DC.

Pandey, R., Sharma, A., Zahoor, A., Sharma, S., Khuller, G.K., Prasad, B. (2003). Poly [DL-lactide-co-glycolide] nanoparticle-based inhalable sustained drug delivery system for experimental tuberculosis. *J. Antimicrob Chemother.* **52(6).**981–986.

Perry, R.H., Green, D.W. (1984). Perry's Chemical Engineers' Handbook. 50th editions. McGraw-Hill Book Co.Singapore.

Pikal, M. J. (1994). Freeze-drying of proteins: process, formulation, and stability. ACS Symposium Series 567(Formulation and Delivery of Proteins and Peptides):120-33.

Pikal, M. J., Shah, S., Roy, M. L., Putman, R. (1990). The secondary drying stage of freeze drying: Drying kinetics as a function of temperature and chamber pressure. *Int. J. Pharm.* **60.** 203-217.

Pikal, M.J., (2003). Heat and Mass Transfer in Low Pressure Gases: Applications to Freeze Drying. Freeze Drying of Pharmaceuticals. Lecture script, University of Connecticut, Storrs.

Pikal, MJ. (2002). Freeze Drying: Encyclopedia of Pharmaceutical Technology. Marcel Dekker, New York,,1299-1326.

Pison, U., Welte, T., Giersig, M., Groneberg, D. A., (2006). Nanomedicine for respiratory diseases. *Eur. J. Pharmacol.* **533(1–3).** 341–350.

Ponchel, G. and Irache, J.M. (1998). Specific and non-specific bioadhesive particulate systems for oral delivery to the gastrointestinal tract. *Adv. Drug Deliv. Rev.* **34(2-3).** 191-219.

Pouton, C.W. (1997). Formulation of self-emulsifying drug delivery systems. *Adv. Drug Deliv. Rev.* **25(1).** 47-58.

Pratsinis, S.E., Vemury, S. (1996). Particle formation in gases: a review. *Powder Technol.* **88(3).** 267-273.

Purvis, T., Vaughn, J. M., Rogers, T. L., Chen, X., Overhoff, K. A., Sinswat, P., Hu, J., McConville, J. T., Johnston, K. P., Williams, R. O. (2006). Cryogenic liquids, nanoparticles, and microencapsulation. *Int. J. Pharm.* **324(1)**. 43–50.

Quenelle, D. C., Staas, J. K., Winchester, G. A., Barrow, E. L., and Barrow, W. W. (1999). Efficacy of microencapsulated rifampin in Mycobacterium tuberculosis-infected mice. *Antimicrob. Agents Chemother.* **43(5).** 1144–1151.

Rambhatla, S., Ramot, R., Pikal, M.J. (2003). The Impact of the Freezing Stage on Lyophilization: Effects of nucleation temperature and pore size. Proc. University of Connecticut. School of Pharmacy, Storrs, CT, USA.

Reddy, R. K., Khalil, S. A., Gonda, M. W. (1976). Effect of dioctyl sodium sulflosuccinate and polaxamer 188 on dissolution and intestinal absorption of sulfadiazine and ulfisoxazole in rats. *J. Pharm. Sci.* **65.** 115–118.

Reverchon, E. (1999). Supercritical antisolvent precipitation of micro- and nano-particles. *J. Supercrit. Fluids.* **15(1).** 1-21.

Reverchon, E., Adami, R. (2006). Nanomaterials and supercritical fluids. *J. of Supercritical Fluids.* **37**. 1–22.

Reverchon, E., Caputo, G., Marco, I. De. (2003). Role of phase behavior and atomization in the supercritical antisolvent precipitation. *Ind. Eng. Chem. Res.* **42(25).** 6406-6414.

Reverchon, E., Spada, A. (2004). Crystalline microparticles of controlled size produced by supercritical-assisted atomization. *Ind. Eng. Chem. Res.* **43(6).**1460-1465.

Riley, R.L., Mills, C.C., Nyka, W., Weinstock, N., Storey, P.B., Sultan, L.U. (1995). Aerial dissemination of pulmonary tuberculosis: a two year study of contagion in a tuberculosis ward. *Am. J. Epidemiol.* **142(1).**1-2.

Rogers, T. L., Johnston, K. P., Williams, R. O. (2001). Solution-based particle formation of pharmaceutical powders by supercritical or compressed fluid CO_2 and cryogenic spray-freezing technologies. *Drug development and industrial pharmacy*. **27(10).** 1003-1016.

Rogers, T.L., Hu, J., Yu, Z., Johnston, K.P., Williams, R.O. (2002). A novel particle engineering technology: spray-freezing into liquid. *Int. J. Pharm.* **(242).** 93–100.

Rogers, T.L., Nelsen, A.C., Hu, J., Brown, J.N., Sarkari, M., Young, T.J., Johnston, K.P., Williams III, R.O. (2002). A novel particle engineering technology to enhance dissolution of poorly water soluble drugs: spray-freezing into liquid. *Eur. J. Pharma. Biopharma.* **54.** 271-280.

Rogers, T.L., Overhoff, K.A., Shah, P., Santiago, P., Yacaman, M.J., Johnston, K.P., Williams III, R.O. (2003). Micronized powders of a poorly water soluble drug

produced by a spray-freezing into liquid-emulsion process. *Eur. J. Pharma. Biopharm.* **55**. 161-172.

Russell, D.G. (2001). Mycobacterium tuberculosis: here today and here tomorrow. *Nat. Rev. Mol. Cell. Biol.* **2**.569–586.

Sauer, H.A. (1969). Method and apparatus for freeze-freeze drying. *Patent US* 3.484.946.

Searles, J.A., Carpenter, J.F., Randolph, T.W. (2001). The Ice Nucleation Temperature Determines the Primary Drying Rate of Lyophilization for Samples Frozen on a Temperature-Controlled Shelf. *J. Pharm. Sci.* **90(7).** 860-871.

Shibata, M., Kokubo, H., Morimoto, K., Ishida, T., Inoue, M. (1983). X-ray structural studies and physicochemical properties of cimetidine polymorphism. *J. Pharm. Sci.* **72**.14-36.

Shirahama, K. (1974). The binding equilibrium of sodium dodecyl sulfate to poly(ethylene oxide) in 0.1 M sodium chloride solution at 30°C. *Colloid Polym. Sci.* **252(11).**978-981.

Strickland, R. F. (1968). Kinetics and Mechanism of Crystallisation. Academic Press, London.74-129

Subramaniam, B., Said, S., Rajewski, R.A., Stella, V. Methods and apparatus for particle precipitation and coating using near-critical and supercritical antisolvents. WO/A1 9731691 (19970904).

Suh, J., Wirtz, D., Hanes, J. (2003). Efficient active transport of gene nanocarriers to the cell nucleus. *Proc. Natl. Acad. Sci. USA.* **100(7).** 3878–3882.

Sung, J.C., Pulliam, B.L., Edwards, D.A. (2007). Nanoparticles for drug delivery to the lungs. *Trends Biotechnol.* **25(12).** 563–570.

Tang, X., Pikal, M.J. (2004). Design of Freeze-Drying Processes for Pharmaceuticals: Practical Advice. *Pharm. Res.* **21(2).**191-200.

Torchilin, V.P., (2001). Structure and design of polymeric surfactant-based drug delivery systems. *J. Controlled Release.* **73(2-3)**. 137-72.

Vaughn, J. M., Gao, X., Yacaman, M. J., Johnston, K.P., Williams III, R. O. (2005). Comparison of powder produced by evaporative precipitation into aqueous solution (EPAS) and spray freezing into liquid (SFL) technologies using Zcontrast STEM and complimentary technologies. *Eur. J. Pharm. Biopharm.***60.**81–89.

Vaughn, J. M., McConville, J. T., Burgess, D., Peters, J. I., Johnston, K. P., Williams, R. O. (2006). Single dose and multiple dose studies of itraconazole nanoparticles. *Euro. J. of Pharm. and Biopharm.* **63**. 95–102.

Wang, W. (2000). Lyophilization and development of solid protein pharmaceuticals. *Inter. Jour. of Pharm.* **203.** 1-60.

Weber A. Production of nanoscale powders from sols using supercritical fluids. DE A1 19904990 (20000427).

Willemer, H., (1992). Measurements of temperatures, ice evaporation rates and residual moisture contents in freeze-drying. *Dev. Biol. Stand.* **74.**123-134.

Williams III, R.O., Johnston, K.P., Young, T.J., Rogers, T.L., Barron, M.K., Yu, Z. (2002). Process for production of nanoparticles and microparticles by spray freezing into liquid. Patent WO 02/060411.

Wisniewski, R., (1998). Large-Scale Cryopreservation of Cells, Cell Components and Biological Solutions. *Biopharm.* **11(9).** 42-50.

Woodward, H.T. (1963). Freeze-drying without vacuum. *Food Eng*. **35**.96–97.

York, P., Hanna, M. Salmeterol xinafoate with controlled particle size. WO A1 9501324 (19950112).

Yu, Z., Garcia, A.S., Johnston, K.P., Williams III, R.O. (2004). Spray freezing into liquid nitrogen for highly stable protein nanostructured microparticles. *Eur. J. Pharm. Biopharm.* **58.** 529-537.

Yu, Z., Rogers, T.L., Hu, J., Johnston, K. P., Williams III, R. O. (2002). Preparation and characterization of microparticles containing peptide produced by a novel process: spray freezing into liquid. *Eur. J. Pharm. Biopharm.* **54.** 221–228.